

# Characterization of photoreceptor gene regulation and modulation of microglial reactivity in the retina

Inaugural Dissertation

zur

Erlangung des Doktorgrades

Dr. nat. med.

der Medizinischen Fakultät

und

der Mathematisch-Naturwissenschaftlichen Fakultät

der Universität zu Köln



vorgelegt von

**Alexander Aslanidis**

aus Regensburg

Köln, 2016

Berichtersteller/Berichterstellerin:

Prof. Dr. Sabine Eming

Prof. Dr. Peter Kloppenburg

Tag der letzten mündlichen Prüfung:

16. November 2015

*For my beloved parents*

# I Table of contents

<b>I Table of contents</b> .....	<b>1</b>
<b>II Summary</b> .....	<b>3</b>
<b>III Zusammenfassung</b> .....	<b>5</b>
<b>1. Introduction</b> .....	<b>7</b>
1.1 Structure and function of the mammalian retina.....	7
1.2 Retinal genetics .....	9
1.2.1 Inherited retinal degenerations .....	9
1.2.2 Regulation of photoreceptor development.....	10
1.2.3 Genome-wide identification of CRX target genes .....	12
1.2.4 Sterile alpha motif containing proteins and SAMD7.....	13
1.3 Microglia .....	14
1.3.1 Microglia in the CNS and retina .....	14
1.3.2 Functions of microglia .....	14
1.3.3 Microglia in retinal degeneration.....	16
1.3.4 Microglial (reactivity) markers.....	19
1.3.5 Microglia as a therapeutic target .....	21
1.3.5.1 Natural compounds .....	22
1.3.5.2 Whey acidic proteins (WAPs) and AMWAP .....	23
1.3.5.3 Translocator protein (18 kDa) (TSPO) and its ligands .....	24
1.4 Aims of the thesis .....	26
<b>2. Results</b> .....	<b>28</b>
2.1 Sterile alpha motif containing 7 (SAMD7) is a novel CRX-regulated transcriptional repressor in the retina.....	28
2.2 Activated microglia/macrophage whey acidic protein (AMWAP) inhibits NFκB signaling and induces a neuroprotective phenotype in microglia .....	30
2.3 Translocator protein (18 kDa) (TSPO) is expressed in reactive retinal microglia and modulates microglial inflammation and phagocytosis .....	32
<b>3. Discussion</b> .....	<b>35</b>
3.1 Results from the three presented studies in summary .....	35
3.2 SAMD7, a novel photoreceptor gene repressor .....	35
3.2.1 Photoreceptor-specific SAMD7 gene regulation .....	36
3.2.2 SAMD7, a gene regulator without DNA binding sequence.....	36
3.2.3 Potential role of SAMD7 in retinal health and disease .....	37
3.3 AMWAP, a counter-regulator of microglial reactivity .....	38
3.3.1 Obtaining recombinant AMWAP for therapy .....	38

3.3.2	AMWAP, an inhibitor of microglial NFκB signaling.....	38
3.3.3	AMWAP induces a neuroprotective microglial phenotype.....	39
3.3.4	AMWAP, current state and future perspectives .....	40
3.4	TSPO, emerging roles in the CNS and retina .....	41
3.4.1	TSPO, a novel marker for reactive retinal microglia.....	41
3.4.2	Functions of TSPO and its ligands in reactive microglia .....	42
3.4.3	TSPO, current state and future perspectives.....	44
3.5	Concluding remarks.....	45
	<b>Reference list .....</b>	<b>46</b>
	<b>Acknowledgements .....</b>	<b>61</b>
	<b>Erklärung.....</b>	<b>62</b>
	<b>Publications .....</b>	<b>63</b>

## II Summary

Photoreceptors are highly specialized cells required for phototransduction within the retina and thus crucial for visual perception. Inherited retinal diseases are mainly caused by mutations in photoreceptor-specific genes, the majority of which is regulated by the key transcription factor cone rod homeobox (CRX). Using genome-wide chromatin immunoprecipitation data (CRX ChIP-seq), we have identified a novel sterile alpha motif (SAM) domain containing protein, SAMD7, as a CRX target. SAMD7 is expressed in the mouse retina and pineal gland and localizes to the cytoplasm and nucleus of photoreceptor cells. SAMD7 expression is regulated by CRX, which binds to two specific regions in the promoter and first intron (enhancer) of the SAMD7 gene. Consequently, CRX knock-down leads to a significant decrease of SAMD7 enhancer activity and protein levels in the retina. Functionally, SAMD7 acts as a transcriptional repressor of CRX-mediated photoreceptor gene expression, indicating that mutations in or dysregulation of SAMD7 could lead to disturbed photoreceptor homeostasis and ultimately retinal degeneration.

Microglial cells are the resident macrophages of the central nervous system (CNS), including the retina, and play pivotal roles in innate immune responses and regulation of homeostasis in the healthy and degenerating CNS. Reactive microgliosis is a common hallmark of neurodegenerative diseases and chronic pro-inflammatory microglial reactivity contributes to disease progression. We have previously identified activated microglia/macrophage whey acidic protein (AMWAP) as a biomarker for microglial reactivity and counter-regulator of pro-inflammatory response. AMWAP is actively secreted from lipopolysaccharide (LPS)-activated microglia and recombinant AMWAP is taken up by microglial cells in a paracrine fashion and effectively reduces TLR2- and TLR4-mediated pro-inflammatory gene expression. AMWAP exerts its anti-inflammatory function through blockade of NF $\kappa$ B activation, as it inhibits proteolysis of the NF $\kappa$ B pathway mediators IRAK-1 and I $\kappa$ B $\alpha$  without preventing I $\kappa$ B $\alpha$  phosphorylation and ubiquitination or affecting overall 20S proteasome activity. Functionally, AMWAP reduces pro-inflammatory microglial nitric oxide (NO) secretion and neurotoxicity on photoreceptor cells *in vitro*. Further, AMWAP promotes filopodia formation of microglia and increases the phagocytic recognition and uptake of apoptotic photoreceptor debris, common features of homeostatic regulatory microglia. We therefore hypothesize that anti-inflammatory whey acidic proteins

(WAPs) could have therapeutic potential in neurodegenerative diseases of the brain and retina.

The translocator protein (18 kDa) (TSPO) is a mitochondrial protein expressed in reactive glial cells and a biomarker for gliosis in the brain but has not been investigated in a retinal context so far. Various TSPO ligands have been shown to reduce neuroinflammation in neurodegenerative mouse models. We could show strong upregulation of TSPO transcript and protein levels in reactive microglial cells *in vitro*, microglia of the retinoschisin-deficient retinal degeneration mouse model as well as TSPO expression in microglia of the human retina. TSPO mRNA expression is high in the developing mouse retina and declines to low levels in the adult tissue. The synthetic TSPO ligand XBD173 effectively suppresses pro-inflammatory microglial gene expression, migration, proliferation, NO secretion and neurotoxicity on photoreceptors *in vitro*. Further, XBD173 treatment promotes filopodia formation and increases the phagocytic recognition and uptake of latex beads and apoptotic photoreceptor debris by murine and human microglial cells *in vitro*. Finally, XBD173 effectively reduces the number of amoeboid alerted microglia in organotypic murine retinal explant cultures stimulated with LPS. In conclusion, we have identified TSPO as a novel marker for microglial reactivity in the retina and a potential therapeutic target to reduce chronic neuroinflammation during retinal degeneration.

In summary, our studies on the novel photoreceptor gene regulator SAMD7 and the microglial reactivity markers AMWAP and TSPO provide insights into potential disease mechanisms of retinal degeneration and suggest future strategies of identifying and therapeutically modulating pro-inflammatory microglial reactivity in degenerative diseases of the CNS and retina.

### III Zusammenfassung

Photorezeptorzellen sind hoch spezialisierte Zellen innerhalb der Netzhaut, welche die Phototransduktion vermitteln und daher essentiell für die Aufnahme und Verarbeitung visueller Sinnesreize sind. Erbliche Netzhautdystrophien werden vornehmlich durch Mutationen in Photorezeptor-spezifischen Genen verursacht, von welchen die Mehrzahl durch den Schlüsseltranskriptionsfaktor cone rod homeobox (CRX) reguliert wird. Mit Hilfe eines genomweiten Chromatin Immunpräzipitations-Datensatzes (CRX ChIP-seq), konnten wir ein neuartiges, sterile alpha motif (SAM) Domänen beinhaltendes Protein, SAMD7, als CRX Zielgen identifizieren. SAMD7 wird in der Mausnetzhaut und Zirbeldrüse exprimiert und lokalisiert im Zytoplasma und Nukleus von Photorezeptorzellen. Die SAMD7 Expression wird durch CRX reguliert, welches an zwei spezifischen Regionen im Promotor und ersten Intron (Enhancer) im SAMD7 Gen bindet. Somit führt CRX knock-down zu einer signifikanten Abnahme der regulatorischen Aktivität des SAMD7 Enhancers und der SAMD7 Proteinlevel in der Netzhaut. Funktionell agiert SAMD7 als Transkriptionsrepressor der CRX-vermittelten Photorezeptor-Genexpression, was darauf hindeutet, dass Mutationen in oder Dysregulation von SAMD7 zu gestörter Photorezeptor-Homöostase und letztlich zu Netzhautdegeneration führen könnten.

Mikrogliazellen sind die gewebsansässigen Makrophagen des zentralen Nervensystems (ZNS), inklusive der Netzhaut, und spielen eine wichtige Rolle in der Immunantwort und Regulation der Homöostase im gesunden sowie degenerierenden ZNS. Reaktive Mikroglie ist ein typisches Merkmal neurodegenerativer Erkrankungen und chronische proinflammatorische Mikrogliaaktivierung beschleunigt den Krankheitsverlauf. Wir konnten in Vorarbeiten das activated microglia/macrophage whey acidic protein (AMWAP) als Biomarker für reaktive Mikroglia und Gegenspieler der proinflammatorischen Mikrogliaantwort identifizieren. AMWAP wird aktiv von Lipopolysaccharid (LPS)-aktivierten Mikroglia sezerniert und rekombinantes AMWAP wird in parakriner Weise von Mikroglia aufgenommen in welchen es effektiv die TLR2- und TLR4-vermittelte proinflammatorische Genexpression reduziert. AMWAP erzielt diese antiinflammatorische Wirkung durch Blockade der NFκB Aktivierung, indem es die Proteolyse der NFκB Signalwegsmediatoren IRAK-1 und IκBα verhindert ohne die IκBα Phosphorylierung, Ubiquitinierung oder die allgemeine 20S Proteasomaktivität zu beeinflussen. Funktionell reduziert AMWAP die proinflam-

matorische mikrogliale Stickstoffoxidsekretion und Neurotoxizität gegenüber Photorezeptorzellen *in vitro*. Des Weiteren induziert AMWAP die Bildung mikroglialer Filopodien und erhöht die phagozytische Aufnahmefähigkeit von apoptotischem Photorezeptordebris, typische Charakteristika homöostatischer und regulatorischer Mikroglia. Wir schließen aus diesen Ergebnissen, dass antiinflammatorische whey acidic proteins (WAPs) therapeutisches Potential in neurodegenerativen Erkrankungen des Gehirns und der Netzhaut haben könnten.

Das Translokatorprotein (18 kDa) (TSPO) ist ein mitochondriales Protein, welches in reaktiven Gliazellen exprimiert ist, als Gliosemarker im Gehirn fungiert und bisher noch nicht im retinalen Kontext untersucht wurde. Verschiedene TSPO Liganden reduzieren Neuroinflammation in neurodegenerativen Mausmodellen. Wir konnten eine starke Hochregulation der TSPO Transkript- und Proteinlevels in reaktiven Mikrogliazellen *in vitro*, Mikroglia des Retinoschisin-defizienten Mausmodells sowie TSPO Expression in Mikroglia der humanen Netzhaut nachweisen. TSPO ist auf mRNA Ebene stark in der sich entwickelnden Mausnetzhaut exprimiert und sinkt auf ein niedrigeres Niveau im adulten Gewebe. Der synthetische TSPO Ligand XBD173 verringert effektiv die proinflammatorische mikrogliale Genexpression, Migration, Proliferation, Stickstoffoxid-Sekretion und Neurotoxizität gegenüber Photorezeptorzellen *in vitro*. Außerdem induziert XBD173 die Bildung mikroglialer Filopodien und erhöht die phagozytische Aufnahmefähigkeit von Latexkügelchen und apoptotischem Photorezeptordebris durch murine und humane Mikrogliazellen *in vitro*. Weiterhin reduziert XBD173-Behandlung effektiv die Zahl amöboider, alarmierter Mikrogliazellen in LPS-stimulierten organotypischen Netzhautexplantatkulturen. Schlussfolgernd konnten wir TSPO als neuartigen Marker der Mikrogliaaktivierung in der Netzhaut und potentielle therapeutische Zielstruktur zur Reduktion chronischer Neuroinflammation während Netzhautdegeneration identifizieren.

Zusammenfassend ermöglichen unsere Untersuchungen zum neuartigen Photorezeptor-Genregulator SAMD7 und den mikroglialen Reaktivitätsmarkern AMWAP und TSPO einen Einblick in mögliche Pathomechanismen retinaler Degeneration und offenbaren Möglichkeiten zur Identifizierung und therapeutischen Modulation pro-inflammatorischer Mikrogliaaktivität in degenerativen Erkrankungen des ZNS und der Netzhaut.

# 1. Introduction

## 1.1 Structure and function of the mammalian retina

Visual perception represents one of our most important senses and enables us to experience our environment in a remarkable fashion and detail. The complex mechanisms underlying the transformation of light into visual stimuli have fascinated humans for centuries. Electromagnetic rays between 400-750 nm wavelengths are recognizable to humans as visible light, and the tissue crucial for this process is the retina with its different cellular layers. In opposition to the peripheral sensory organs, the retina is a direct component of the central nervous system (CNS), as it developmentally represents an evagination of the diencephalon.

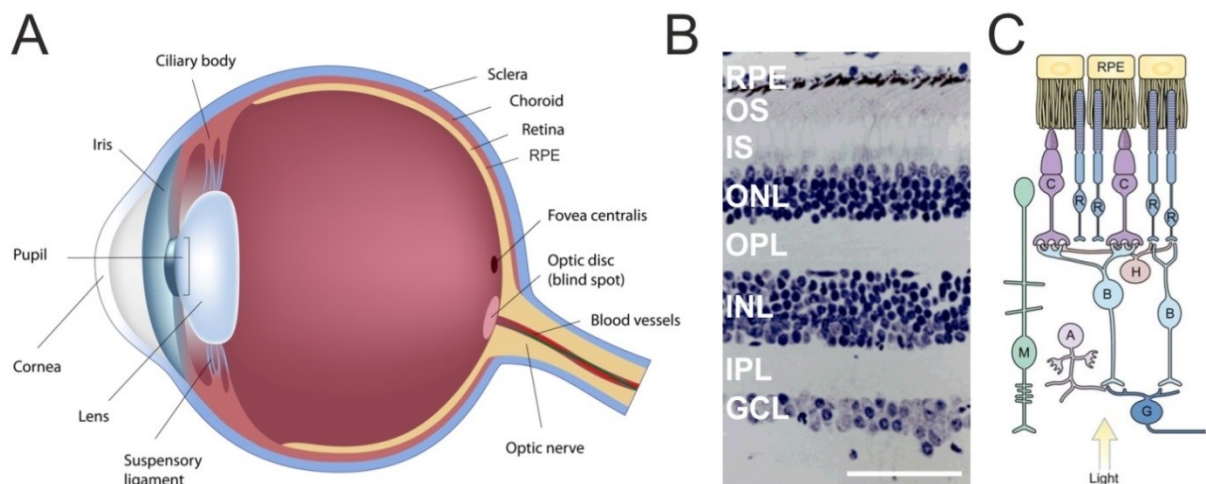


**Figure 1: Gross anatomy of the eyeball and detailed cross-section of the retina and its different cell types.**

(A) The retina lines the posterior segment of the eyeball and lies adjacent on top of the retinal pigment epithelium (RPE). (B) Histological cross-section of the retina depicting its different cell layers. GCL, ganglion cell layer; IPL, inner plexiform layer; INL, inner nuclear layer; OPL, outer plexiform layer; ONL, outer nuclear layer; IS, photoreceptor inner segment; OS, photoreceptor outer segment; RPE, retinal pigment epithelium. (C) Schematic overview of the different cell types within the retinal layers. G, ganglion cell; A, amacrine cell; B, bipolar cell; H, horizontal cell; M, Müller cell; R, rod photoreceptor; C, cone photoreceptor; RPE, retinal pigment epithelium. (Eyeball modified from <http://www.garetina.com/about-the-eye>, retinal cross section modified from <http://www.oculist.net/downaton502/prof/ebook/duanes/pages/v8/v8c013.html>, schematic section adapted from Sung and Chuang, 2010).

Within the eye, the retina lies directly adjacent on top of the retinal pigment epithelium (RPE) (Fig. 1 A), which has important housekeeping functions like vitamin A metabolism, heat regulation and constant shedding of photoreceptor outer segments containing the visual pigment (opsins) through phagocytosis. Further, the

RPE functions as outer blood retinal barrier, ensuring that only molecules below a certain size translocate from the choroidea into the neuroretina. The choroidea serves as a key structure for supporting blood vessels, and the sclera, as the outermost layer of the eye, provides stability and is attached to the ocular muscles. In spite of being only ~200  $\mu\text{m}$  thick, the retina consists of three distinct cellular layers, harboring many different cell classes (Fig. 1 B, C) (Klinke et al., 2003). The innermost layer consists of ganglion cells (GCs), whose axons converge to form the optic nerve and transmit visual signals to the brain. Adjacent layers are the inner nuclear layer (INL), consisting of amacrine, bipolar and horizontal cells, preprocessing visual signals and increasing contrast. After passing through these layers, light reaches the outer nuclear layer (ONL), which harbors the cell bodies of photoreceptors. There are two distinct types of photoreceptors: cones and rods. The human retina harbors around 130 million photoreceptors, of which 95% represent rods (Sung and Chuang, 2010). Cones are responsible for high resolution color vision and the perception of objects in bright light conditions (photopic vision), whereas rods are responsible for perception in dim light conditions and night vision (scotopic vision) (Baylor et al., 1979, Klinke et al., 2003).

Absorption of photons by opsins in the photoreceptor outer segment (OS) leads to isomerization of 11-cis retinal to all-trans retinal and triggers the phototransduction cascade including hyperpolarization of photoreceptor cell membranes. The signal is then transmitted to the neurons of the INL and finally reaches the ganglion cells, which possess long axons that unite at the so-called “blind spot”, which is devoid of photoreceptors and where the optic nerve exits the eyeball. Roughly 3.5 mm distant lies the fovea centralis (in the center of the macula), which is comprised solely of cones and represents the area enabling sharp central vision within the retina. In the fovea, each cone cell is connected to a single bipolar and ganglion cell, enabling particularly focused vision in this area compared to the peripheral retina. Mueller cells represent one out of three glial cell moieties in the retina (Mueller glia, astroglia and microglia). They serve as support cells for retinal neurons and span throughout all retinal layers. In recent years, an additional function of Mueller cells as optic fibers facilitating the transmission of light through the retina towards the photoreceptors has been described (Reichenbach and Bringmann, 2013).

The retina is devoid of pain receptors, therefore neuroretinal diseases remain largely pain-free and impairment of visual perception should be monitored and examined thoroughly. One of the main causes of impaired vision in inherited retinal degenerations is the irreversible loss of photoreceptors due to retinal damage or mutations in photoreceptor-specific genes leading to apoptosis (Rattner et al., 1999).

The murine retina is to a large extent structurally similar to the human retina, there are however certain distinctions to be considered. Around 75% of the murine retina account for photoreceptors, of which 97% are rods. Mice almost exclusively rely on rod-mediated scotopic vision and, in contrast to humans (red, green and blue), are only equipped with two types of cones for either short or middle-to-long wavelengths of light (Morrow et al., 1998). Most importantly, the murine retina does not harbor a macula or fovea.

## **1.2 Retinal genetics**

### **1.2.1 Inherited retinal degenerations**

Since the retina is comprised of a complex network of highly specialized cells, it is highly susceptible to genetic defects leading to hereditary retinal dystrophies, a major cause of legal blindness worldwide. To date, the Retnet database (<https://sph.uth.edu/retnet/> as of July 28<sup>th</sup> 2015) lists a total of 278 genes and loci linked with retinal degenerations. 64 of these genes are causative for the most frequent monogenic group of disorders, retinitis pigmentosa (RP). On the other hand, the leading cause of legal blindness in the elderly of industrialized nations today is age-related macular degeneration (AMD), a complex genetic disease. In contrast to RP, a multitude of genetic risk variants as well as environmental risk factors contribute to the development of AMD and ultimately loss of vision (Jager et al., 2008, Chen et al., 2010).

Various animal models have been generated over the last decades, mimicking hereditary retinal degenerative diseases like retinitis pigmentosa (Rivas and Vecino, 2009). X-linked juvenile retinoschisis is another retinal dystrophy affecting patients as early as in their adolescence. Retinoschisin-deficient ( $Rs1h^{-Y}$ ) mice show an early splitting (schisis) of the inner retinal layers followed by photoreceptor degeneration

(Weber et al., 2002). Although a plethora of different cellular malfunctions can be the underlying cause for monogenic or complex inherited retinal degeneration, photoreceptor apoptosis represents a common hallmark of all retinal dystrophies during disease progression (Portera-Cailliau et al., 1994, Sancho-Pelluz et al., 2008). Within the large group of causative genes, defects in retina-specific genes and master transcription factors are frequently associated with inherited retinal dystrophies (Rattner et al., 1999, Tran and Chen, 2014). Photoreceptors are highly specialized cells with a multitude of intracellular components and functions and therefore highly prone to various genetic malfunctions, ultimately leading to photoreceptor degeneration (Bramall et al., 2010). High transcript levels of a gene in photoreceptors and a dysfunction of the corresponding protein are tightly associated with retinal degeneration, indicating that knowledge about abundantly expressed photoreceptor-specific genes, transcription factors and their regulation may help to identify novel retinal disease genes (Blackshaw et al., 2001, Wagner et al., 2013).

### **1.2.2 Regulation of photoreceptor development**

Photoreceptors have a bridging function between our environment and central nervous system as they transform light into visual signals within the retina. The development of retinal progenitor cells into differentiated, fully functional photoreceptors is orchestrated by many regulatory events like expression of transcription factors, their target genes and cis-regulatory elements that mediate their interaction (Hsiau et al., 2007).

During early retinal development, expression of the transcription factor OTX2 (orthodenticle homeobox 2) in retinal progenitor cells directs them towards a photoreceptor cell fate (Nishida et al., 2003). 12.5 days into the mouse embryonal stage (E12.5) OTX2 induces expression of another photoreceptor-specific key transcription factor, CRX (cone rod homeobox), in the developing rods and cones (Furukawa et al., 1997). From then on, CRX is highly expressed in developing and mature photoreceptors indicating its important role in photoreceptor function and homeostasis. Additionally, CRX interacts with a variety of other transcription factors to influence photoreceptor development and function (Fig. 2). CRX orchestrates this network of transcription factors, which regulates whether a progenitor develops into a rod or cone photoreceptor. TRB2 (thyroid hormone receptor  $\beta$ 2) and RORB (retinoid-

related orphan receptor  $\beta$ ) are crucial factors towards a cone cell fate (Yanagi et al., 2002, Srinivas et al., 2006), whereas NRL (neural retina leucine zipper) and NR2E3 (nuclear receptor subfamily 2, group E, member 3) are important mediators of a rod cell fate and predominantly expressed in rods (Mears et al., 2001, Milam et al., 2002).

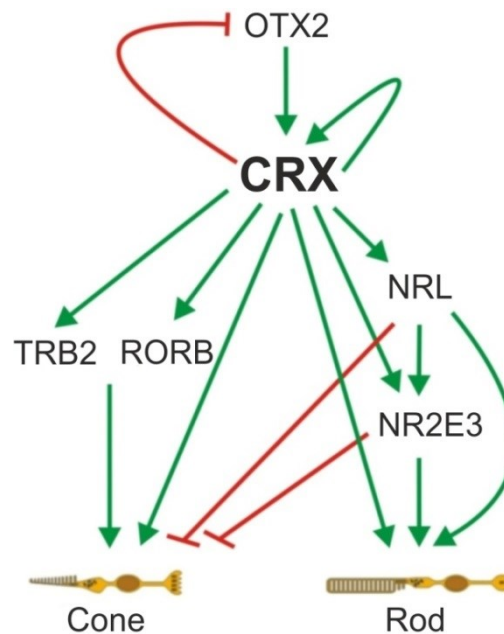


**Figure 2: The transcriptional network of photoreceptor development.** The key transcription factor CRX is induced by OTX2, represses OTX2 and regulates its own expression. CRX further activates a variety of transcription factors important for either a cone or rod photoreceptor cell fate. Activatory (green) and repressory (red) influences are depicted as arrows. (Modified from Hsiau et al., 2007).

This is in line with the observation that NRL- and NR2E3-mutant mice exhibit a significant transformation of rods into cones or cone-like photoreceptors (Mears et al., 2001, Corbo and Cepko, 2005). CRX interacts synergistically with NRL in mature photoreceptors to regulate the expression of rod-specific genes like rhodopsin (Mitton et al., 2000). Among the above described, a multitude of additional transcription factors play subordinate roles in photoreceptor development (Hsiau et al., 2007). It is however fair to say that the beforementioned factors, majorly orchestrated by CRX, play the central part (Hennig et al., 2008).

Severe retinal diseases like cone-rod dystrophy or Leber's congenital amaurosis are caused by mutations in the human CRX gene (Freund et al., 1997, Freund et al., 1998, Sohocki et al., 1998), while NRL mutations have been associated with retinitis pigmentosa (Bessant et al., 1999). CRX overexpression leads to a disproportionately

high number of rods and CRX-mutant mice develop photoreceptors lacking outer segments and are therefore devoid of visual function (Furukawa et al., 1999).

### **1.2.3 Genome-wide identification of CRX target genes**

In a genome-wide approach to identify potential novel photoreceptor-specific genes including potential disease genes using CRX chromatin immunoprecipitation coupled with massively parallel sequencing (CRX ChIP-seq), we could previously identify 5,595 CRX-bound regions (CBRs) in the regulatory regions of murine photoreceptor genes (Corbo et al., 2010). These CBRs show high phylogenetic conservation, indicating their functional importance in photoreceptor gene regulation (Visel et al., 2007). After mapping those target genes to their human orthologues, a total of 724 CRX-regulated genes, containing a large number of confirmed retinal disease genes, could be identified. Employing this dataset, two novel retinitis pigmentosa genes, FAM161A and MAK could already be identified (Langmann et al., 2010, Ozgul et al., 2011) and a recently generated mouse model showing severe FAM161A-associated retinal ciliopathy confirmed its role in photoreceptor degeneration (Karlstetter et al., 2014b). Moreover, the gene causative for cone dystrophy with supernormal rod response (CDSRR), KCNV2, was also identified to be highly CRX-regulated which we could previously confirm employing electroporation reporter assays in living mouse retinas (Aslanidis et al., 2014).

Interestingly, among the most prominently CRX-bound genes not only known disease genes, but also genes that have not been investigated in a retinal context so far, were identified. One prominent example of such a gene was sterile alpha motif containing 7 (SAMD7). Out of all identified CRX target genes, SAMD7 shows the highest CRX binding affinity towards its two single CBRs in the promoter region and the first intron, respectively. CRX ChIP-seq of *NRL*<sup>-/-</sup> retinas still revealed SAMD7 to be highly CRX-bound, indicating that SAMD7 is expressed in both rods and cones, since *NRL*-deficient mice are largely cone-enriched. Additionally, a recent genome-wide *NRL* ChIP-seq study confirmed binding of *NRL* at the above mentioned SAMD7 cis-regulatory elements (Hao et al., 2012). Further, another ChIP-on-Chip study has shown that the promoter region and first intron of SAMD7 are actively bound by RNA-polymerase II and are thus active transcription start sites in the adult retina (Tummala et al., 2010). These findings on SAMD7 as a novel heavily CRX- and *NRL*-regulated

gene in photoreceptors prompted us to take a closer look into its expression, regulation and function in the retina.

#### **1.2.4 Sterile alpha motif containing proteins and SAMD7**

Sterile alpha motif (SAM) domains are ~70 amino acid long protein-protein interaction domains present in a variety of proteins of different function (Qiao and Bowie, 2005). Their initial identification and role in yeast and drosophila fertility together with their proposed  $\alpha$ -helical structure coined their nomenclature (Ponting, 1995). Around 1,000 proteins containing SAM domains are found in eukaryotes and some bacteria. However, no common functional theme exists for SAM domains (Kim and Bowie, 2003). These proteins can self-assemble via their SAM domain to build functional complexes as well as bind to many other proteins lacking a SAM domain (Kim and Bowie, 2003). SAM domain proteins can therefore fulfil a multitude of functions like acting as kinases (Tu et al., 1997), regulatory enzymes (Harada et al., 2008), scaffolding proteins (Baron et al., 2006), RNA-binding proteins (Aviv et al., 2003) and transcriptional regulators (Slupsky et al., 1998).

Little is known about the role of SAM domain proteins in a retinal context. The SAM domain containing ETS transcription factor Yan acts as a negative regulator of photoreceptor development in drosophila (Lai and Rubin, 1992) and recently the first SAM domain protein exclusively expressed in mouse photoreceptors and the pineal gland, Mr-s alias SAMD11 was identified. SAMD11 is CRX-regulated and functions as a repressor of CRX-mediated photoreceptor gene expression (Inoue et al., 2006). Interestingly, *in situ* hybridization experiments describe high SAMD7 transcript levels in the developing and adult mouse retina (Blackshaw et al., 2001). The emerging role of SAM domain proteins in retinal photoreceptors, together with the identification of SAMD7 as a highly CRX-regulated gene via CRX ChIP-seq therefore make SAMD7 a promising gene with potentially important function in photoreceptor development and homeostasis. Indeed, we could recently show that SAMD7 acts as a CRX-regulated repressor of CRX-mediated photoreceptor gene expression in the retina (Hlawatsch et al., 2013).

## **1.3 Microglia**

### **1.3.1 Microglia in the CNS and retina**

Microglial cells are the resident macrophages of the CNS, including the retina, and play pivotal roles in innate immune responses and regulation of homeostasis in the healthy and degenerating CNS (Hanisch and Kettenmann, 2007, Streit, 2002). Initially observed by Rio-Hortega as distinct cells with long cellular processes within the brain parenchyma, he hypothesized that microglia are mobile, macrophage-like cells playing a role in inflammatory nerve tissue (Rio-Hortega, 1939). This hypothesis was later confirmed by showing that microglia are indeed bone marrow-derived immune-competent cells of the CNS (Hickey and Kimura, 1988). It is now an established concept that microglia play important roles in the maintenance of the healthy and degenerating CNS in various neurodegenerative diseases (Hanisch and Kettenmann, 2007, Heneka et al., 2014). In contrast to macrophages, which are derived from postnatal hematopoietic progenitors, microglia originate from myeloid precursor cells in the yolk sac during early embryogenesis and populate their respective resident tissues in the CNS before formation of the blood-brain and blood-retina barrier (Ginhoux et al., 2010, Ginhoux and Jung, 2014). Under healthy homeostatic conditions, microglia exhibit a ramified morphology with small somata and long cellular protrusions, actively scanning their microenvironment for changes or injuries in the neuronal tissue (Raivich, 2005). These protrusions are highly motile to ensure complete monitoring of the brain parenchyma every few hours (Nimmerjahn et al., 2005). In the healthy retina, microglia reside in the inner and outer plexiform layers with their small cell bodies, branching their long protrusions into the nuclear layers actively surveying the retinal microenvironment (Hume et al., 1983, Langmann, 2007, Karlstetter et al., 2015).

### **1.3.2 Functions of microglia**

Microglia carry out a multitude of physiological functions in the developing and adult CNS such as regulating apoptosis of specific subpopulations of developing neurons, synaptic pruning, modeling and regulation of synaptic plasticity (Marin-Teva et al., 2004, Coull et al., 2005, Casano and Peri, 2015, Salter and Beggs, 2014). In contrast to other neuroglia, microglial cells keep their distance to one another with each single

cell surveying its individual territory. It is therefore likely that microglia signal through auto- and paracrine mechanisms. Neuron-microglia crosstalk takes place through various ligands, receptors, neurotransmitters and neurotrophins (Biber et al., 2007, Pocock and Kettenmann, 2007, Vecino et al., 2015). As an example, two well characterized ligands, CD200 (cluster of differentiation 200) and CX3CL1 (CX3C chemokine ligand 1, alias fractalkine) find their corresponding receptors expressed on microglia (Hoek et al., 2000, Cardona et al., 2006). Signaling between those ligands and receptors leads to an immunosuppression of microglia, preventing them from becoming reactive as well as maintaining their homeostatic regulatory state. In addition, these ligands affect microglial migration and ramification movements, contributing to the effective monitoring function of microglia (Cardona et al., 2006). Another example is the exposition of glycocalyx components on the surface of healthy neurons, which microglia recognize via specific Siglec (sialic acid-binding immunoglobulin like lectins) receptors (Linnartz-Gerlach et al., 2014). Upon ligand binding, Siglecs signal through an immunoreceptor tyrosine-based inhibition motif (ITIM) to keep the microglial cell in a regulatory homeostatic state (Wang and Neumann, 2010, Claude et al., 2013). However, in early neuronal damage, loss of these glycocalyx components leads to rapid complement-mediated pro-inflammatory activation of microglia through an immunoreceptor tyrosine-based activation motif (ITAM).

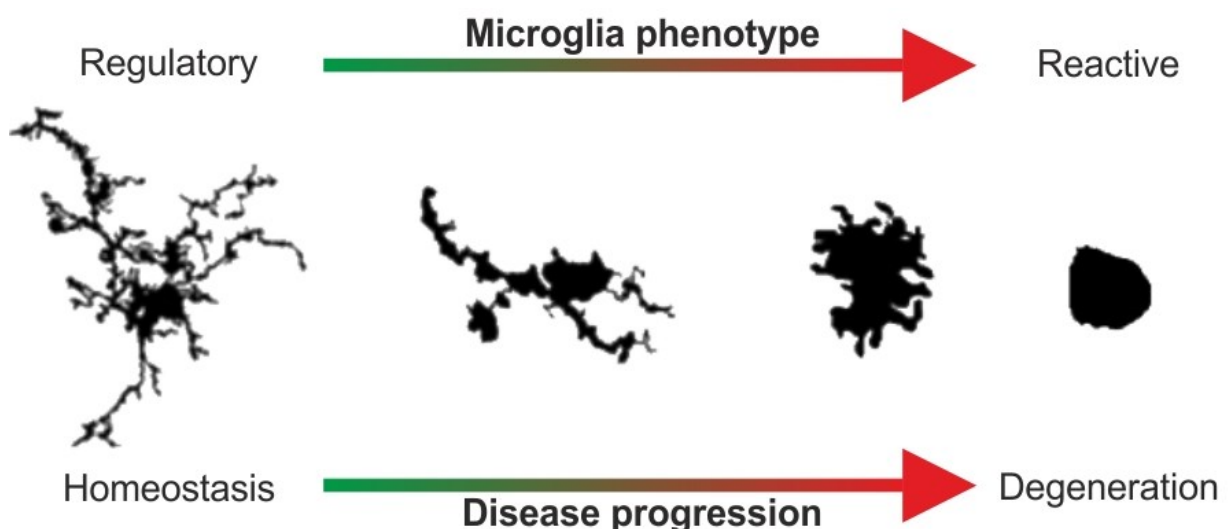


**Figure 3: Phenotypic plasticity of microglia in the healthy and diseased CNS.** Under homeostatic conditions (left), microglia exhibit small somata with long, branched protrusions to actively scan their microenvironment and carry out tissue maintenance tasks. During degenerative processes in the CNS, microglia are early sensors of perturbed tissue homeostasis and undergo a gradual morphological transition (middle) towards amoeboid pro-inflammatory reactive phagocytes (right). (microglia drawings modified from Karperien et al. (2013)).

Upon recognition of disturbed or insulted tissue integrity, microglia undergo morphological changes, retracting their cellular protrusions and adopting an amoeboid reactive phenotype (Fig. 3) (Hanisch and Kettenmann, 2007). These microglial activation cues include damage-associated molecular patterns (DAMPs) released from neurons, which are recognized by microglia and lead to toll-like receptor (TLR)-mediated pro-inflammatory microglial reactivity (Gao et al., 2011). Upon activation, these amoeboid microglia actively migrate towards the lesion site where they proliferate, phagocytose apoptotic cells and secrete pro-inflammatory cytokines and chemokines like IL6 (interleukin 6), TNF $\alpha$  (tumor necrosis factor  $\alpha$ ) or CCL2 (chemokine (C-C motif) ligand 2) (Banati et al., 1993). Further, they actively secrete reactive oxygen species (ROS) and nitric oxide (NO) (Minghetti and Levi, 1998, Agostinho et al., 2010). Microglia represent the first line of damage response, as microglial reactivity occurs very early in response to tissue damage, often preceding physiological reactions of any other cell type, like apoptosis (Gehrmann et al., 1995). Only minutes after injury, microglia polarize their processes towards the lesion site and initiate the inflammatory response (Nimmerjahn et al., 2005). Once the pro-inflammatory stimulus has resolved, microglia will return to their regulatory state. However, in the case of prolonged insult or neurodegenerative disease, these mechanisms may become dysregulated, leading to chronic neuroinflammation which can have neurotoxic and detrimental effects including microglial phagocytosis of still viable neurons (Block et al., 2007, Brown and Neher, 2014, Zhao et al., 2015). The contribution of this reactive microgliosis is nowadays recognized to play a role in various neurodegenerative diseases including Alzheimer's disease, Parkinson's disease, multiple sclerosis, inherited retinal degenerations and several other retinal diseases (Perry et al., 2010, Orr et al., 2002, Raivich and Banati, 2004, Langmann, 2007, Karlstetter et al., 2015).

### **1.3.3 Microglia in retinal degeneration**

As the retina is part of the CNS, microglia also exert their physiological and immunoregulatory functions in this tissue. Regardless of the underlying genetic defect or source of retinal injury, pro-inflammatory microglial reactivity is an early hallmark and active contributor in retinal degeneration (Thanos, 1991, Langmann, 2007, Karlstetter et al., 2015). At early stages of disease progression in various

retinal degeneration models, reactive retinal microglia retract their cellular protrusions and migrate from the plexiform layers to the areas of tissue damage, e.g. the outer nuclear layer (ONL) containing photoreceptors, where they act as pro-inflammatory phagocytes as mentioned above (Fig. 4) (Zeiss and Johnson, 2004, Combadiere et al., 2007, Cuenca et al., 2014).

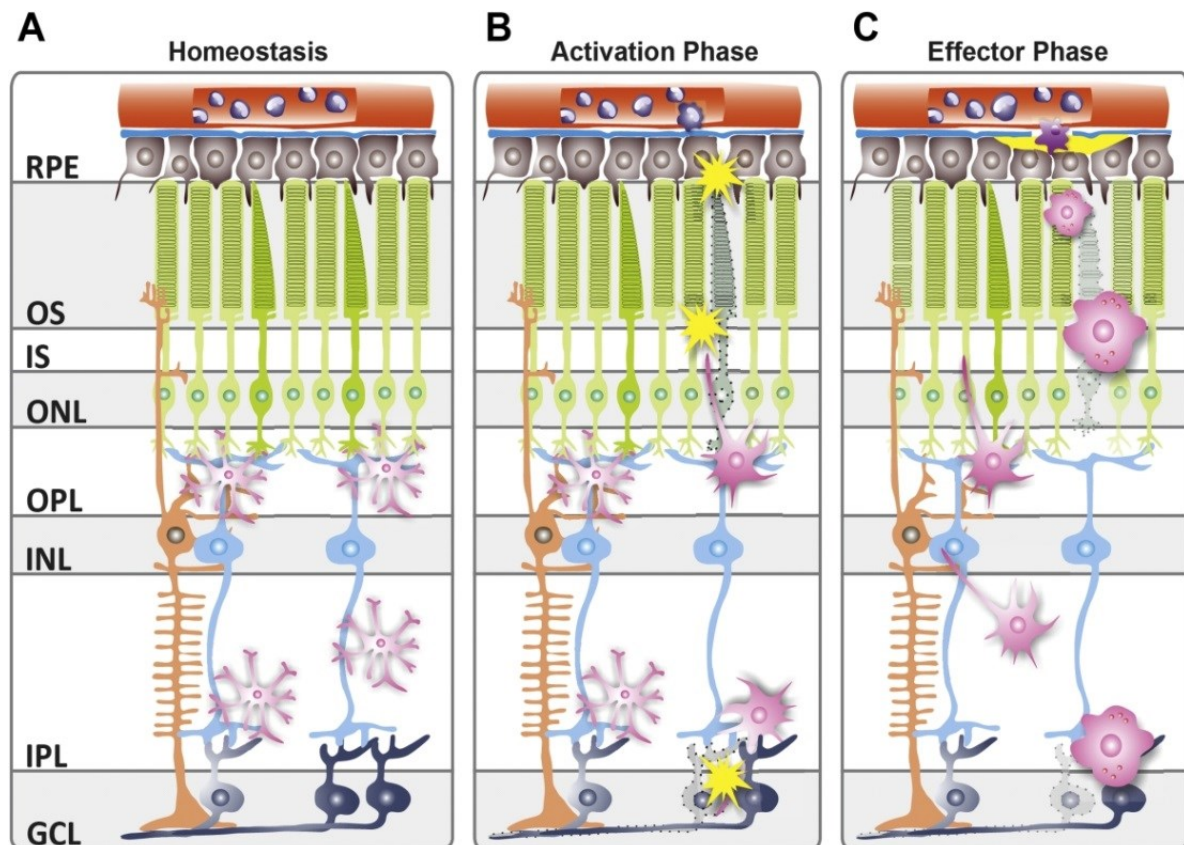


**Figure 4: Schematic overview of microglial distribution and behavior in retinal health and disease. (A)** In the healthy retina, microglia reside in the plexiform layers, actively scanning their microenvironment with their long protrusions (simplified depiction), phagocytosing insoluble metabolites and cellular debris. **(B)** Upon sensing tissue damage, microglia get alarmed, retract their protrusions and migrate into the sites of lesion, where they become full-blown pro-inflammatory phagocytes **(C)**, phagocytosing apoptotic cells, secreting cytokines, chemokines and neurotoxic radicals. GCL, ganglion cell layer; IPL, inner plexiform layer; INL, inner nuclear layer; OPL, outer plexiform layer; ONL, outer nuclear layer; IS, inner segment; OS, outer segment; RPE, retinal pigment epithelium. (Karlstetter et al., 2015).

In the PDE6B (phosphodiesterase 6b)-deficient rd1 and rd10 mouse models, which exhibit strong photoreceptor degeneration, a significant number of reactive microglial cells is found in the outer nuclear layer secreting high amounts of the pro-inflammatory mediators TNF $\alpha$ , CCL2 and CCL5 (Zeng et al., 2005, Yoshida et al., 2013). Further, a recent study has shown that phagocytosis of living photoreceptors by reactive microglia contributes to disease progression in the rd10 mouse model

(Zhao et al., 2015). In the murine model of X-linked juvenile retinoschisis (Weber et al., 2002), an early transformation of microglia into reactive phagocytes, even before retinal neurons undergo apoptosis, is observed (Gehrig et al., 2007, Ebert et al., 2009). These microglial cells show elevated pro-inflammatory transcript expression days before neuronal cell death is observable. We recently described a novel model of FAM161A-associated photoreceptor ciliopathy, which also exhibits strong microgliosis accompanied by pro-inflammatory microglial gene expression in the ONL during disease progression which seems to partially resolve after most photoreceptors are lost in late disease stages (Karlstetter et al., 2014b). These findings indicate that microglial reactivity is a key event in the onset and progression of retinal degeneration.

There is now ample evidence that inflammation and microglia also play important roles in the onset and disease progression of AMD (Newman et al., 2012, Penfold et al., 2001). In accordance, in post mortem retinas from human AMD and RP patients, the presence of reactive microglia bearing phagocytosed apoptotic photoreceptor debris was confirmed in the ONL (Gupta et al., 2003). Since mice harbor no macula and no archetypical murine AMD model exists to this date, most AMD models focus on mimicking single pathological features of the disease like deposition of drusen, RPE damage or choroidal neovascularization leading to photoreceptor degeneration. In a model of geographic atrophy, which accumulates drusen-like deposits in the RPE, reactive phagocytes including microglia accumulate in the outer retina by a CCR2 (C-C chemokine receptor type 2)-dependent recruiting mechanism (Hollyfield et al., 2010, Cruz-Guilloty et al., 2013). Another strategy of mimicking photo-oxidative damage and retinal degeneration present in AMD is irradiation with focused blue or intense white light. Blue light-damaged retinas show a high focal accumulation of blood-derived macrophages and reactive retinal microglia, and transcriptomic analyses confirm the strong inflammatory response of these cells as early as a few hours after light damage (Joly et al., 2009, Ebert et al., 2012). Similar observations have been made for microglia in the white light damage model which shows early CCL2-mediated chemotaxis of reactive microglia to the outer nuclear layer (Santos et al., 2010, Suzuki et al., 2012). In recent years, animal models mimicking the wet form of AMD including choroidal neovascularization (CNV), employing local rupture of the Bruch's membrane through laser coagulation have proven to be successful (Lambert et al., 2013). In this model, reactive microglia are recruited to the lesion site within

four hours and peak numbers of reactive phagocytes are found in the subretinal space two days after laser damage, long before CNV can be observed (Eter et al., 2008, Liu et al., 2013).

These findings indicate the key role of microglia and inflammatory processes during early pathogenesis and disease progression of monogenic inherited retinal degenerations as well as complex retinal diseases like AMD.

### **1.3.4 Microglial (reactivity) markers**

With microglia playing a key role in the onset and progression of neurodegenerative diseases of the CNS and retina, there is a high interest in discovering microglia-specific markers to allow for their identification and discrimination between regulatory and reactive microglia. Lacking microglia-specific candidates, for decades classical macrophage markers like F4/80, CD68 and CD11b were employed to identify microglia in the brain and retina (Hume et al., 1983, Xu et al., 2007). In recent years, however, IBA1 (ionized calcium-binding adapter molecule 1) has emerged as the most reliable and widely used target structure for immunohistochemical detection of microglia in the CNS and retina (Ito et al., 1998, Ohsawa et al., 2000).

Transgenic mice harboring GFP (green fluorescent protein)-positive macrophages and microglia are also widely used to simplify recognition of microglia in the immune-privileged CNS, which is devoid of macrophages under healthy conditions. The CX3CR1-GFP knock-in mouse is a widely used example, where all myeloid cells express GFP under control of the cell type-specific CX3CR1 promoter on one of their CX3CR1 gene copies (Jung et al., 2000). This model has enabled *in vivo* and live-imaging of microglial distribution, dynamics and behavior in the healthy and degenerating retina (Eter et al., 2008, Lee et al., 2008, Liang et al., 2009). Another microglial reporter animal model is the MacGreen mouse. In comparison to the CX3CR1-GFP knock-in mouse, this model has the advantage of not replacing a functional locus and therefore homozygous mice with potentially stronger GFP expression can be used without altering microglial behavior (Sasmono et al., 2003). GFP is expressed under the control of the macrophage-specific c-fms (colony stimulating factor 1 receptor) promoter and GFP signals in the healthy and

degenerating retina overlap nicely with classical immunohistochemical markers IBA1 and F4/80 (Fig. 5) (Ebert et al., 2009).

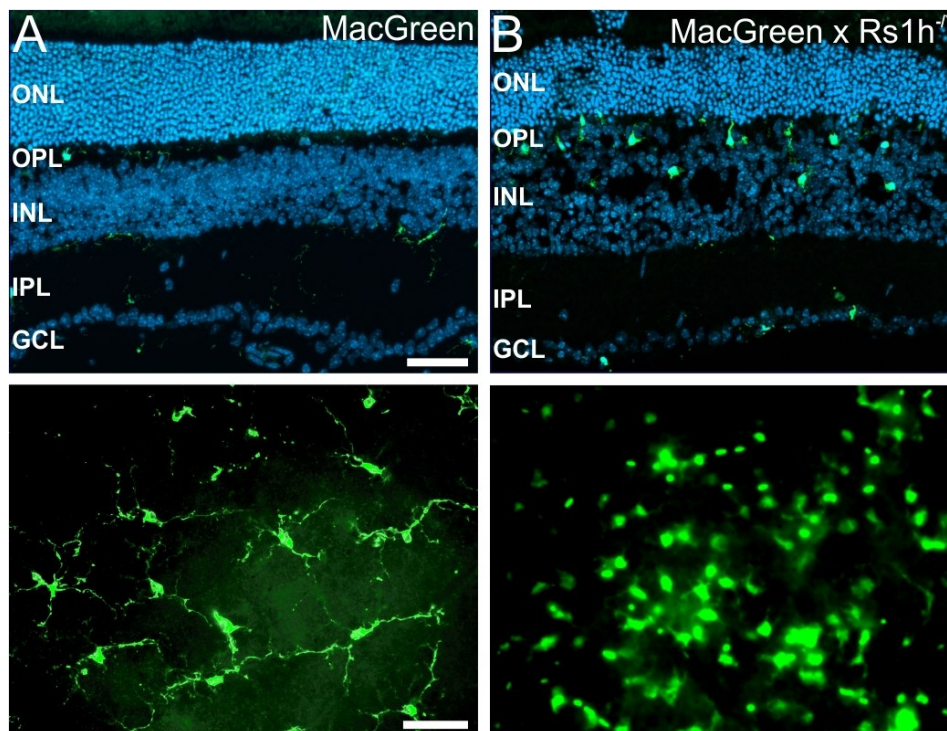


**Figure 5: Microglial reactivity in the retinoschisin-deficient ( $Rs1h^{-/-}$ ) mouse retina. (A)** In the healthy MacGreen GFP reporter mouse, microglia reside in the plexiform layers, exhibit small somata with long cellular protrusions (top) and populate the retina in an evenly distributed fashion as shown in retinal flat mount microscopy (bottom). **(B)** In the dystrophic retina, microglia adopt an amoeboid phenotype, lose their even distribution and migrate into the site of retinal damage, in this model an early splitting (schisis) of the inner nuclear layer, where they act as pro-inflammatory phagocytes. Scale bar, 50  $\mu$ m. (Flat mount pictures modified from Ebert et. al, 2009).

Reactive microglia express and secrete a plethora of molecules including classical pro-inflammatory mediators like IL1, IL6 and TNF $\alpha$  (Banati et al., 1993, Perry et al., 2010). This response is largely triggered by pro-inflammatory cytokines like IFN $\gamma$  (interferon  $\gamma$ ), TNFs or pathogen-associated molecular patterns (PAMPs) like bacterial lipopolysaccharide (LPS) and leads to a classical activation of microglia towards an aggressive M1-like macrophage phenotype (Laskin, 2009). However, alternative activation of microglia through IL10 or TGF $\beta$  (transforming growth factor  $\beta$ ) towards an M2-like phenotype is associated with resolution of inflammation, reduced pro-inflammatory gene expression and increased expression of neurotrophic factors, a phenotype more favorable during neurodegenerative diseases (Duffield, 2003, Cherry et al., 2014). Knowledge about microglial reactivity markers and their function is therefore crucial for understanding their individual role in degenerative diseases of the CNS and retina.

Employing genome-wide expression profiling of microglia from the  $Rs1h^{-Y}$  mouse retina, we could recently identify activated microglia/macrophage whey acidic protein (AMWAP, alias WFDC17, Gm11428) as a novel marker for microglial reactivity, counter-regulating their inflammatory response and thereby serving as a feedback-loop mechanism to help attenuate pro-inflammatory microgliosis (Gehrig et al., 2007, Karlstetter et al., 2010, Aslanidis et al., 2015). We could also show induction of AMWAP gene expression in the FAM161A-deficient retinal ciliopathy mouse model, congruent with the course and severity of observed microgliosis (Karlstetter et al., 2014b). In addition, in a recent study we also observed elevated AMWAP transcript levels in the retina of the acid sphingomyelinase (aSMase)-deficient mouse model of impaired retinal function and reactive microgliosis (Dannhausen et al., 2015). Interestingly, transcriptomic profiling using microarray analysis of isolated microglia previously also reported a strong upregulation of the back then uncharacterized AMWAP transcript (Gm11428) in reactive microglia in a mouse model of severe neuronal impairment (Huyghe et al., 2006).

Further, we and others could show that reactive retinal microglia from  $Rs1h^{-Y}$  and aSMase-deficient mice as well as *in vitro* exhibit strong upregulation of the mitochondrial translocator protein (18 kDa) (TSPO) (Karlstetter et al., 2014a, Dannhausen et al., 2015, Wang et al., 2014b). These are the first reports of TSPO as a microglia reactivity marker and potential therapeutic target in the retina, while TSPO has already been implicated to play a role in neuroinflammation of the brain and CNS (Girard et al., 2012, Chen and Guilarte, 2008).

These novel microgliosis markers now serve as assessment tools to evaluate microglial reactivity in the retina and are subject of further investigation to elucidate their function and employ them as potential mediators of anti-inflammatory immunotherapy.

### **1.3.5 Microglia as a therapeutic target**

Given the important and often detrimental role of chronic pro-inflammatory microglial reactivity in degenerative diseases of the CNS and retina, there is a growing interest in modulating microglia towards a regulatory, homeostatic phenotype in a therapeutic fashion (Schuetz and Thanos, 2004, Karlstetter et al., 2015). Various therapeutic

strategies have been investigated so far, including the use of natural compounds, endogenous microglial factors as well as synthetic immunoregulatory pharmaceuticals.

### **1.3.5.1 Natural compounds**

Curcumin, a major constituent of turmeric, has been used in Ayurvedic medicine for centuries and has broad anti-inflammatory properties (Ammon and Wahl, 1991). Curcumin treatment effectively reduces microglial NO secretion, pro-inflammatory cytokine expression and migration *in vitro* (Karlstetter et al., 2011). It further attenuates microglial reactivity via blockade of NFκB signaling and is neuroprotective in mouse models of intracerebral hemorrhage and traumatic brain injury (Yang et al., 2014, Zhu et al., 2014a). It was also shown to be protective in various retinal degeneration models, inhibiting microglial neurotoxicity and attenuating photoreceptor degeneration (Mirza et al., 2013, Gupta et al., 2011, Vasireddy et al., 2011).

Luteolin, another natural compound, is a flavonoid abundant in parsley, green pepper and celery. Luteolin acts anti-inflammatory through inhibition of pro-inflammatory NFκB and AP-1 signaling as well as acting as a radical scavenger (Jang et al., 2008, Chen et al., 2007). We could previously show that Luteolin triggers global changes in the microglial transcriptome inducing an anti-inflammatory, anti-oxidative and neuroprotective phenotype *in vitro* (Dirscherl et al., 2010). Luteolin further blocks pro-inflammatory NFκB activation and microglial neurotoxicity *in vitro* (Zhu et al., 2014b). Finally, Luteolin reduces the neurotoxicity of microglia cells on primary hippocampal neurons and enhances spatial working memory in aged mice by reducing microglia-mediated inflammation in the hippocampus (Zhu et al., 2011, Jang et al., 2010).

Docosahexaenoic acid (DHA) is a polyunsaturated fatty acid enriched in fish oil and is highly abundant in the retina as a precursor of neuroprotectin D1 (NPD1), which promotes the survival of RPE and photoreceptor cells (Bazan et al., 2010). DHA levels were shown to be decreased in various retinal degenerations and DHA is therefore regarded as a potential compound for beneficial dietary supplementation (Anderson et al., 2002, Schaefer et al., 1995). DHA reduces microglial reactivity through inhibition of NFκB signaling and confers neuroprotection in animal models of

spinal cord compression and experimental stroke (Wang et al., 2015, Lim et al., 2013, Eady et al., 2014). In the eye, DHA protects from microglia-mediated retinal degeneration in mouse models of X-linked juvenile retinoschisis and neuronal ceroid lipofuscinosis (NCL) (Ebert et al., 2009, Mirza et al., 2013).

### **1.3.5.2 Whey acidic proteins (WAPs) and AMWAP**

Whey acidic proteins (WAPs) are a group of secreted proteins carrying one or more WAP four-disulfide core (WFDC) domains, which comprise eight cysteines forming four disulfide bonds in a specific manner (Simpson and Nicholas, 2002). They are highly enriched at mucosal surfaces like the lung, oral cavity or colon and also expressed by neutrophils and macrophages. They fulfil a role as “alarmins”, since they are upregulated and actively secreted during tissue damage and inflammation (Bingle and Vyakarnam, 2008). They have a broad range of functions, including anti-microbial, anti-protease and anti-inflammatory potential in the respective tissues (Moreau et al., 2008). The best characterized WAPs are secretory leukocyte protease inhibitor (SLPI) and elafin (Scott et al., 2011). Both these WAPs serve as markers in inflammatory diseases of the lung and colon and have been shown to be beneficial for the resolution of inflammation (Tsoumakidou et al., 2010, Eriksson et al., 2008, Small et al., 2015, Marino et al., 2011, Reardon et al., 2011). Functionally, they can inhibit pro-inflammatory NF $\kappa$ B and AP-1 signaling in innate immune cells, restoring a regulatory protective phenotype (Greene et al., 2004, Butler et al., 2006, Taggart et al., 2005).

Over the last years, an emerging role of WAPs in the onset and resolution of neuroinflammation in the CNS has been proposed (Hannila, 2014). SLPI is upregulated in various CNS pathologies, including animal models of multiple sclerosis and stroke, as well as in amyotrophic lateral sclerosis (ALS) patients (Mueller et al., 2008, Wang et al., 2003, Lilo et al., 2013). In addition, SLPI was shown to be immunomodulatory and neuroprotective in models of optic nerve and spinal cord injury, multiple sclerosis and stroke (Hannila et al., 2013, Ghasemlou et al., 2010, Mueller et al., 2008, Wang et al., 2003). We have previously identified the novel activated microglia/macrophage whey acidic protein (AMWAP) as a highly upregulated molecule in microglia from Rs1h<sup>-Y</sup>, the FAM161A- and aSMase-deficient retina as well as reactive microglia and macrophages *in vitro* (Gehrig et al., 2007,

Karlstetter et al., 2010, Karlstetter et al., 2014b, Dannhausen et al., 2015). AMWAP is a 76 aa polypeptide containing a single WAP domain and a N-terminal signaling peptide for cellular export. AMWAP overexpression in cultured microglia reduces their pro-inflammatory gene expression, induces expression of alternative activation markers and reduces microglial migration, whereas RNAi-mediated AMWAP knock-down has adverse effects (Karlstetter et al., 2010). In addition, we could recently show that AMWAP is actively secreted from reactive microglia *in vitro* to counter-balance pro-inflammatory microglial activation through inhibition of NF $\kappa$ B signaling in a paracrine fashion (Aslanidis et al., 2015).

### **1.3.5.3 Translocator protein (18 kDa) (TSPO) and its ligands**

The translocator protein (18 kDa) (TSPO), formerly known as peripheral benzodiazepine receptor (PBR), is a transmembrane protein located in the outer mitochondrial membrane, highly expressed in steroidogenic cells of the adrenal gland, gonad and brain (Papadopoulos et al., 2006, Rupprecht et al., 2010). Within the CNS, TSPO is expressed predominantly in glial cells and to a lesser extent in certain neurons, e.g. of the olfactory bulb or dorsal root ganglia sensory neurons (Casellas et al., 2002, Zhang et al., 2007, Karchewski et al., 2004, Maeda et al., 2007). One of the main functions of TSPO is the cholesterol transport from the outer to the inner mitochondrial membrane, which is a crucial step in steroid hormone and neurosteroid synthesis (Papadopoulos et al., 2006). Additionally, TSPO plays a role in mitochondrial respiration and permeability, apoptosis and cell proliferation (Casellas et al., 2002, Maeda et al., 2007, Karchewski et al., 2004).

Over the last years, many studies have surfaced observing an upregulation of TSPO expression during CNS pathologies (Chen and Guilarte, 2008, Rupprecht et al., 2010). For example, TSPO expression was shown to be induced in Alzheimer's disease, Huntington's disease, Parkinson's disease as well as in psychiatric disorders like anxiety or post-traumatic stress disorder (Yasuno et al., 2008, Politis et al., 2012, Nakamura et al., 2002, Da Pozzo et al., 2012). In a retinal context, we and others could recently show microglial upregulation of TSPO in the Rs1h<sup>-Y</sup> mouse model of retinal degeneration, the aSMase-deficient retina as well as in an *in vivo* model of LPS-induced retinal microglia activation (Karlstetter et al., 2014a, Dannhausen et al., 2015, Wang et al., 2014b). The selective upregulation of TSPO in

microglia and astrocytes during CNS pathologies makes it a suitable biomarker to monitor the location, course and severity of neuroinflammatory processes. Therefore, TSPO serves as a target structure for neuroimaging procedures and specific TSPO ligands are employed as diagnostic tools e.g. for positron emission tomography (PET) (Chen and Guilarte, 2008).

Since TSPO is selectively upregulated in pathologies of the CNS, in recent years growing interest in the use of specific TSPO ligands as a strategy to attenuate neuroinflammation has emerged (Rupprecht et al., 2010, Nothdurfter et al., 2012). TSPO has a number of endogenous ligands like cholesterol, porphyrins or endozepines (Li and Papadopoulos, 1998, Gavish et al., 1992, Costa and Guidotti, 1991). Especially endozepines have been found to be highly produced during CNS inflammation, indicating that paracrine mechanisms of modulating glial reactivity through TSPO may exist. As an example, it was recently shown that Mueller cells and astrocytes express and secrete diazepam binding inhibitor (DBI) in the inflamed retina, which effectively reduces pro-inflammatory microglial cytokine expression and ROS secretion (Wang et al., 2014b).

These mechanisms raised the interest in developing highly specific synthetic TSPO ligands as therapeutic tools to attenuate neuroinflammation. The isoquinoline carboxamide derivative PK11195, used as a radioligand in PET studies and the benzodiazepine diazepam as a classic anxiolytic drug are prime examples for synthetic TSPO ligands (Venneti et al., 2013, Gavish et al., 1992). It was implicated that TSPO ligands can act therapeutically through induction of anti-inflammatory cytokine and neurotrophic factor expression in microglia and protective effects have already been shown for ALS, neuropathic pain, brain inflammation, depression and anxiety disorders (Bordet et al., 2007, Wei et al., 2013, Papadopoulos and Lecanu, 2009, Rupprecht et al., 2010). Further, TSPO ligands have been shown to reduce pro-inflammatory microglia reactivity and the production of pro-inflammatory cytokines in animal models of hippocampal and striatal brain damage (Veiga et al., 2005, Ryu et al., 2005). Novel synthetic ligands include etifoxine (Stresam<sup>®</sup>) and XBD173 (Emapunil<sup>®</sup>). Etifoxine reduces neuroinflammation and is protective and regenerative in a mouse model of multiple sclerosis (Daugherty et al., 2013). XBD173 is a phenylpurine, which binds TSPO at a nanomolar affinity (Kita et al., 2004). XBD173 was shown to possess potent anxiolytic functions in rodents and

humans, without exerting negative diazepam-like side effects like sedation or habit formation (Rupprecht et al., 2009). In addition, we could recently show that XBD173 is a potent anti-inflammatory mediator and modulates microglial reactivity, neurotoxicity and phagocytosis towards a regulatory phenotype (Karlstetter et al., 2014a).

The exact mechanisms, through which TSPO ligands modulate microglial reactivity and exert their neuroprotective effects, are still largely unknown. Possible mechanisms include the modulation of the mitochondrial transmembrane potential, leading to reduced ROS production and preventing neuronal damage (Carayon et al., 1996, Chelli et al., 2004). Another suggestion is a reduction of apoptosis-related caspase activation by attenuating mitochondrial cytochrome C release (Strohmeier et al., 2002, Veiga et al., 2005). However, since TSPO ligands increase neurosteroid synthesis in the CNS, which exert immunomodulatory and neuroprotective functions, it is likely that this could be a key mechanism of their protective action (Schule et al., 2011). It remains to be elucidated how specific TSPO ligands fulfill their therapeutic function in detail, and it is likely that a combination of the described effects contributes to their effectiveness.

## **1.4 Aims of the thesis**

In a comprehensive approach, we focused on the understanding of photoreceptor homeostasis and disease mechanisms, the identification and characterization of novel microglial markers as well as potential future therapeutics in neurodegenerative diseases with an emphasis on microglia-directed anti-inflammatory therapy in the brain and retina.

Thus, one aim of this work was to investigate the novel CRX-regulated gene SAMD7 in the retina. Elucidating its spatiotemporal expression pattern, the exact regulatory fine-tuning of SAMD7 by the photoreceptor-specific transcription factor CRX and the putative function of SAMD7 as a repressor of CRX-mediated photoreceptor gene expression, we aimed to gain understanding into the fine-tuning of photoreceptor homeostasis and potential disease mechanisms of inherited retinal degenerations.

Another goal was to elucidate the paracrine anti-inflammatory potential of the novel activated microglia/macrophage whey acidic protein (AMWAP) in microglial cells.

Using recombinant AMWAP, we sought to shed light on AMWAPs effects on microglial NF $\kappa$ B signaling and classical physiological functions of microglia *in vitro*, with the aim of establishing whey acidic proteins as potential future therapeutics in neurodegenerative diseases of the brain and retina.

Finally, we were interested in the role of the translocator protein (18 kDa) (TSPO) in the context of neuroinflammation in the retina. Investigating its potential as a novel biomarker for pro-inflammatory microglia activation in the degenerating retina and employing the specific TSPO ligand XBD173 to modulate microglial reactivity *in vitro* and *ex vivo*, we aimed to establish TSPO as a potential target structure for microglia-directed anti-inflammatory therapy in the brain and retina.

## 2. Results

### 2.1 Sterile alpha motif containing 7 (SAMD7) is a novel CRX-regulated transcriptional repressor in the retina

Julia Hlawatsch\*, Marcus Karlstetter\*, Alexander Aslanidis\*, Anika Lückoff, Yana Walczak, Michael Plank, Julia Böck, and Thomas Langmann

\*these authors contributed equally

Inherited retinal diseases are mainly caused by mutations in genes that are highly expressed in photoreceptors of the retina. The majority of these genes is under the control of the transcription factor Cone rod homeobox (CRX), which acts as a master transcription factor in photoreceptors. Using a genome-wide chromatin immunoprecipitation dataset that highlights all potential *in vivo* targets of CRX, we have identified a novel sterile alpha motif (SAM) domain containing protein, SAMD7. mRNA Expression of SAMD7 was confined to the late postnatal and adult mouse retina as well as the pineal gland. Using immunohistochemistry and Western blot, we could detect SAMD7 protein in the outer nuclear layer of adult mouse retina. Ectopic over-expression in HEK293 cells demonstrated that SAMD7 resides in the cytoplasm as well as the nucleus. *In vitro* electroporation of fluorescent reporters into living mouse retinal cultures revealed that transcription of the SAMD7 gene depends on evolutionary conserved CRX motifs located in the first intron enhancer. Moreover, CRX knock-down with shRNA strongly reduced SAMD7 reporter activity and endogenous SAMD7 protein, indicating that CRX is required for retinal expression of SAMD7. Finally, using co-transfections in luciferase reporter assays we found that SAMD7 interferes with CRX-dependent transcription. SAMD7 suppressed luciferase activity from a reporter plasmid with five CRX consensus repeats in a dose dependent manner and reduced CRX-mediated transactivation of regulatory sequences in the retinoschisin gene and the SAMD7 gene itself. Taken together, we have identified a novel retinal SAM domain protein, SAMD7, which could act as a transcriptional repressor involved in fine-tuning of CRX-regulated gene expression.

**Own contribution to publication I:**

I carried out the characterization of the novel SAMD7 gene by analyzing its tissue-specific mRNA expression (Fig. 2 B) and its expression in the pineal gland (Fig. 2 C). I further elucidated the retina-specific localization of SAMD7 protein to the photoreceptor layer using immunohistochemistry (Fig. 3 A). Further, I established, designed, performed and analyzed *ex vivo* electroporation knock-down experiments in murine retinal explants combined with immunohistochemistry to show the CRX-dependent regulation and expression of SAMD7 (Fig. 5 A,B). Finally, I demonstrated the important transcriptional repression function of SAMD7 using Luciferase reporter assays in HEK293 cells, after optimizing the protocol (Fig. 6 A-D). I co-supervised Bachelor student Michael Plank, who also contributed experimentally to this project. All images depicting my experimental data were created by me. I presented posters and oral presentations as first author on this project at both national and international symposia during my PhD.

**Contribution of co-authors to publication I:**

Dr. Julia Hlawatsch was a medical student, who participated in the early stages of the project and helped to establish anti-SAMD7 immunohistochemistry. Dr. Marcus Karlstetter carried out bioinformatic analysis (Fig. 1 A-D) and characterization of the SAMD7 protein, helped with dissection of pineal glands and carried out Flag-SAMD7 transfections and immunocytochemistry in HEK293 cells (Fig. 3 E-P). Anika Lückoff cloned the Flag-SAMD7 construct, carried out transfection of HEK293 cells and Western blot analysis (Fig. 3 B-D). Yana Walczak carried out SAMD7 qRT-PCR of postnatal murine retinas (Fig. 2 D). Michael Plank and Julia Böck performed *ex vivo* electroporation of SAMD7 reporter constructs into living mouse retinas under my co-supervision (Fig. 4 C-E). Prof. Thomas Langmann, as principal investigator, supervised the study and wrote the manuscript.

## 2.2 Activated microglia/macrophage whey acidic protein (AMWAP) inhibits NF $\kappa$ B signaling and induces a neuroprotective phenotype in microglia

Alexander Aslanidis, Marcus Karlstetter, Rebecca Scholz, Sascha Fauser, Harald Neumann, Cora Fried, Markus Pietsch\* and Thomas Langmann\*

\*these authors contributed equally

**Background:** Microglia reactivity is a hallmark of neurodegenerative diseases. We have previously identified activated microglia/macrophage whey acidic protein (AMWAP) as a counter-regulator of pro-inflammatory response. Here, we studied its mechanisms of action with a focus on toll-like receptor (TLR) and nuclear factor  $\kappa$ B (NF $\kappa$ B) signaling.

**Methods:** Recombinant AMWAP was produced in *Escherichia coli* and HEK293 EBNA cells and purified by affinity chromatography. AMWAP uptake was identified by fluorescent labeling, and pro-inflammatory microglia markers were measured by qRT-PCR after stimulation with TLR ligands. NF $\kappa$ B pathway proteins were assessed by immunocytochemistry, Western blot, and immunoprecipitation. A 20S proteasome activity assay was used to investigate the anti-peptidase activity of AMWAP. Microglial neurotoxicity was estimated by nitrite measurement and quantification of caspase 3/7 levels in 661W photoreceptors cultured in the presence of microglia-conditioned medium. Microglial proliferation was investigated using flow cytometry, and their phagocytosis was monitored by the uptake of 661W photoreceptor debris.

**Results:** AMWAP was secreted from lipopolysaccharide (LPS)-activated microglia and recombinant AMWAP reduced gene transcription of IL6, iNOS, CCL2, CASP11, and TNF $\alpha$  in BV-2 microglia treated with LPS as TLR4 ligand. This effect was replicated with murine embryonic stem cell-derived microglia (ESdM) and primary brain microglia. AMWAP also diminished pro-inflammatory markers in microglia activated with the TLR2 ligand zymosan but had no effects on IL6, iNOS, and CCL2 transcription in cells treated with CpG oligodeoxynucleotides as TLR9 ligand. Microglial uptake of AMWAP effectively inhibited TLR4-dependent NF $\kappa$ B activation by preventing IRAK-1 and I $\kappa$ B $\alpha$  proteolysis. No inhibition of I $\kappa$ B $\alpha$  phosphorylation or ubiquitination and no influence on overall 20S proteasome activity were observed. Functionally, both microglial nitric oxide (NO) secretion and 661W photoreceptor

apoptosis were significantly reduced after AMWAP treatment. AMWAP promoted the filopodia formation of microglia and increased the phagocytic uptake of apoptotic 661W photoreceptor cells.

**Conclusions:** AMWAP is secreted from reactive microglia and acts in a paracrine fashion to counter-balance TLR2/TLR4-induced reactivity through NF $\kappa$ B inhibition. AMWAP also induces a neuroprotective microglial phenotype with reduced neurotoxicity and increased phagocytosis. We therefore hypothesize that anti-inflammatory whey acidic proteins could have a therapeutic potential in neurodegenerative diseases of the brain and the retina.

#### **Own contribution to publication II:**

This was one of my main DFG-funded PhD projects. I designed, performed and analyzed all experiments, assisted with CFSE-proliferation assays, created all images except CFSE-proliferation assay image, which I finalized, and wrote the manuscript draft. I independently handled the revision phase of this project. I presented posters and oral presentations on this project at both national and international symposia during my PhD.

#### **Contribution of co-authors to publication II:**

Dr. Marcus Karlstetter provided the AMWAP-His expression plasmid and the previously created AMWAP antibody, further he provided suggestions towards possible experimental strategies. Rebecca Scholz established, performed and analyzed CFSE-proliferation experiments using flow cytometry and created the image (Fig. 10 B). Prof. Sascha Fauser provided suggestions and critically read the manuscript. Prof. Harald Neumann provided embryonic stem cell-derived microglia. Dr. Markus Pietsch and Cora Fried introduced me to recombinant protein expression and purification from HEK293 EBNA cells, which I then carried out in their laboratory. Prof. Thomas Langmann, as principal investigator, obtained funding, supervised the project and corrected the manuscript.

## 2.3 Translocator protein (18 kDa) (TSPO) is expressed in reactive retinal microglia and modulates microglial inflammation and phagocytosis

Marcus Karlstetter\*, Caroline Nothdurfter\*, Alexander Aslanidis, Katharina Moeller, Felicitas Horn, Rebecca Scholz, Harald Neumann, Bernhard H F Weber, Rainer Rupprecht\* and Thomas Langmann\*

\*these authors contributed equally

**Background:** The translocator protein (18 kDa) (TSPO) is a mitochondrial protein expressed on reactive glial cells and a biomarker for gliosis in the brain. TSPO ligands have been shown to reduce neuroinflammation in several mouse models of neurodegeneration. Here, we analyzed TSPO expression in mouse and human retinal microglia and studied the effects of the TSPO ligand XBD173 on microglial functions.

**Methods:** TSPO protein analyses were performed in retinoschisin-deficient mouse retinas and human retinas. Lipopolysaccharide (LPS)-challenged BV-2 microglial cells were treated with XBD173 and TSPO shRNAs *in vitro* and pro-inflammatory markers were determined by qRT-PCR. The migration potential of microglia was determined with wound healing assays and the proliferation was studied with Fluorescence Activated Cell Sorting (FACS) analysis. Microglial neurotoxicity was estimated by nitrite measurement and quantification of caspase 3/7 levels in 661 W photoreceptors cultured in the presence of microglia-conditioned medium. The effects of XBD173 on filopodia formation and phagocytosis were analyzed in BV-2 cells and human induced pluripotent stem (iPS) cell-derived microglia (iPSdM). The morphology of microglia was quantified in mouse retinal explants treated with XBD173.

**Results:** TSPO was strongly up-regulated in microglial cells of the dystrophic mouse retina and also co-localized with microglia in human retinas. Constitutive TSPO expression was high in the early postnatal Day 3 mouse retina and declined to low levels in the adult tissue. TSPO mRNA and protein were also strongly induced in LPS-challenged BV-2 microglia while the TSPO ligand XBD173 efficiently suppressed transcription of the pro-inflammatory marker genes chemokine (C-C motif) ligand 2 (CCL2), interleukin 6 (IL6) and inducible nitric oxide (NO)-synthase

(iNOS). Moreover, treatment with XBD173 significantly reduced the migratory capacity and proliferation of microglia, their level of NO secretion and their neurotoxic activity on 661 W photoreceptor cells. Furthermore, XBD173 treatment of murine and human microglial cells promoted the formation of filopodia and increased their phagocytic capacity to ingest latex beads or photoreceptor debris. Finally, treatment with XBD173 reversed the amoeboid alerted phenotype of microglial cells in explanted organotypic mouse retinal cultures after challenge with LPS.

**Conclusions:** These findings suggest that TSPO is highly expressed in reactive retinal microglia and a promising target to control microglial reactivity during retinal degeneration.

### **Own contribution to publication III:**

This was another important project, for which I obtained funding through a PhD scholarship by the Pro Retina Germany foundation. I carried out the spatiotemporal expression analysis and characterization of TSPO as a marker for microgliosis in the retina using immunohistochemistry (Fig. 1 A-I), quantitative real-time PCR and Western blot (Fig. 2 A-E) on various samples. I further established, performed and analyzed scratch wound healing assays (Fig. 4 A, B) and phenotyping of microglial morphology using Phalloidin-TRITC staining (Fig. 5 A-D). In addition, I established, performed and analyzed microglial phagocytosis assays employing either latex beads or apoptotic photoreceptor fragments as bait (Fig. 6 A-D). I supervised Master student Felicitas Horn, who also contributed experimentally during the revision phase of this publication. All images depicting my experimental data were created by me. I presented posters and oral presentations as first author on this project at both national and international symposia during my PhD.

### **Contribution of co-authors to publication III:**

Dr. Marcus Karlstetter conceptualized parts of the project, finalized images, managed collaborations and carried out qRT-PCR analysis and neurotoxicity assays to show the anti-inflammatory effect of the TSPO ligand XBD173 (Fig. 3 A-H). Dr. Caroline Nothdurfter carried out pregnenolone ELISA (Fig. 7 A). Katharina Moeller performed aminoglutethimide phagocytosis assays (Fig. 7 B) and optimized and carried out

retinal explant experiments (Fig. 8 A-E). Felicitas Horn, under my supervision, performed Phalloidin staining and phagocytosis assays using iPScM cells (Fig. 5 E-H, Fig. 6 E-H). Rebecca Scholz established, performed and analyzed TSPO/GFAP and TSPO/MAP2 immunohistochemistry as well as CFSE-proliferation assays (Fig. 1 J-M, Fig. 4 C). Prof. Harald Neumann provided iPScM cells. Prof. Bernhard Weber provided valuable suggestions and critically read the manuscript. Prof. Rainer Rupprecht supplied the synthetic TSPO ligand XBD173 and provided valuable suggestions. Prof. Thomas Langmann, as principal investigator, coordinated the project and wrote the manuscript.

## 3. Discussion

### 3.1 Results from the three presented studies in summary

1. Sterile alpha motif containing 7 (SAMD7) is expressed in retinal photoreceptors and the pineal gland and its expression is regulated by the photoreceptor key transcription factor CRX. SAMD7 localizes to the cytosol and nucleus and acts as a transcriptional repressor of CRX-mediated photoreceptor gene expression.
2. Activated microglia/macrophage whey acidic protein (AMWAP) is actively secreted from reactive microglia and reduces TLR-mediated pro-inflammatory gene expression through inhibition of NF $\kappa$ B signaling in a paracrine fashion. AMWAP further reduces microglial neurotoxicity, promotes filopodia formation and increases microglial phagocytosis *in vitro*, typical hallmarks of a regulatory phenotype.
3. The translocator protein (18 kDa) (TSPO) is a biomarker for microglial reactivity in the dystrophic mouse retina and also expressed in human retinal microglia. It is further induced in reactive microglia *in vitro*. The specific TSPO ligand XBD173 effectively reduces pro-inflammatory microglial gene expression, proliferation, migration and neurotoxicity *in vitro*. XBD173 further induces filopodia formation and increases microglial phagocytosis in murine and human microglia. Finally, XBD173 reduces the number of pro-inflammatory amoeboid microglia in *ex vivo* organotypic murine retinal explant cultures.

### 3.2 SAMD7, a novel photoreceptor gene repressor

In the first study, we could identify SAMD7 as a novel CRX-regulated photoreceptor-specific gene, which acts as a repressor of CRX-mediated photoreceptor gene transcription (Hlawatsch et al., 2013). SAMD7 is the hitherto second SAM domain containing protein next to its closest phylogenetic relative SAMD11. SAMD7 and SAMD11 show a similar spatiotemporal expression profile in photoreceptors and the pineal gland. SAMD11 was previously also described to act as a repressor of CRX-

dependent photoreceptor gene expression (Inoue et al., 2006). Since this family of proteins is known to interact through their SAM domains (Kim and Bowie, 2003), it will be interesting to investigate whether SAMD7 and SAMD11 interact to modulate photoreceptor gene expression in a combinatorial fashion.

### **3.2.1 Photoreceptor-specific SAMD7 gene regulation**

CRX ChIP-seq revealed SAMD7 to be strongly CRX-regulated by binding CRX in the promoter and first intron (CBR1 and CBR2). Interestingly, the promoter CBR (CBR1) alone was not sufficient to induce reporter expression in the *ex vivo* electroporation experiments and required the presence of the enhancing CBR2. CBR2 contains two crucial individual CRX binding sites (CBS), which exhibit the perfect CRX consensus sequence (5'-GATTA-3'), as previously identified from over 5,595 CRX-bound regions (Corbo et al., 2010). These findings strengthen the notion that photoreceptor-specific genes, including most disease genes, are tightly regulated by a number of cis-regulatory elements binding CRX. In addition, SAMD7 was shown to be NRL-regulated, as NRL binds to the same cis-regulatory regions as CRX (Hao et al., 2012, Aslanidis et al., 2013). In further experiments, we could indeed verify a reduced enhancer activity of SAMD7 CBR2 as well as reduced SAMD7 protein levels in photoreceptors after NRL knock-down using *ex vivo* electroporation into living mouse retinas (Aslanidis et al., 2013). CRX is known to synergistically interact with NRL to regulate photoreceptor-specific gene expression in many cases (Mitton et al., 2000). It is therefore not clear if the observed SAMD7 downregulation after NRL knock-down is solely due to reduced NRL-mediated SAMD7 transcription or a combinatorial effect. Interestingly, SAMD7 mRNA levels are strongly reduced in the OTX2-deficient retina (Omori et al., 2011). However, it is also unclear if SAMD7 is directly regulated by OTX2 or the loss of SAMD7 expression is a secondary effect due to reduced CRX levels in OTX2-deficient photoreceptors. Further experiments will be helpful in deciphering the exact cis-regulatory architecture of the SAMD7 gene.

### **3.2.2 SAMD7, a gene regulator without DNA binding sequence**

Functionally, using Luciferase assays we could show that SAMD7 interferes with the CRX-mediated gene transcription at photoreceptor-specific promoters. This is

particularly interesting, as SAMD7 lacks an obvious DNA binding domain. The drosophila SAM domain protein Mae, also carrying a single SAM domain and lacking a DNA binding domain, interacts with the SAM domain of the transcriptional repressor Yan which leads to a termination of repressor activity by translocation to the cytoplasm (Baker et al., 2001, Qiao et al., 2004). It is therefore imaginable that SAMD7 exerts its repressor function by forming non-active protein complexes with CRX. SAMD7 could also fulfil its function through chromatin remodeling, as the SAM domain containing PRC2 (polycomb repressive complex 2) has been shown to silence gene expression through this mechanism (Aldiri and Vetter, 2012). Recently, another repressor of CRX-mediated photoreceptor gene expression, PANKY-A, was identified, which inhibits the DNA binding activity of CRX (Sanuki et al., 2010). Further analyses will be required to reveal the exact mechanisms of SAMD7 repressor function. We could so far show that SAMD7 represses gene transcription from three different CRX-dependent promoters. Future experiments employing SAMD7-deficient or knock-down retinas will be particularly helpful in identifying a comprehensive list of *in vivo* target genes affected by SAMD7.

### **3.2.3 Potential role of SAMD7 in retinal health and disease**

In an ongoing collaborative effort, we and others could recently identify mutations of regulatory CRX target regions in the SAMD7 gene in a family of retinitis pigmentosa patients (Van Schil et al., 2015). *Ex vivo* electroporation and luciferase reporter assays show a significant loss of cis-regulatory activity of the mutant sequences. This is the first description of regulatory SAMD7 mutations in humans, which could have a potential modifying effect on the observed disease phenotype. Of note, a recent study reports the presence of multiple SAMD11 alternative splice variants in the human retina (Jin et al., 2013). It will be interesting to focus research on SAMD7 also in this regard and potentially identify novel splice variants with different functions in human photoreceptor health and disease.

### 3.3 AMWAP, a counter-regulator of microglial reactivity

In the second study, we could demonstrate that the activated microglia/macrophage whey acidic protein (AMWAP) is actively secreted from reactive microglia to reduce pro-inflammatory microglial activation in a paracrine fashion and therefore serves as a negative feedback-loop to counter-regulate neuroinflammation (Aslanidis et al., 2015). Recombinant AMWAP elicits this effect through inhibition of NFκB signaling and induces an overall neuroprotective phenotype in microglia *in vitro*.

#### 3.3.1 Obtaining recombinant AMWAP for therapy

We observed a rapid induction and secretion of AMWAP after LPS stimulation of microglial cells *in vitro*. This notion is in coherence with the transcriptional control of the AMWAP gene by NFκB, as we could previously show that blockade of NFκB signaling inhibits TLR4-mediated AMWAP expression (Karlstetter et al., 2010). This finding prompted us to investigate the physiological functions of recombinantly expressed AMWAP with a focus on its microglia-modulating therapeutic potential. When producing potential anti-inflammatory mediators through recombinant protein expression and purification, we observed that it is more feasible to employ a eukaryotic organism like HEK293 EBNA cells for expression, as a prokaryotic source like *E. coli* bears the risk of LPS contamination of the purified protein, which leads to high immunogenicity. In addition, proper protein folding and disulfide bond formation are also ensured when using eukaryotic expression systems as previously demonstrated for the whey acidic protein SLPI expressed in the yeast *Pichia pastoris* (Li et al., 2009, Li et al., 2010).

#### 3.3.2 AMWAP, an inhibitor of microglial NFκB signaling

We could show that recombinant AMWAP is gradually being taken up by microglial cells and localizes to the cytoplasm in a patchy perinuclear fashion, an observation reminiscent of SLPI in neutrophils (Jacobsen et al., 2008). In contrast to SLPI, which was previously described by Taggart and colleagues to also act in the nucleus by inhibiting NFκB binding to its pro-inflammatory gene promoters, we did not observe any nuclear uptake of AMWAP in microglia (Taggart et al., 2005). AMWAP inhibits

NFκB signaling and effectively reduces TLR2- and TLR4-mediated pro-inflammatory gene expression in microglia cells from different sources *in vitro*. The lack of this effect when cells are activated through TLR9 signaling could be due to the fact that TLR2 and TLR4 signal mainly through NFκB, which is effectively inhibited by AMWAP, but TLR9 signals majorly through interferon regulatory factors (IRFs) (O'Neill et al., 2013). These findings are in coherence with the report of SLPI inhibiting pro-inflammatory TLR2 and TLR4 responses in human monocytes (Greene et al., 2004).

Mechanistically we could show that AMWAP exerts its NFκB inhibitory effect through blocking the proteolytic degradation of the NFκB pathway mediators IRAK-1 and IκBα without affecting IκBα phosphorylation, ubiquitination or any of the 20S proteasome peptidase activities directly. A similar function has been described for the whey acidic proteins SLPI and elafin in monocytes as well as for the antibacterial peptide PR39, where IκBα gets labeled properly for proteolytic degradation but does not get cleaved by the proteasome, therefore keeping its NFκB regulatory function (Taggart et al., 2002, Butler et al., 2006, Gao et al., 2000). There is conflicting evidence whether the NFκB inhibitory effect of whey acidic proteins is dependent on the anti-protease activity of their WAP domain (Williams et al., 2006, Yang et al., 2005). Future experiments will have to show which elements of AMWAP are accountable for its anti-inflammatory function.

### **3.3.3 AMWAP induces a neuroprotective microglial phenotype**

Functionally we could show that AMWAP induces a regulatory neuroprotective phenotype in microglia *in vitro*. AMWAP significantly reduces microglial NO secretion and neurotoxicity on photoreceptor cells. In coherence with these findings, SLPI overexpression was previously shown to reduce macrophage NO secretion (Jin et al., 1997, Yang et al., 2005). In addition, SLPI reduces LPS-induced neutrophil apoptosis while a lack of SLPI leads to increased apoptosis of myeloid cells (Subramaniam et al., 2011, Klimenkova et al., 2014).

We could demonstrate that AMWAP induces a ramified microglial phenotype, and even reverses the pro-inflammatory amoeboid phenotype observed after LPS stimulation, which is regarded as an anti-inflammatory feature (Nimmerjahn et al.,

2005). Further, the recognition and phagocytic clearance of apoptotic cell debris is also a typical characteristic of a regulatory microglial phenotype (Sierra et al., 2013, Karlstetter et al., 2014a). In line with this, we could show increased phagocytic uptake of apoptotic photoreceptor cells by AMWAP-treated microglia, regardless of further LPS stimulation, as apoptotic cells alone serve as an activatory stimulus for microglia (Heneka et al., 2014). Interestingly, elafin was previously shown to protect macrophages from degradation of their receptors for apoptotic cell recognition, effectively restoring their phagocytic activity and clearance potential, and a similar mechanism can be imagined for AMWAP (Henriksen et al., 2004).

Increased proliferation rates are a typical hallmark of reactive microglia (Perry et al., 2010, Chen and Guilarte, 2008). However, we did not observe an anti-mitotic effect of AMWAP on microglial cells. It is noteworthy that there is conflicting evidence in the literature regarding the anti-proliferative potential of WAPs with one study even showing a SLPI-induced increase in stem cell proliferation towards an oligodendroglial cell fate via induction of Cyclin D1 (Mueller et al., 2008). Future experiments employing *ex vivo* organotypic retinal explant cultures or *in vivo* models of retinal degeneration will be needed to potentially translate the AMWAP-induced beneficial regulatory microglia phenotype into living tissues.

### 3.3.4 AMWAP, current state and future perspectives

In sum, our studies on the novel activated microglia/macrophage whey acidic protein (AMWAP) as a marker and modulator of pro-inflammatory microglial activation have enabled us to gain insight into mechanisms of microglial reactivity in neuro-inflammatory settings (Karlstetter et al., 2010, Aslanidis et al., 2015). Today, we employ AMWAP as a reliable *bona fide* transcriptional biomarker to monitor microglial activation states in various genetic or light-induced retinal degenerative mouse models as well as *in vitro* (Karlstetter et al., 2014b, Dannhausen et al., 2015). We could show that AMWAP is secreted from pro-inflammatory microglia and serves as a negative feedback-loop to counter-regulate microglial reactivity. Future experiments using recombinant AMWAP or AAV-mediated AMWAP overexpression in the retina of murine retinal degeneration models will have to demonstrate the therapeutic value of whey acidic proteins as a microglia-directed immunotherapy in neurodegenerative diseases.

### 3.4 TSPO, emerging roles in the CNS and retina

In the third study, we could establish the translocator protein (18 kDa) (TSPO) as a novel biomarker for reactive microgliosis in the degenerating retina as well as *in vitro* (Karlstetter et al., 2014a). Treatment of murine and human microglia with the specific synthetic TSPO ligand XBD173 effectively reduces microglial reactivity and induces a neuroprotective phenotype *in vitro*. In addition, XBD173 effectively reduces the number of LPS-induced reactive amoeboid microglia in organotypic *ex vivo* retinal explant cultures.

#### 3.4.1 TSPO, a novel marker for reactive retinal microglia

We and others present the first report of TSPO as a marker for reactive microglia during retinal degeneration (Karlstetter et al., 2014a, Wang et al., 2014b). The observed elevated microglial TSPO protein levels are in perfect overlap with the course of microglia activation in the *Rs1h<sup>-/-</sup>* mouse model (Karlstetter et al., 2010). Since we also observed an upregulation of TSPO in LPS-activated microglial cells *in vitro*, a potential TLR4-mediated mechanism of induction can be imagined. In line with this, blockade of TLR4 signaling was shown to inhibit TSPO induction in a rat model of neuropathic pain (Wei et al., 2013). It is therefore imaginable, that damage-associated molecular patterns (DAMPs) from dying neurons could induce TSPO expression through stimulating TLR4 on microglia (Frank et al., 2015). We also observed a peak of TSPO mRNA levels in the healthy early postnatal (P3) retina before decline to basal levels in the adult retina. This is in accordance with the notion that microglia are initially mitotic, amoeboid and phagocytically active in early postnatal neuronal development, before they gradually adopt their ramified and surveillant phenotype (Prinz and Mildner, 2011, Schlegelmilch et al., 2011). Our findings expand the use of TSPO as a potential microgliosis biomarker, e.g. for radiolabeling and live imaging techniques, from the brain to the retinal context (Trapani et al., 2013). In addition, we could very recently demonstrate an increase of TSPO expression in reactive retinal microglia in the *aSMase*-deficient mouse model (Dannhausen et al., 2015). Future analyses of various genetic or induced retinal degeneration animal models will have to prove the reliability of assessing retinal microgliosis through TSPO quantification.

### 3.4.2 Functions of TSPO and its ligands in reactive microglia

We could show various anti-inflammatory effects of the synthetic TSPO ligand XBD173 on microglial cells *in vitro* and *ex vivo*. XBD173 effectively reduces LPS-induced pro-inflammatory gene expression in microglia, an effect also observed for the TSPO ligand PK11195 via modulation of  $\text{Ca}^{2+}$ -mediated signaling pathways (Choi et al., 2002). PK11195 further proved to be anti-inflammatory and neuroprotective in a rat model of quinolinic acid-induced brain damage (Ryu et al., 2005). We could show that the reduced pro-inflammatory gene expression in microglia after XBD173 treatment is indeed dependent on TSPO, as shRNA-mediated TSPO knock-down abolished the therapeutic effect (Karlstetter et al., 2014a).

A potential mechanism by which XBD173 acts anti-inflammatory could be through inhibition of NF $\kappa$ B and AP-1 signaling, as another TSPO ligand, vinpocetine, was previously shown to reduce pro-inflammatory cytokine production and neurotoxicity in microglia *in vitro* and *in vivo* in this fashion (Zhao et al., 2011, Wang et al., 2014a). Another potential mechanism by which XBD173 exerts its anti-inflammatory function could be by elevating neurosteroid production. Indeed, we could show that XBD173 enhances the synthesis of the neurosteroid precursor pregnenolone in microglial cells *in vitro* and another TSPO ligand, etifoxine, exerts a similar effect in the rat brain (Karlstetter et al., 2014a, Verleye et al., 2005). In addition, elevated neurosteroid levels were shown to be protective in animal models of motoneuron degradation and multiple sclerosis (Ferzaz et al., 2002, Giatti et al., 2012).

We observed an induction of microglial filopodia formation after treating murine and human microglia with XBD173, a typical hallmark of homeostatic microglia. A potential mechanism, through which XBD173 exerts its effects on the microglial f-actin cytoskeleton, could be by modulation of intracellular  $\text{Ca}^{2+}$  signaling. It was previously described that LPS stimulation of microglia and neutrophils leads to an increase in cytosolic  $\text{Ca}^{2+}$  and subsequent remodeling of the f-actin cytoskeleton (Bader et al., 1994, Yee and Christou, 1993). Interestingly, PK11195 reduces the LPS-induced elevation of  $\text{Ca}^{2+}$  levels, which is generally considered a hallmark of regulatory microglia (Hong et al., 2006, Choi et al., 2002).

We could demonstrate increased TSPO expression, migration and proliferation in LPS-activated microglial cells *in vitro*, which was effectively reduced after XBD173

treatment. In accordance, TSPO overexpression was shown to increase migration and proliferation of C6 rat glioma cells and treatment with the TSPO ligand PK11195 exerts a strong anti-proliferative and pro-apoptotic effect on these cells (Rechichi et al., 2008). A potential mechanism by which XBD173 executes its effects on microglia migration and proliferation could be by modulation of phosphatidylinositol-3 kinase (PI3K) signaling or Ca<sup>2+</sup>-dependent protein kinase C (PKC) activation, two events that were previously shown to be influenced by TSPO and its ligands (Venneti et al., 2007, Azarashvili et al., 2007, Batarseh et al., 2010). Activation of either PI3K or PKC has been implicated in the signaling cascade associated with the migratory and proliferative activity of microglia (Suh et al., 2005, Zassler et al., 2003). In addition to these findings, other TSPO ligands have previously been shown to influence chemotactic and phagocytic behavior in monocytes and neutrophils (Ruff et al., 1985, Cosentino et al., 2000, Marino et al., 2001).

We could also show a XBD173-induced elevation of microglial phagocytic clearance of both latex beads and apoptotic photoreceptor debris. Interestingly, blockade of pregnenolone synthesis using aminoglutethimide (AMG) reversed this effect (Karlstetter et al., 2014a). This indicates neurosteroid synthesis being a prerequisite for microglial phagocytosis in our experimental system. Interestingly, estrogen was previously shown to enhance phagocytosis of amyloid- $\beta$  in human cortical microglia cultures (Li et al., 2000). Accordingly, another study also observed increased phagocytic clearance by microglia after treatment with the TSPO ligands PK11195 and Ro-4864 (Choi et al., 2011). As introduced above, activation of PI3K and PKC have been implicated in the signaling cascade associated with the phagocytic activity of macrophages and microglia (Makranz et al., 2004, Cohen et al., 2006, Rotshenker et al., 2008).

We observed a significantly reduced number of LPS-alerted amoeboid microglia in living retinal explants after treatment with XBD173. Interestingly, however, the overall fraction of ramified cells was not increased by XBD173. These findings indicate that TSPO may control microglial dynamics and behavior during the onset and resolution of retinal damage. Within the retina, endogenous ligands (endozepines) may serve as TSPO-directed modulators of microglial reactivity to fulfil this function. One example is the diazepam binding inhibitor (DBI), which was previously shown to be actively secreted from Mueller cells and astrocytes (Wang et al., 2014b, Alho et al.,

1994). DBI then acts through TSPO to reduce pro-inflammatory microglial ROS production, cytokine expression and secretion as well as proliferation (Wang et al., 2014b). Further, DBI can be cleaved into several active peptide fragments which then stimulate neurosteroid synthesis (Costa et al., 1994).

### 3.4.3 TSPO, current state and future perspectives

With TSPO fulfilling a multitude of different functions in many different cell types, including glial cells of the CNS, there is a growing interest in revealing its functions in the context of health and disease. For this purpose, various approaches of generating and characterizing TSPO-deficient mouse models have been undertaken over the last couple of years (Gut et al., 2015). First attempts of generating TSPO<sup>-/-</sup> mice reported early embryonal lethality, implicating vital potentially steroidogenic functions of TSPO during embryogenesis (Papadopoulos et al., 1997). In heavy contrast, recent studies of novel TSPO knock-out mouse strains could not confirm a crucial role of TSPO in steroid synthesis, mitochondrial permeability, survival or reproduction (Banati et al., 2014, Sileikyte et al., 2014, Tu et al., 2014, Morohaku et al., 2014, Tu et al., 2015). These observations call for a reassessment of the dogmatic indispensable importance of TSPO for life in general (Campanella, 2015). Interestingly, however, it was reported that microglial cells from a global TSPO knock-out mouse line show significantly reduced mitochondrial ATP production, suggesting reduced metabolic activity and potential effects on microglial behavior in the healthy and degenerating CNS (Banati et al., 2014, Rodriguez et al., 2013). Future experiments employing microglia-specific conditional TSPO knock-out mice will therefore be valuable tools to assess the functions of TSPO in the healthy and degenerating CNS and retina.

We observed a potentially NFκB-mediated induction of TSPO expression in microglial cells and bioinformatic analysis revealed a putative NFκB binding site in the TSPO promoter region. As TSPO is expressed in a multitude of different tissues and cells, a variety of transcription factors were found to bind to its promoter. The TATA-less, GC-rich promoter contains five tandem binding sites for Sp factors, a typical characteristic of housekeeping genes (Batarseh and Papadopoulos, 2010). However, a similar structure is found in growth factor receptor genes important for cell proliferation (DiMario, 2002). Mechanisms of TSPO induction include the PKC-

mediated activation of the mitogen-activated protein kinase (MAPK) and signal transducer and activator of transcription 3 (STAT3) (Batarseh et al., 2010). Ongoing investigations on microglia-specific transcriptional TSPO regulation in homeostatic and reactive states will shed light on mechanisms of TSPO induction during neuroinflammation.

In summary, we present the first report of TSPO as a microglial biomarker and potential therapeutic target to attenuate neuroinflammation in retinal degeneration. Future experiments employing TSPO ligands like XBD173 as microglia-directed therapy in animal models of retinal degeneration will have to prove their feasibility as a novel treatment option.

### **3.5 Concluding remarks**

Loss of vision due to inherited retinal degeneration is a devastating and in most cases unstoppable prognosis and accompanied by large constraints in the life quality of affected patients. In our studies, we contribute to the understanding of retinal homeostasis in health and disease by characterization of the novel photoreceptor gene regulator SAMD7, which could have future implications as an elicitor or modulator of retinal degenerative phenotypes.

Neuroinflammation and reactive microgliosis are common hallmarks and early indicators of retinal degeneration, and chronic neurotoxic microglial reactivity has detrimental effects and contributes to disease progression. Therefore, there is a high interest in discovering novel microglial reactivity biomarkers and potential microglia-directed therapeutic approaches to attenuate neuroinflammation. We could establish AMWAP and TSPO as suitable microgliosis markers and could show their therapeutic potential either as an anti-inflammatory peptide or target structure for pharmacotherapy in degenerative diseases of the CNS and retina.

## Reference list

- AGOSTINHO, P., CUNHA, R. A. & OLIVEIRA, C. 2010. Neuroinflammation, oxidative stress and the pathogenesis of Alzheimer's disease. *Curr Pharm Des*, 16, 2766-78.
- ALDIRI, I. & VETTER, M. L. 2012. PRC2 during vertebrate organogenesis: a complex in transition. *Dev Biol*, 367, 91-9.
- ALHO, H., VARGA, V. & KRUEGER, K. E. 1994. Expression of mitochondrial benzodiazepine receptor and its putative endogenous ligand diazepam binding inhibitor in cultured primary astrocytes and C-6 cells: relation to cell growth. *Cell Growth Differ*, 5, 1005-14.
- AMMON, H. P. & WAHL, M. A. 1991. Pharmacology of *Curcuma longa*. *Planta Med*, 57, 1-7.
- ANDERSON, R. E., MAUDE, M. B., MCCLELLAN, M., MATTHES, M. T., YASUMURA, D. & LAVAIL, M. M. 2002. Low docosahexaenoic acid levels in rod outer segments of rats with P23H and S334ter rhodopsin mutations. *Mol Vis*, 8, 351-8.
- ASLANIDIS, A., KARLSTETTER, M., SCHOLZ, R., FAUSER, S., NEUMANN, H., FRIED, C., PIETSCH, M. & LANGMANN, T. 2015. Activated microglia/macrophage whey acidic protein (AMWAP) inhibits NFkappaB signaling and induces a neuroprotective phenotype in microglia. *J Neuroinflammation*, 12, 77.
- ASLANIDIS, A., KARLSTETTER, M., WALCZAK, Y., JAGLE, H. & LANGMANN, T. 2014. RETINA-specific expression of *Kcnv2* is controlled by cone-rod homeobox (*Crx*) and neural retina leucine zipper (*Nrl*). *Adv Exp Med Biol*, 801, 31-41.
- ASLANIDIS, A., KARLSTETTER, M., WALCZAK, Y., LÜCKOFF, A., SCHEIFFERT, E., BREMICKER, N. & LANGMANN, T. 2013. Sterile alpha motif containing 7 (*Samd7*) is a novel *Crx*- and *Nrl*-regulated transcriptional repressor in the retina. *Investigative Ophthalmology & Visual Science*, June 2013, Vol.54.
- AVIV, T., LIN, Z., LAU, S., RENDL, L. M., SICHERI, F. & SMIBERT, C. A. 2003. The RNA-binding SAM domain of Smaug defines a new family of post-transcriptional regulators. *Nat Struct Biol*, 10, 614-21.
- AZARASHVILI, T., GRACHEV, D., KRESTININA, O., EVTODIENKO, Y., YURKOV, I., PAPADOPOULOS, V. & REISER, G. 2007. The peripheral-type benzodiazepine receptor is involved in control of Ca<sup>2+</sup>-induced permeability transition pore opening in rat brain mitochondria. *Cell Calcium*, 42, 27-39.
- BADER, M. F., TAUPENOT, L., ULRICH, G., AUNIS, D. & CIESIELSKI-TRESKA, J. 1994. Bacterial endotoxin induces [Ca<sup>2+</sup>]<sub>i</sub> transients and changes the organization of actin in microglia. *Glia*, 11, 336-44.
- BAKER, D. A., MILLE-BAKER, B., WAINWRIGHT, S. M., ISH-HOROWICZ, D. & DIBB, N. J. 2001. Mae mediates MAP kinase phosphorylation of Ets transcription factors in *Drosophila*. *Nature*, 411, 330-4.
- BANATI, R. B., GEHRMANN, J., SCHUBERT, P. & KREUTZBERG, G. W. 1993. Cytotoxicity of microglia. *Glia*, 7, 111-8.
- BANATI, R. B., MIDDLETON, R. J., CHAN, R., HATTY, C. R., KAM, W. W., QUIN, C., GRAEBER, M. B., PARMAR, A., ZAHRA, D., CALLAGHAN, P., FOK, S., HOWELL, N. R., GREGOIRE, M., SZABO, A., PHAM, T., DAVIS, E. & LIU, G. J. 2014. Positron emission tomography and functional characterization of a complete PBR/TSPO knockout. *Nat Commun*, 5, 5452.
- BARON, M. K., BOECKERS, T. M., VAIDA, B., FAHAM, S., GINGERY, M., SAWAYA, M. R., SALYER, D., GUNDELFINGER, E. D. & BOWIE, J. U. 2006. An architectural framework that may lie at the core of the postsynaptic density. *Science*, 311, 531-5.
- BATARSEH, A., LI, J. & PAPADOPOULOS, V. 2010. Protein kinase C epsilon regulation of translocator protein (18 kDa) *Tspo* gene expression is mediated through a MAPK pathway targeting STAT3 and c-Jun transcription factors. *Biochemistry*, 49, 4766-78.

- BATARSEH, A. & PAPADOPOULOS, V. 2010. Regulation of translocator protein 18 kDa (TSPO) expression in health and disease states. *Mol Cell Endocrinol*, 327, 1-12.
- BAYLOR, D. A., LAMB, T. D. & YAU, K. W. 1979. Responses of retinal rods to single photons. *J Physiol*, 288, 613-34.
- BAZAN, N. G., CALANDRIA, J. M. & SERHAN, C. N. 2010. Rescue and repair during photoreceptor cell renewal mediated by docosahexaenoic acid-derived neuroprotectin D1. *J Lipid Res*, 51, 2018-31.
- BESSANT, D. A., PAYNE, A. M., MITTON, K. P., WANG, Q. L., SWAIN, P. K., PLANT, C., BIRD, A. C., ZACK, D. J., SWAROOP, A. & BHATTACHARYA, S. S. 1999. A mutation in NRL is associated with autosomal dominant retinitis pigmentosa. *Nat Genet*, 21, 355-6.
- BIBER, K., NEUMANN, H., INOUE, K. & BODDEKE, H. W. 2007. Neuronal 'On' and 'Off' signals control microglia. *Trends Neurosci*, 30, 596-602.
- BINGLE, C. D. & VYAKARNAM, A. 2008. Novel innate immune functions of the whey acidic protein family. *Trends Immunol*, 29, 444-53.
- BLACKSHAW, S., FRAIOLI, R. E., FURUKAWA, T. & CEPKO, C. L. 2001. Comprehensive analysis of photoreceptor gene expression and the identification of candidate retinal disease genes. *Cell*, 107, 579-89.
- BLOCK, M. L., ZECCA, L. & HONG, J. S. 2007. Microglia-mediated neurotoxicity: uncovering the molecular mechanisms. *Nat Rev Neurosci*, 8, 57-69.
- BORDET, T., BUISSON, B., MICHAUD, M., DROUOT, C., GALEA, P., DELAAGE, P., AKENTIEVA, N. P., EVERS, A. S., COVEY, D. F., OSTUNI, M. A., LACAPERRE, J. J., MASSAAD, C., SCHUMACHER, M., STEIDL, E. M., MAUX, D., DELAAGE, M., HENDERSON, C. E. & PRUSS, R. M. 2007. Identification and characterization of cholest-4-en-3-one, oxime (TRO19622), a novel drug candidate for amyotrophic lateral sclerosis. *J Pharmacol Exp Ther*, 322, 709-20.
- BRAMALL, A. N., WRIGHT, A. F., JACOBSON, S. G. & MCINNES, R. R. 2010. The genomic, biochemical, and cellular responses of the retina in inherited photoreceptor degenerations and prospects for the treatment of these disorders. *Annu Rev Neurosci*, 33, 441-72.
- BROWN, G. C. & NEHER, J. J. 2014. Microglial phagocytosis of live neurons. *Nat Rev Neurosci*, 15, 209-16.
- BUTLER, M. W., ROBERTSON, I., GREENE, C. M., O'NEILL, S. J., TAGGART, C. C. & MCELVANEY, N. G. 2006. Elafin prevents lipopolysaccharide-induced AP-1 and NF-kappaB activation via an effect on the ubiquitin-proteasome pathway. *J Biol Chem*, 281, 34730-5.
- CAMPANELLA, M. 2015. TSPO the unrested: challenged opinions of a resourceful mitochondrial protein. *Trends Endocrinol Metab*, 26, 333-4.
- CARAYON, P., PORTIER, M., DUSSOSSOY, D., BORD, A., PETITPRETRE, G., CANAT, X., LE FUR, G. & CASELLAS, P. 1996. Involvement of peripheral benzodiazepine receptors in the protection of hematopoietic cells against oxygen radical damage. *Blood*, 87, 3170-8.
- CARDONA, A. E., PIORO, E. P., SASSE, M. E., KOSTENKO, V., CARDONA, S. M., DIJKSTRA, I. M., HUANG, D., KIDD, G., DOMBROWSKI, S., DUTTA, R., LEE, J. C., COOK, D. N., JUNG, S., LIRA, S. A., LITTMAN, D. R. & RANSOHOFF, R. M. 2006. Control of microglial neurotoxicity by the fractalkine receptor. *Nat Neurosci*, 9, 917-24.
- CASANO, A. M. & PERI, F. 2015. Microglia: multitasking specialists of the brain. *Dev Cell*, 32, 469-77.
- CASELLAS, P., GALIEGUE, S. & BASILE, A. S. 2002. Peripheral benzodiazepine receptors and mitochondrial function. *Neurochem Int*, 40, 475-86.
- CHELLI, B., LENA, A., VANACORE, R., DA POZZO, E., COSTA, B., ROSSI, L., SALVETTI, A., SCATENA, F., CERUTI, S., ABBRACCHIO, M. P., GREMIGNI, V. & MARTINI, C. 2004. Peripheral benzodiazepine receptor ligands: mitochondrial transmembrane potential depolarization and apoptosis induction in rat C6 glioma cells. *Biochem Pharmacol*, 68, 125-34.

- CHEN, C. Y., PENG, W. H., TSAI, K. D. & HSU, S. L. 2007. Luteolin suppresses inflammation-associated gene expression by blocking NF-kappaB and AP-1 activation pathway in mouse alveolar macrophages. *Life Sci*, 81, 1602-14.
- CHEN, M. K. & GUILARTE, T. R. 2008. Translocator protein 18 kDa (TSPO): molecular sensor of brain injury and repair. *Pharmacol Ther*, 118, 1-17.
- CHEN, Y., BEDELL, M. & ZHANG, K. 2010. Age-related macular degeneration: genetic and environmental factors of disease. *Mol Interv*, 10, 271-81.
- CHERRY, J. D., OLSCHOWKA, J. A. & O'BANION, M. K. 2014. Neuroinflammation and M2 microglia: the good, the bad, and the inflamed. *J Neuroinflammation*, 11, 98.
- CHOI, H. B., KHOO, C., RYU, J. K., VAN BREEMEN, E., KIM, S. U. & MCLARNON, J. G. 2002. Inhibition of lipopolysaccharide-induced cyclooxygenase-2, tumor necrosis factor-alpha and [Ca<sup>2+</sup>]<sub>i</sub> responses in human microglia by the peripheral benzodiazepine receptor ligand PK11195. *J Neurochem*, 83, 546-55.
- CHOI, J., IFUKU, M., NODA, M. & GUILARTE, T. R. 2011. Translocator protein (18 kDa)/peripheral benzodiazepine receptor specific ligands induce microglia functions consistent with an activated state. *Glia*, 59, 219-30.
- CLAUDE, J., LINNARTZ-GERLACH, B., KUDIN, A. P., KUNZ, W. S. & NEUMANN, H. 2013. Microglial CD33-related Siglec-E inhibits neurotoxicity by preventing the phagocytosis-associated oxidative burst. *J Neurosci*, 33, 18270-6.
- COHEN, G., MAKRANZ, C., SPIRA, M., KODAMA, T., REICHERT, F. & ROTSHENKER, S. 2006. Non-PKC DAG/phorbol-ester receptor(s) inhibit complement receptor-3 and nPKC inhibit scavenger receptor-AI/II-mediated myelin phagocytosis but cPKC, PI3k, and PLCgamma activate myelin phagocytosis by both. *Glia*, 53, 538-50.
- COMBADIÈRE, C., FEUMI, C., RAOUL, W., KELLER, N., RODERO, M., PEZARD, A., LAVALETTE, S., HOUSSIER, M., JONET, L., PICARD, E., DEBRE, P., SIRINYAN, M., DETERRE, P., FERROUKHI, T., COHEN, S. Y., CHAUVAUD, D., JEANNY, J. C., CHEMTOB, S., BEHAR-COHEN, F. & SENNLAUB, F. 2007. CX3CR1-dependent subretinal microglia cell accumulation is associated with cardinal features of age-related macular degeneration. *J Clin Invest*, 117, 2920-8.
- CORBO, J. C. & CEPKO, C. L. 2005. A hybrid photoreceptor expressing both rod and cone genes in a mouse model of enhanced S-cone syndrome. *PLoS Genet*, 1, e11.
- CORBO, J. C., LAWRENCE, K. A., KARLSTETTER, M., MYERS, C. A., ABDELAZIZ, M., DIRKES, W., WEIGELT, K., SEIFERT, M., BENES, V., FRITSCHKE, L. G., WEBER, B. H. & LANGMANN, T. 2010. CRX ChIP-seq reveals the cis-regulatory architecture of mouse photoreceptors. *Genome Res*, 20, 1512-25.
- COSENTINO, M., MARINO, F., CATTANEO, S., DI GRAZIA, L., FRANCIOLI, C., FIETTA, A. M., LECCHINI, S. & FRIGO, G. 2000. Diazepam-binding inhibitor-derived peptides induce intracellular calcium changes and modulate human neutrophil function. *J Leukoc Biol*, 67, 637-43.
- COSTA, E., AUTA, J., GUIDOTTI, A., KORNEYEV, A. & ROMEO, E. 1994. The pharmacology of neurosteroidogenesis. *J Steroid Biochem Mol Biol*, 49, 385-9.
- COSTA, E. & GUIDOTTI, A. 1991. Diazepam binding inhibitor (DBI): a peptide with multiple biological actions. *Life Sci*, 49, 325-44.
- COULL, J. A., BEGGS, S., BOUDREAU, D., BOIVIN, D., TSUDA, M., INOUE, K., GRAVEL, C., SALTER, M. W. & DE KONINCK, Y. 2005. BDNF from microglia causes the shift in neuronal anion gradient underlying neuropathic pain. *Nature*, 438, 1017-21.
- CRUZ-GUILLOT, F., SAEED, A. M., ECHEGARAY, J. J., DUFFORT, S., BALLMICK, A., TAN, Y., BETANCOURT, M., VITERI, E., RAMKHELLAWAN, G. C., EWALD, E., FEUER, W., HUANG, D., WEN, R., HONG, L., WANG, H., LAIRD, J. M., SENE, A., APTE, R. S., SALOMON, R. G., HOLLYFIELD, J. G. & PEREZ, V. L. 2013. Infiltration of proinflammatory m1 macrophages into the outer retina precedes damage in a mouse model of age-related macular degeneration. *Int J Inflamm*, 2013, 503725.

- CUENCA, N., FERNANDEZ-SANCHEZ, L., CAMPELLO, L., MANEU, V., DE LA VILLA, P., LAX, P. & PINILLA, I. 2014. Cellular responses following retinal injuries and therapeutic approaches for neurodegenerative diseases. *Prog Retin Eye Res*, 43, 17-75.
- DA POZZO, E., COSTA, B. & MARTINI, C. 2012. Translocator protein (TSPO) and neurosteroids: implications in psychiatric disorders. *Curr Mol Med*, 12, 426-42.
- DANNHAUSEN, K., KARLSTETTER, M., CARAMOY, A., VOLZ, C., JAGLE, H., LIEBISCH, G., UTERMOHLEN, O. & LANGMANN, T. 2015. Acid sphingomyelinase (aSMase) deficiency leads to abnormal microglia behavior and disturbed retinal function. *Biochem Biophys Res Commun*.
- DAUGHERTY, D. J., SELVARAJ, V., CHECHNEVA, O. V., LIU, X. B., PLEASURE, D. E. & DENG, W. 2013. A TSPO ligand is protective in a mouse model of multiple sclerosis. *EMBO Mol Med*, 5, 891-903.
- DIMARIO, J. X. 2002. Activation and repression of growth factor receptor gene transcription (Review). *Int J Mol Med*, 10, 65-71.
- DIRSCHERL, K., KARLSTETTER, M., EBERT, S., KRAUS, D., HLAWATSCH, J., WALCZAK, Y., MOEHLE, C., FUCHSHOFER, R. & LANGMANN, T. 2010. Luteolin triggers global changes in the microglial transcriptome leading to a unique anti-inflammatory and neuroprotective phenotype. *J Neuroinflammation*, 7, 3.
- DUFFIELD, J. S. 2003. The inflammatory macrophage: a story of Jekyll and Hyde. *Clin Sci (Lond)*, 104, 27-38.
- EADY, T. N., KHOUTOROVA, L., OBENAU, A., MOHD-YUSOF, A., BAZAN, N. G. & BELAYEV, L. 2014. Docosahexaenoic acid complexed to albumin provides neuroprotection after experimental stroke in aged rats. *Neurobiol Dis*, 62, 1-7.
- EBERT, S., WALCZAK, Y., REME, C. & LANGMANN, T. 2012. Microglial activation and transcriptomic changes in the blue light-exposed mouse retina. *Adv Exp Med Biol*, 723, 619-32.
- EBERT, S., WEIGELT, K., WALCZAK, Y., DROBNIK, W., MAUERER, R., HUME, D. A., WEBER, B. H. & LANGMANN, T. 2009. Docosahexaenoic acid attenuates microglial activation and delays early retinal degeneration. *J Neurochem*, 110, 1863-75.
- ERIKSSON, A., FLACH, C. F., LINDGREN, A., KVIFORS, E. & LANGE, S. 2008. Five mucosal transcripts of interest in ulcerative colitis identified by quantitative real-time PCR: a prospective study. *BMC Gastroenterol*, 8, 34.
- ETER, N., ENGEL, D. R., MEYER, L., HELB, H. M., ROTH, F., MAURER, J., HOLZ, F. G. & KURTS, C. 2008. In vivo visualization of dendritic cells, macrophages, and microglial cells responding to laser-induced damage in the fundus of the eye. *Invest Ophthalmol Vis Sci*, 49, 3649-58.
- FERZAZ, B., BRAULT, E., BOURLIAUD, G., ROBERT, J. P., POUGHON, G., CLAUSTRE, Y., MARGUET, F., LIERE, P., SCHUMACHER, M., NOWICKI, J. P., FOURNIER, J., MARABOUT, B., SEVRIN, M., GEORGE, P., SOUBRIE, P., BENAVIDES, J. & SCATTON, B. 2002. SSR180575 (7-chloro-N,N,5-trimethyl-4-oxo-3-phenyl-3,5-dihydro-4H-pyridazino[4,5-b]indole-1-acetamide), a peripheral benzodiazepine receptor ligand, promotes neuronal survival and repair. *J Pharmacol Exp Ther*, 301, 1067-78.
- FRANK, M. G., WEBER, M. D., WATKINS, L. R. & MAIER, S. F. 2015. Stress sounds the alarmin: The role of the danger-associated molecular pattern HMGB1 in stress-induced neuroinflammatory priming. *Brain Behav Immun*.
- FREUND, C. L., GREGORY-EVANS, C. Y., FURUKAWA, T., PAPAIOANNOU, M., LOOSER, J., PLODER, L., BELLINGHAM, J., NG, D., HERBRICK, J. A., DUNCAN, A., SCHERER, S. W., TSUI, L. C., LOUTRADIS-ANAGNOSTOU, A., JACOBSON, S. G., CEPKO, C. L., BHATTACHARYA, S. S. & MCINNES, R. R. 1997. Cone-rod dystrophy due to mutations in a novel photoreceptor-specific homeobox gene (CRX) essential for maintenance of the photoreceptor. *Cell*, 91, 543-53.
- FREUND, C. L., WANG, Q. L., CHEN, S., MUSKAT, B. L., WILES, C. D., SHEFFIELD, V. C., JACOBSON, S. G., MCINNES, R. R., ZACK, D. J. & STONE, E. M. 1998. De

- novo mutations in the CRX homeobox gene associated with Leber congenital amaurosis. *Nat Genet*, 18, 311-2.
- FURUKAWA, T., MORROW, E. M. & CEPKO, C. L. 1997. Crx, a novel otx-like homeobox gene, shows photoreceptor-specific expression and regulates photoreceptor differentiation. *Cell*, 91, 531-41.
- FURUKAWA, T., MORROW, E. M., LI, T., DAVIS, F. C. & CEPKO, C. L. 1999. Retinopathy and attenuated circadian entrainment in Crx-deficient mice. *Nat Genet*, 23, 466-70.
- GAO, H. M., ZHOU, H., ZHANG, F., WILSON, B. C., KAM, W. & HONG, J. S. 2011. HMGB1 acts on microglia Mac1 to mediate chronic neuroinflammation that drives progressive neurodegeneration. *J Neurosci*, 31, 1081-92.
- GAO, Y., LECKER, S., POST, M. J., HIETARANTA, A. J., LI, J., VOLK, R., LI, M., SATO, K., SALUJA, A. K., STEER, M. L., GOLDBERG, A. L. & SIMONS, M. 2000. Inhibition of ubiquitin-proteasome pathway-mediated I kappa B alpha degradation by a naturally occurring antibacterial peptide. *J Clin Invest*, 106, 439-48.
- GAVISH, M., KATZ, Y., BAR-AMI, S. & WEIZMAN, R. 1992. Biochemical, physiological, and pathological aspects of the peripheral benzodiazepine receptor. *J Neurochem*, 58, 1589-601.
- GEHRIG, A., LANGMANN, T., HORLING, F., JANSSEN, A., BONIN, M., WALTER, M., POTHS, S. & WEBER, B. H. 2007. Genome-wide expression profiling of the retinoschisin-deficient retina in early postnatal mouse development. *Invest Ophthalmol Vis Sci*, 48, 891-900.
- GEHRMANN, J., MATSUMOTO, Y. & KREUTZBERG, G. W. 1995. Microglia: intrinsic immune effector cell of the brain. *Brain Res Brain Res Rev*, 20, 269-87.
- GHASEMLOU, N., BOUHY, D., YANG, J., LOPEZ-VALES, R., HABER, M., THURASINGAM, T., HE, G., RADZIOCH, D., DING, A. & DAVID, S. 2010. Beneficial effects of secretory leukocyte protease inhibitor after spinal cord injury. *Brain*, 133, 126-38.
- GIATTI, S., CARUSO, D., BORASO, M., ABBIATI, F., BALLARINI, E., CALABRESE, D., PESARESI, M., RIGOLIO, R., SANTOS-GALINDO, M., VIVIANI, B., CAVALETTI, G., GARCIA-SEGURA, L. M. & MELCANGI, R. C. 2012. Neuroprotective effects of progesterone in chronic experimental autoimmune encephalomyelitis. *J Neuroendocrinol*, 24, 851-61.
- GINHOUX, F., GRETER, M., LEBOEUF, M., NANDI, S., SEE, P., GOKHAN, S., MEHLER, M. F., CONWAY, S. J., NG, L. G., STANLEY, E. R., SAMOKHVALOV, I. M. & MERAD, M. 2010. Fate mapping analysis reveals that adult microglia derive from primitive macrophages. *Science*, 330, 841-5.
- GINHOUX, F. & JUNG, S. 2014. Monocytes and macrophages: developmental pathways and tissue homeostasis. *Nat Rev Immunol*, 14, 392-404.
- GIRARD, C., LIU, S., ADAMS, D., LACROIX, C., SINEUS, M., BOUCHER, C., PAPADOPOULOS, V., RUPPRECHT, R., SCHUMACHER, M. & GROYSER, G. 2012. Axonal regeneration and neuroinflammation: roles for the translocator protein 18 kDa. *J Neuroendocrinol*, 24, 71-81.
- GREENE, C. M., MCELVANEY, N. G., O'NEILL, S. J. & TAGGART, C. C. 2004. Secretory leucoprotease inhibitor impairs Toll-like receptor 2- and 4-mediated responses in monocytic cells. *Infect Immun*, 72, 3684-7.
- GUPTA, N., BROWN, K. E. & MILAM, A. H. 2003. Activated microglia in human retinitis pigmentosa, late-onset retinal degeneration, and age-related macular degeneration. *Exp Eye Res*, 76, 463-71.
- GUPTA, S. K., KUMAR, B., NAG, T. C., AGRAWAL, S. S., AGRAWAL, R., AGRAWAL, P., SAXENA, R. & SRIVASTAVA, S. 2011. Curcumin prevents experimental diabetic retinopathy in rats through its hypoglycemic, antioxidant, and anti-inflammatory mechanisms. *J Ocul Pharmacol Ther*, 27, 123-30.
- GUT, P., ZWECKSTETTER, M. & BANATI, R. B. 2015. Lost in translocation: the functions of the 18-kD translocator protein. *Trends Endocrinol Metab*.

- HANISCH, U. K. & KETTENMANN, H. 2007. Microglia: active sensor and versatile effector cells in the normal and pathologic brain. *Nat Neurosci*, 10, 1387-94.
- HANNILA, S. S. 2014. Secretory Leukocyte Protease Inhibitor (SLPI): Emerging Roles in CNS Trauma and Repair. *Neuroscientist*.
- HANNILA, S. S., SIDDIQ, M. M., CARMEL, J. B., HOU, J., CHAUDHRY, N., BRADLEY, P. M., HILAIRE, M., RICHMAN, E. L., HART, R. P. & FILBIN, M. T. 2013. Secretory leukocyte protease inhibitor reverses inhibition by CNS myelin, promotes regeneration in the optic nerve, and suppresses expression of the transforming growth factor-beta signaling protein Smad2. *J Neurosci*, 33, 5138-51.
- HAO, H., KIM, D. S., KLOCKE, B., JOHNSON, K. R., CUI, K., GOTOH, N., ZANG, C., GREGORSKI, J., GIESER, L., PENG, W., FANN, Y., SEIFERT, M., ZHAO, K. & SWAROOP, A. 2012. Transcriptional regulation of rod photoreceptor homeostasis revealed by in vivo NRL targetome analysis. *PLoS Genet*, 8, e1002649.
- HARADA, B. T., KNIGHT, M. J., IMAI, S., QIAO, F., RAMACHANDER, R., SAWAYA, M. R., GINGERY, M., SAKANE, F. & BOWIE, J. U. 2008. Regulation of enzyme localization by polymerization: polymer formation by the SAM domain of diacylglycerol kinase delta1. *Structure*, 16, 380-7.
- HENEKA, M. T., KUMMER, M. P. & LATZ, E. 2014. Innate immune activation in neurodegenerative disease. *Nat Rev Immunol*, 14, 463-77.
- HENNIG, A. K., PENG, G. H. & CHEN, S. 2008. Regulation of photoreceptor gene expression by Crx-associated transcription factor network. *Brain Res*, 1192, 114-33.
- HENRIKSEN, P. A., DEVITT, A., KOTELEVTSYEV, Y. & SALLENAVE, J. M. 2004. Gene delivery of the elastase inhibitor elafin protects macrophages from neutrophil elastase-mediated impairment of apoptotic cell recognition. *FEBS Lett*, 574, 80-4.
- HICKEY, W. F. & KIMURA, H. 1988. Perivascular microglial cells of the CNS are bone marrow-derived and present antigen in vivo. *Science*, 239, 290-2.
- HLAWATSCH, J., KARLSTETTER, M., ASLANIDIS, A., LUCKOFF, A., WALCZAK, Y., PLANK, M., BOCK, J. & LANGMANN, T. 2013. Sterile alpha motif containing 7 (samd7) is a novel crx-regulated transcriptional repressor in the retina. *PLoS One*, 8, e60633.
- HOEK, R. M., RUULS, S. R., MURPHY, C. A., WRIGHT, G. J., GODDARD, R., ZURAWSKI, S. M., BLOM, B., HOMOLA, M. E., STREIT, W. J., BROWN, M. H., BARCLAY, A. N. & SEDGWICK, J. D. 2000. Down-regulation of the macrophage lineage through interaction with OX2 (CD200). *Science*, 290, 1768-71.
- HOLLYFIELD, J. G., PEREZ, V. L. & SALOMON, R. G. 2010. A hapten generated from an oxidation fragment of docosahexaenoic acid is sufficient to initiate age-related macular degeneration. *Mol Neurobiol*, 41, 290-8.
- HONG, S. H., CHOI, H. B., KIM, S. U. & MCLARNON, J. G. 2006. Mitochondrial ligand inhibits store-operated calcium influx and COX-2 production in human microglia. *J Neurosci Res*, 83, 1293-8.
- HSIAU, T. H., DIACONU, C., MYERS, C. A., LEE, J., CEPKO, C. L. & CORBO, J. C. 2007. The cis-regulatory logic of the mammalian photoreceptor transcriptional network. *PLoS One*, 2, e643.
- HUME, D. A., PERRY, V. H. & GORDON, S. 1983. Immunohistochemical localization of a macrophage-specific antigen in developing mouse retina: phagocytosis of dying neurons and differentiation of microglial cells to form a regular array in the plexiform layers. *J Cell Biol*, 97, 253-7.
- HUYGHE, S., SCHMALBRUCH, H., HULSHAGEN, L., VELDHOVEN, P. V., BAES, M. & HARTMANN, D. 2006. Peroxisomal multifunctional protein-2 deficiency causes motor deficits and glial lesions in the adult central nervous system. *Am J Pathol*, 168, 1321-34.
- INOUE, T., TERADA, K., FURUKAWA, A., KOIKE, C., TAMAKI, Y., ARAIE, M. & FURUKAWA, T. 2006. Cloning and characterization of mr-s, a novel SAM

- domain protein, predominantly expressed in retinal photoreceptor cells. *BMC Dev Biol*, 6, 15.
- ITO, D., IMAI, Y., OHSAWA, K., NAKAJIMA, K., FUKUUCHI, Y. & KOHSAKA, S. 1998. Microglia-specific localisation of a novel calcium binding protein, Iba1. *Brain Res Mol Brain Res*, 57, 1-9.
- JACOBSEN, L. C., SORENSEN, O. E., COWLAND, J. B., BORREGAARD, N. & THEILGAARD-MONCH, K. 2008. The secretory leukocyte protease inhibitor (SLPI) and the secondary granule protein lactoferrin are synthesized in myelocytes, colocalize in subcellular fractions of neutrophils, and are coreleased by activated neutrophils. *J Leukoc Biol*, 83, 1155-64.
- JAGER, R. D., MIELER, W. F. & MILLER, J. W. 2008. Age-related macular degeneration. *N Engl J Med*, 358, 2606-17.
- JANG, S., DILGER, R. N. & JOHNSON, R. W. 2010. Luteolin inhibits microglia and alters hippocampal-dependent spatial working memory in aged mice. *J Nutr*, 140, 1892-8.
- JANG, S., KELLEY, K. W. & JOHNSON, R. W. 2008. Luteolin reduces IL-6 production in microglia by inhibiting JNK phosphorylation and activation of AP-1. *Proc Natl Acad Sci U S A*, 105, 7534-9.
- JIN, F. Y., NATHAN, C., RADZIOCH, D. & DING, A. 1997. Secretory leukocyte protease inhibitor: a macrophage product induced by and antagonistic to bacterial lipopolysaccharide. *Cell*, 88, 417-26.
- JIN, G., LONG, C., LIU, W., TANG, Y., ZHU, Y., ZHOU, X., AI, Y., ZHANG, Q. & SHEN, H. 2013. Identification and characterization of novel alternative splice variants of human SAMD11. *Gene*, 530, 215-21.
- JOLY, S., FRANCKE, M., ULBRICHT, E., BECK, S., SEELIGER, M., HIRRLINGER, P., HIRRLINGER, J., LANG, K. S., ZINKERNAGEL, M., ODERMATT, B., SAMARDZIJA, M., REICHENBACH, A., GRIMM, C. & REME, C. E. 2009. Cooperative phagocytes: resident microglia and bone marrow immigrants remove dead photoreceptors in retinal lesions. *Am J Pathol*, 174, 2310-23.
- JUNG, S., ALIBERTI, J., GRAEMMEL, P., SUNSHINE, M. J., KREUTZBERG, G. W., SHER, A. & LITTMAN, D. R. 2000. Analysis of fractalkine receptor CX(3)CR1 function by targeted deletion and green fluorescent protein reporter gene insertion. *Mol Cell Biol*, 20, 4106-14.
- KARCHEWSKI, L. A., BLOECHLINGER, S. & WOOLF, C. J. 2004. Axonal injury-dependent induction of the peripheral benzodiazepine receptor in small-diameter adult rat primary sensory neurons. *Eur J Neurosci*, 20, 671-83.
- KARLSTETTER, M., LIPPE, E., WALCZAK, Y., MOEHLE, C., ASLANIDIS, A., MIRZA, M. & LANGMANN, T. 2011. Curcumin is a potent modulator of microglial gene expression and migration. *J Neuroinflammation*, 8, 125.
- KARLSTETTER, M., NOTHDURFTE, C., ASLANIDIS, A., MOELLER, K., HORN, F., SCHOLZ, R., NEUMANN, H., WEBER, B. H., RUPPRECHT, R. & LANGMANN, T. 2014a. Translocator protein (18 kDa) (TSPO) is expressed in reactive retinal microglia and modulates microglial inflammation and phagocytosis. *J Neuroinflammation*, 11, 3.
- KARLSTETTER, M., SCHOLZ, R., RUTAR, M., WONG, W. T., PROVIS, J. M. & LANGMANN, T. 2015. Retinal microglia: just bystander or target for therapy? *Prog Retin Eye Res*, 45, 30-57.
- KARLSTETTER, M., SORUSCH, N., CARAMOY, A., DANNHAUSEN, K., ASLANIDIS, A., FAUSER, S., BOESL, M. R., NAGEL-WOLFRUM, K., TAMM, E. R., JAGLE, H., STOEHR, H., WOLFRUM, U. & LANGMANN, T. 2014b. Disruption of the retinitis pigmentosa 28 gene Fam161a in mice affects photoreceptor ciliary structure and leads to progressive retinal degeneration. *Hum Mol Genet*, 23, 5197-210.
- KARLSTETTER, M., WALCZAK, Y., WEIGELT, K., EBERT, S., VAN DEN BRULLE, J., SCHWER, H., FUCHSHOFER, R. & LANGMANN, T. 2010. The novel activated microglia/macrophage WAP domain protein, AMWAP, acts as a counter-regulator of proinflammatory response. *J Immunol*, 185, 3379-90.

- KARPERIEN, A., AHAMMER, H. & JELINEK, H. F. 2013. Quantitating the subtleties of microglial morphology with fractal analysis. *Front Cell Neurosci*, 7, 3.
- KIM, C. A. & BOWIE, J. U. 2003. SAM domains: uniform structure, diversity of function. *Trends Biochem Sci*, 28, 625-8.
- KITA, A., KOHAYAKAWA, H., KINOSHITA, T., OCHI, Y., NAKAMICHI, K., KURUMIYA, S., FURUKAWA, K. & OKA, M. 2004. Antianxiety and antidepressant-like effects of AC-5216, a novel mitochondrial benzodiazepine receptor ligand. *Br J Pharmacol*, 142, 1059-72.
- KLIMENKOVA, O., ELLERBECK, W., KLIMIANKOU, M., UNALAN, M., KANDABARAU, S., GIGINA, A., HUSSEIN, K., ZEIDLER, C., WELTE, K. & SKOKOWA, J. 2014. A lack of secretory leukocyte protease inhibitor (SLPI) causes defects in granulocytic differentiation. *Blood*, 123, 1239-49.
- KLINKE, R., BAUER, C. & SILBERNAGL, S. 2003. *Lehrbuch der Physiologie*.
- LAI, Z. C. & RUBIN, G. M. 1992. Negative control of photoreceptor development in *Drosophila* by the product of the *yan* gene, an ETS domain protein. *Cell*, 70, 609-20.
- LAMBERT, V., LECOMTE, J., HANSEN, S., BLACHER, S., GONZALEZ, M. L., STRUMAN, I., SOUNNI, N. E., ROZET, E., DE TULLIO, P., FOIDART, J. M., RAKIC, J. M. & NOEL, A. 2013. Laser-induced choroidal neovascularization model to study age-related macular degeneration in mice. *Nat Protoc*, 8, 2197-211.
- LANGMANN, T. 2007. Microglia activation in retinal degeneration. *J Leukoc Biol*, 81, 1345-51.
- LANGMANN, T., DI GIOIA, S. A., RAU, I., STOHR, H., MAKSIMOVIC, N. S., CORBO, J. C., RENNER, A. B., ZRENNER, E., KUMARAMANICKAVEL, G., KARLSTETTER, M., ARSENIJEVIC, Y., WEBER, B. H., GAL, A. & RIVOLTA, C. 2010. Nonsense mutations in FAM161A cause RP28-associated recessive retinitis pigmentosa. *Am J Hum Genet*, 87, 376-81.
- LASKIN, D. L. 2009. Macrophages and inflammatory mediators in chemical toxicity: a battle of forces. *Chem Res Toxicol*, 22, 1376-85.
- LEE, J. E., LIANG, K. J., FARISS, R. N. & WONG, W. T. 2008. Ex vivo dynamic imaging of retinal microglia using time-lapse confocal microscopy. *Invest Ophthalmol Vis Sci*, 49, 4169-76.
- LI, H. & PAPADOPOULOS, V. 1998. Peripheral-type benzodiazepine receptor function in cholesterol transport. Identification of a putative cholesterol recognition/interaction amino acid sequence and consensus pattern. *Endocrinology*, 139, 4991-7.
- LI, R., SHEN, Y., YANG, L. B., LUE, L. F., FINCH, C. & ROGERS, J. 2000. Estrogen enhances uptake of amyloid beta-protein by microglia derived from the human cortex. *J Neurochem*, 75, 1447-54.
- LI, Z., MOY, A., GOMEZ, S. R., FRANZ, A. H., LIN-CEREGHINO, J. & LIN-CEREGHINO, G. P. 2010. An improved method for enhanced production and biological activity of human secretory leukocyte protease inhibitor (SLPI) in *Pichia pastoris*. *Biochem Biophys Res Commun*, 402, 519-24.
- LI, Z., MOY, A., SOHAL, K., DAM, C., KUO, P., WHITTAKER, J., WHITTAKER, M., DUZGUNES, N., KONOPKA, K., FRANZ, A. H., LIN-CEREGHINO, J. & LIN-CEREGHINO, G. P. 2009. Expression and characterization of recombinant human secretory leukocyte protease inhibitor (SLPI) protein from *Pichia pastoris*. *Protein Expr Purif*, 67, 175-81.
- LIANG, K. J., LEE, J. E., WANG, Y. D., MA, W., FONTAINHAS, A. M., FARISS, R. N. & WONG, W. T. 2009. Regulation of dynamic behavior of retinal microglia by CX3CR1 signaling. *Invest Ophthalmol Vis Sci*, 50, 4444-51.
- LILLO, E., WALD-ALTMAN, S., SOLMESKY, L. J., BEN YAAKOV, K., GERSHONI-EMEK, N., BULVIK, S., KASSIS, I., KARUSSIS, D., PERLSON, E. & WEIL, M. 2013. Characterization of human sporadic ALS biomarkers in the familial ALS transgenic mSOD1(G93A) mouse model. *Hum Mol Genet*, 22, 4720-5.

- LIM, S. N., HUANG, W., HALL, J. C., MICHAEL-TITUS, A. T. & PRIESTLEY, J. V. 2013. Improved outcome after spinal cord compression injury in mice treated with docosahexaenoic acid. *Exp Neurol*, 239, 13-27.
- LINNARTZ-GERLACH, B., KOPATZ, J. & NEUMANN, H. 2014. Siglec functions of microglia. *Glycobiology*, 24, 794-9.
- LIU, J., COPLAND, D. A., HORIE, S., WU, W. K., CHEN, M., XU, Y., PAUL MORGAN, B., MACK, M., XU, H., NICHOLSON, L. B. & DICK, A. D. 2013. Myeloid cells expressing VEGF and arginase-1 following uptake of damaged retinal pigment epithelium suggests potential mechanism that drives the onset of choroidal angiogenesis in mice. *PLoS One*, 8, e72935.
- MAEDA, J., HIGUCHI, M., INAJI, M., JI, B., HANEDA, E., OKAUCHI, T., ZHANG, M. R., SUZUKI, K. & SUHARA, T. 2007. Phase-dependent roles of reactive microglia and astrocytes in nervous system injury as delineated by imaging of peripheral benzodiazepine receptor. *Brain Res*, 1157, 100-11.
- MAKRANZ, C., COHEN, G., BARON, A., LEVIDOR, L., KODAMA, T., REICHERT, F. & ROTSHENKER, S. 2004. Phosphatidylinositol 3-kinase, phosphoinositide-specific phospholipase-Cgamma and protein kinase-C signal myelin phagocytosis mediated by complement receptor-3 alone and combined with scavenger receptor-AI/II in macrophages. *Neurobiol Dis*, 15, 279-86.
- MARIN-TEVA, J. L., DUSART, I., COLIN, C., GERVAIS, A., VAN ROOIJEN, N. & MALLAT, M. 2004. Microglia promote the death of developing Purkinje cells. *Neuron*, 41, 535-47.
- MARINO, F., CATTANEO, S., COSENTINO, M., RASINI, E., DI GRAZIA, L., FIETTA, A. M., LECCHINI, S. & FRIGO, G. 2001. Diazepam stimulates migration and phagocytosis of human neutrophils: possible contribution of peripheral-type benzodiazepine receptors and intracellular calcium. *Pharmacology*, 63, 42-9.
- MARINO, R., THURAISSINGAM, T., CAMATEROS, P., KANAGARATHAM, C., XU, Y. Z., HENRI, J., YANG, J., HE, G., DING, A. & RADZIOCH, D. 2011. Secretory leukocyte protease inhibitor plays an important role in the regulation of allergic asthma in mice. *J Immunol*, 186, 4433-42.
- MEARS, A. J., KONDO, M., SWAIN, P. K., TAKADA, Y., BUSH, R. A., SAUNDERS, T. L., SIEVING, P. A. & SWAROOP, A. 2001. Nrl is required for rod photoreceptor development. *Nat Genet*, 29, 447-52.
- MILAM, A. H., ROSE, L., CIDECIYAN, A. V., BARAKAT, M. R., TANG, W. X., GUPTA, N., ALEMAN, T. S., WRIGHT, A. F., STONE, E. M., SHEFFIELD, V. C. & JACOBSON, S. G. 2002. The nuclear receptor NR2E3 plays a role in human retinal photoreceptor differentiation and degeneration. *Proc Natl Acad Sci U S A*, 99, 473-8.
- MINGHETTI, L. & LEVI, G. 1998. Microglia as effector cells in brain damage and repair: focus on prostanoids and nitric oxide. *Prog Neurobiol*, 54, 99-125.
- MIRZA, M., VOLZ, C., KARLSTETTER, M., LANGIU, M., SOMOGYI, A., RUONALA, M. O., TAMM, E. R., JAGLE, H. & LANGMANN, T. 2013. Progressive retinal degeneration and glial activation in the CLN6 (nclf) mouse model of neuronal ceroid lipofuscinosis: a beneficial effect of DHA and curcumin supplementation. *PLoS One*, 8, e75963.
- MITTON, K. P., SWAIN, P. K., CHEN, S., XU, S., ZACK, D. J. & SWAROOP, A. 2000. The leucine zipper of NRL interacts with the CRX homeodomain. A possible mechanism of transcriptional synergy in rhodopsin regulation. *J Biol Chem*, 275, 29794-9.
- MOREAU, T., BARANGER, K., DADE, S., DALLET-CHOISY, S., GUYOT, N. & ZANI, M. L. 2008. Multifaceted roles of human elafin and secretory leukocyte proteinase inhibitor (SLPI), two serine protease inhibitors of the chelonianin family. *Biochimie*, 90, 284-95.
- MOROHAKU, K., PELTON, S. H., DAUGHERTY, D. J., BUTLER, W. R., DENG, W. & SELVARAJ, V. 2014. Translocator protein/peripheral benzodiazepine receptor is not required for steroid hormone biosynthesis. *Endocrinology*, 155, 89-97.

- MORROW, E. M., FURUKAWA, T. & CEPKO, C. L. 1998. Vertebrate photoreceptor cell development and disease. *Trends Cell Biol*, 8, 353-8.
- MUELLER, A. M., PEDRE, X., STEMPFL, T., KLEITER, I., COUILLARD-DESPRES, S., AIGNER, L., GIEGERICH, G. & STEINBRECHER, A. 2008. Novel role for SLPI in MOG-induced EAE revealed by spinal cord expression analysis. *J Neuroinflammation*, 5, 20.
- NAKAMURA, K., FUKUNISHI, I., NAKAMOTO, Y., IWAHASHI, K. & YOSHII, M. 2002. Peripheral-type benzodiazepine receptors on platelets are correlated with the degrees of anxiety in normal human subjects. *Psychopharmacology (Berl)*, 162, 301-3.
- NEWMAN, A. M., GALLO, N. B., HANCOX, L. S., MILLER, N. J., RADEKE, C. M., MALONEY, M. A., COOPER, J. B., HAGEMAN, G. S., ANDERSON, D. H., JOHNSON, L. V. & RADEKE, M. J. 2012. Systems-level analysis of age-related macular degeneration reveals global biomarkers and phenotype-specific functional networks. *Genome Med*, 4, 16.
- NIMMERJAHN, A., KIRCHHOFF, F. & HELMCHEN, F. 2005. Resting microglial cells are highly dynamic surveillants of brain parenchyma in vivo. *Science*, 308, 1314-8.
- NISHIDA, A., FURUKAWA, A., KOIKE, C., TANO, Y., AIZAWA, S., MATSUO, I. & FURUKAWA, T. 2003. Otx2 homeobox gene controls retinal photoreceptor cell fate and pineal gland development. *Nat Neurosci*, 6, 1255-63.
- NOTHDURFTER, C., BAGHAI, T. C., SCHULE, C. & RUPPRECHT, R. 2012. Translocator protein (18 kDa) (TSPO) as a therapeutic target for anxiety and neurologic disorders. *Eur Arch Psychiatry Clin Neurosci*, 262 Suppl 2, S107-12.
- O'NEILL, L. A., GOLENBOCK, D. & BOWIE, A. G. 2013. The history of Toll-like receptors - redefining innate immunity. *Nat Rev Immunol*, 13, 453-60.
- OHSAWA, K., IMAI, Y., KANAZAWA, H., SASAKI, Y. & KOHSAKA, S. 2000. Involvement of Iba1 in membrane ruffling and phagocytosis of macrophages/microglia. *J Cell Sci*, 113 ( Pt 17), 3073-84.
- OMORI, Y., KATOH, K., SATO, S., MURANISHI, Y., CHAYA, T., ONISHI, A., MINAMI, T., FUJIKADO, T. & FURUKAWA, T. 2011. Analysis of transcriptional regulatory pathways of photoreceptor genes by expression profiling of the Otx2-deficient retina. *PLoS One*, 6, e19685.
- ORR, C. F., ROWE, D. B. & HALLIDAY, G. M. 2002. An inflammatory review of Parkinson's disease. *Prog Neurobiol*, 68, 325-40.
- OZGUL, R. K., SIEMIATKOWSKA, A. M., YUCEL, D., MYERS, C. A., COLLIN, R. W., ZONNEVELD, M. N., BERYOZKIN, A., BANIN, E., HOYNG, C. B., VAN DEN BORN, L. I., EUROPEAN RETINAL DISEASE, C., BOSE, R., SHEN, W., SHARON, D., CREMERS, F. P., KLEVERING, B. J., DEN HOLLANDER, A. I. & CORBO, J. C. 2011. Exome sequencing and cis-regulatory mapping identify mutations in MAK, a gene encoding a regulator of ciliary length, as a cause of retinitis pigmentosa. *Am J Hum Genet*, 89, 253-64.
- PAPADOPOULOS, V., AMRI, H., BOUJRAD, N., CASCIO, C., CULTY, M., GARNIER, M., HARDWICK, M., LI, H., VIDIC, B., BROWN, A. S., REVERSA, J. L., BERNASSAU, J. M. & DRIEU, K. 1997. Peripheral benzodiazepine receptor in cholesterol transport and steroidogenesis. *Steroids*, 62, 21-8.
- PAPADOPOULOS, V., BARALDI, M., GUILARTE, T. R., KNUDSEN, T. B., LACAPERE, J. J., LINDEMANN, P., NORENBURG, M. D., NUTT, D., WEIZMAN, A., ZHANG, M. R. & GAVISH, M. 2006. Translocator protein (18kDa): new nomenclature for the peripheral-type benzodiazepine receptor based on its structure and molecular function. *Trends Pharmacol Sci*, 27, 402-9.
- PAPADOPOULOS, V. & LECANU, L. 2009. Translocator protein (18 kDa) TSPO: an emerging therapeutic target in neurotrauma. *Exp Neurol*, 219, 53-7.
- PENFOLD, P. L., MADIGAN, M. C., GILLIES, M. C. & PROVIS, J. M. 2001. Immunological and aetiological aspects of macular degeneration. *Prog Retin Eye Res*, 20, 385-414.

- PERRY, V. H., NICOLL, J. A. & HOLMES, C. 2010. Microglia in neurodegenerative disease. *Nat Rev Neurol*, 6, 193-201.
- POCOCK, J. M. & KETTENMANN, H. 2007. Neurotransmitter receptors on microglia. *Trends Neurosci*, 30, 527-35.
- POLITIS, M., SU, P. & PICCINI, P. 2012. Imaging of microglia in patients with neurodegenerative disorders. *Front Pharmacol*, 3, 96.
- PONTING, C. P. 1995. SAM: a novel motif in yeast sterile and *Drosophila* polyhomeotic proteins. *Protein Sci*, 4, 1928-30.
- PORTERA-CAILLIAU, C., SUNG, C. H., NATHANS, J. & ADLER, R. 1994. Apoptotic photoreceptor cell death in mouse models of retinitis pigmentosa. *Proc Natl Acad Sci U S A*, 91, 974-8.
- PRINZ, M. & MILDNER, A. 2011. Microglia in the CNS: immigrants from another world. *Glia*, 59, 177-87.
- QIAO, F. & BOWIE, J. U. 2005. The many faces of SAM. *Sci STKE*, 2005, re7.
- QIAO, F., SONG, H., KIM, C. A., SAWAYA, M. R., HUNTER, J. B., GINGERY, M., REBAY, I., COUREY, A. J. & BOWIE, J. U. 2004. Derepression by depolymerization; structural insights into the regulation of Yan by Mae. *Cell*, 118, 163-73.
- RAIVICH, G. 2005. Like cops on the beat: the active role of resting microglia. *Trends Neurosci*, 28, 571-3.
- RAIVICH, G. & BANATI, R. 2004. Brain microglia and blood-derived macrophages: molecular profiles and functional roles in multiple sclerosis and animal models of autoimmune demyelinating disease. *Brain Res Brain Res Rev*, 46, 261-81.
- RATTNER, A., SUN, H. & NATHANS, J. 1999. Molecular genetics of human retinal disease. *Annu Rev Genet*, 33, 89-131.
- REARDON, C., LECHMANN, M., BRUSTLE, A., GAREAU, M. G., SHUMAN, N., PHILPOTT, D., ZIEGLER, S. F. & MAK, T. W. 2011. Thymic stromal lymphopoietin-induced expression of the endogenous inhibitory enzyme SLPI mediates recovery from colonic inflammation. *Immunity*, 35, 223-35.
- RECHICHI, M., SALVETTI, A., CHELLI, B., COSTA, B., DA POZZO, E., SPINETTI, F., LENA, A., EVANGELISTA, M., RAINALDI, G., MARTINI, C., GREMIGNI, V. & ROSSI, L. 2008. TSPO over-expression increases motility, transmigration and proliferation properties of C6 rat glioma cells. *Biochim Biophys Acta*, 1782, 118-25.
- REICHENBACH, A. & BRINGMANN, A. 2013. New functions of Muller cells. *Glia*, 61, 651-78.
- RIO-HORTEGA, P. D. 1939. THE MICROGLIA. *The Lancet*, 233(6036), pp.1023-1026.
- RIVAS, M. A. & VECINO, E. 2009. Animal models and different therapies for treatment of retinitis pigmentosa. *Histol Histopathol*, 24, 1295-322.
- RODRIGUEZ, M. J., MARTINEZ-MORENO, M., ORTEGA, F. J. & MAHY, N. 2013. Targeting microglial K(ATP) channels to treat neurodegenerative diseases: a mitochondrial issue. *Oxid Med Cell Longev*, 2013, 194546.
- ROTSCHENKER, S., REICHERT, F., GITIK, M., HAKLAI, R., ELAD-SFADIA, G. & KLOOG, Y. 2008. Galectin-3/MAC-2, Ras and PI3K activate complement receptor-3 and scavenger receptor-AI/II mediated myelin phagocytosis in microglia. *Glia*, 56, 1607-13.
- RUFF, M. R., PERT, C. B., WEBER, R. J., WAHL, L. M., WAHL, S. M. & PAUL, S. M. 1985. Benzodiazepine receptor-mediated chemotaxis of human monocytes. *Science*, 229, 1281-3.
- RUPPRECHT, R., PAPADOPOULOS, V., RAMMES, G., BAGHAI, T. C., FAN, J., AKULA, N., GROVER, G., ADAMS, D. & SCHUMACHER, M. 2010. Translocator protein (18 kDa) (TSPO) as a therapeutic target for neurological and psychiatric disorders. *Nat Rev Drug Discov*, 9, 971-88.
- RUPPRECHT, R., RAMMES, G., ESER, D., BAGHAI, T. C., SCHULE, C., NOTHDURFTER, C., TROXLER, T., GENTSCH, C., KALKMAN, H. O., CHAPERON, F., UZUNOV, V., MCALLISTER, K. H., BERTAINA-ANGLADE, V., LA ROCHELLE, C. D., TUERCK, D., FLOESSER, A., KIESE, B., SCHUMACHER, M., LANDGRAF, R., HOLSBOER,

- F. & KUCHER, K. 2009. Translocator protein (18 kD) as target for anxiolytics without benzodiazepine-like side effects. *Science*, 325, 490-3.
- RYU, J. K., CHOI, H. B. & MCLARNON, J. G. 2005. Peripheral benzodiazepine receptor ligand PK11195 reduces microglial activation and neuronal death in quinolinic acid-injected rat striatum. *Neurobiol Dis*, 20, 550-61.
- SALTER, M. W. & BEGGS, S. 2014. Sublime microglia: expanding roles for the guardians of the CNS. *Cell*, 158, 15-24.
- SANCHO-PELLUZ, J., ARANGO-GONZALEZ, B., KUSTERMANN, S., ROMERO, F. J., VAN VEEN, T., ZRENNER, E., EKSTROM, P. & PAQUET-DURAND, F. 2008. Photoreceptor cell death mechanisms in inherited retinal degeneration. *Mol Neurobiol*, 38, 253-69.
- SANTOS, A. M., MARTIN-OLIVA, D., FERRER-MARTIN, R. M., TASSI, M., CALVENTE, R., SIERRA, A., CARRASCO, M. C., MARIN-TEVA, J. L., NAVASCUES, J. & CUADROS, M. A. 2010. Microglial response to light-induced photoreceptor degeneration in the mouse retina. *J Comp Neurol*, 518, 477-92.
- SANUKI, R., OMORI, Y., KOIKE, C., SATO, S. & FURUKAWA, T. 2010. Panky, a novel photoreceptor-specific ankyrin repeat protein, is a transcriptional cofactor that suppresses CRX-regulated photoreceptor genes. *FEBS Lett*, 584, 753-8.
- SASMONO, R. T., OCEANDY, D., POLLARD, J. W., TONG, W., PAVLI, P., WAINWRIGHT, B. J., OSTROWSKI, M. C., HIMES, S. R. & HUME, D. A. 2003. A macrophage colony-stimulating factor receptor-green fluorescent protein transgene is expressed throughout the mononuclear phagocyte system of the mouse. *Blood*, 101, 1155-63.
- SCHAEFER, E. J., ROBINS, S. J., PATTON, G. M., SANDBERG, M. A., WEIGEL-DIFRANCO, C. A., ROSNER, B. & BERSON, E. L. 1995. Red blood cell membrane phosphatidylethanolamine fatty acid content in various forms of retinitis pigmentosa. *J Lipid Res*, 36, 1427-33.
- SCHLEGELMILCH, T., HENKE, K. & PERI, F. 2011. Microglia in the developing brain: from immunity to behaviour. *Curr Opin Neurobiol*, 21, 5-10.
- SCHUETZ, E. & THANOS, S. 2004. Microglia-targeted pharmacotherapy in retinal neurodegenerative diseases. *Curr Drug Targets*, 5, 619-27.
- SCHULE, C., ESER, D., BAGHAI, T. C., NOTHDURFTER, C., KESSLER, J. S. & RUPPRECHT, R. 2011. Neuroactive steroids in affective disorders: target for novel antidepressant or anxiolytic drugs? *Neuroscience*, 191, 55-77.
- SCOTT, A., WELDON, S. & TAGGART, C. C. 2011. SLPI and elafin: multifunctional antiproteases of the WFDC family. *Biochem Soc Trans*, 39, 1437-40.
- SIERRA, A., ABIEGA, O., SHAHRAZ, A. & NEUMANN, H. 2013. Janus-faced microglia: beneficial and detrimental consequences of microglial phagocytosis. *Front Cell Neurosci*, 7, 6.
- SILEIKYTE, J., BLACHLY-DYSON, E., SEWELL, R., CARPI, A., MENABO, R., DI LISA, F., RICCHELLI, F., BERNARDI, P. & FORTE, M. 2014. Regulation of the mitochondrial permeability transition pore by the outer membrane does not involve the peripheral benzodiazepine receptor (Translocator Protein of 18 kDa (TSPO)). *J Biol Chem*, 289, 13769-81.
- SIMPSON, K. J. & NICHOLAS, K. R. 2002. The comparative biology of whey proteins. *J Mammary Gland Biol Neoplasia*, 7, 313-26.
- SLUPSKY, C. M., GENTILE, L. N., DONALDSON, L. W., MACKERETH, C. D., SEIDEL, J. J., GRAVES, B. J. & MCINTOSH, L. P. 1998. Structure of the Ets-1 pointed domain and mitogen-activated protein kinase phosphorylation site. *Proc Natl Acad Sci U S A*, 95, 12129-34.
- SMALL, D. M., ZANI, M. L., QUINN, D. J., DALLET-CHOISY, S., GLASGOW, A. M., O'KANE, C., MCAULEY, D. F., MCNALLY, P., WELDON, S., MOREAU, T. & TAGGART, C. C. 2015. A functional variant of elafin with improved anti-inflammatory activity for pulmonary inflammation. *Mol Ther*, 23, 24-31.
- SOHOCKI, M. M., SULLIVAN, L. S., MINTZ-HITTNER, H. A., BIRCH, D., HECKENLIVELY, J. R., FREUND, C. L., MCINNES, R. R. & DAIGER, S. P. 1998. A range of clinical

- phenotypes associated with mutations in CRX, a photoreceptor transcription-factor gene. *Am J Hum Genet*, 63, 1307-15.
- SRINIVAS, M., NG, L., LIU, H., JIA, L. & FORREST, D. 2006. Activation of the blue opsin gene in cone photoreceptor development by retinoid-related orphan receptor beta. *Mol Endocrinol*, 20, 1728-41.
- STREIT, W. J. 2002. Microglia as neuroprotective, immunocompetent cells of the CNS. *Glia*, 40, 133-9.
- STROHMEIER, R., ROLLER, M., SANGER, N., KNECHT, R. & KUHL, H. 2002. Modulation of tamoxifen-induced apoptosis by peripheral benzodiazepine receptor ligands in breast cancer cells. *Biochem Pharmacol*, 64, 99-107.
- SUBRAMANIAM, D., HOLLANDER, C., WESTIN, U., ERJEFALT, J., STEVENS, T. & JANCIAUSKIENE, S. 2011. Secretory leukocyte protease inhibitor inhibits neutrophil apoptosis. *Respirology*, 16, 300-7.
- SUH, H. S., KIM, M. O. & LEE, S. C. 2005. Inhibition of granulocyte-macrophage colony-stimulating factor signaling and microglial proliferation by anti-CD45RO: role of Hck tyrosine kinase and phosphatidylinositol 3-kinase/Akt. *J Immunol*, 174, 2712-9.
- SUNG, C. H. & CHUANG, J. Z. 2010. The cell biology of vision. *J Cell Biol*, 190, 953-63.
- SUZUKI, M., TSUJIKAWA, M., ITABE, H., DU, Z. J., XIE, P., MATSUMURA, N., FU, X., ZHANG, R., SONODA, K. H., EGASHIRA, K., HAZEN, S. L. & KAMEI, M. 2012. Chronic photo-oxidative stress and subsequent MCP-1 activation as causative factors for age-related macular degeneration. *J Cell Sci*, 125, 2407-15.
- TAGGART, C. C., CRYAN, S. A., WELDON, S., GIBBONS, A., GREENE, C. M., KELLY, E., LOW, T. B., O'NEILL, S. J. & MCELVANEY, N. G. 2005. Secretory leucoprotease inhibitor binds to NF-kappaB binding sites in monocytes and inhibits p65 binding. *J Exp Med*, 202, 1659-68.
- TAGGART, C. C., GREENE, C. M., MCELVANEY, N. G. & O'NEILL, S. 2002. Secretory leucoprotease inhibitor prevents lipopolysaccharide-induced IkappaBalpha degradation without affecting phosphorylation or ubiquitination. *J Biol Chem*, 277, 33648-53.
- THANOS, S. 1991. The Relationship of Microglial Cells to Dying Neurons During Natural Neuronal Cell Death and Axotomy-induced Degeneration of the Rat Retina. *Eur J Neurosci*, 3, 1189-1207.
- TRAN, N. M. & CHEN, S. 2014. Mechanisms of blindness: animal models provide insight into distinct CRX-associated retinopathies. *Dev Dyn*, 243, 1153-66.
- TRAPANI, A., PALAZZO, C., DE CANDIA, M., LASORSA, F. M. & TRAPANI, G. 2013. Targeting of the translocator protein 18 kDa (TSPO): a valuable approach for nuclear and optical imaging of activated microglia. *Bioconjug Chem*, 24, 1415-28.
- TSOUMAKIDOU, M., BOULOUKAKI, I., THIMAKI, K., TZANAKIS, N. & SIAFAKAS, N. M. 2010. Innate immunity proteins in chronic obstructive pulmonary disease and idiopathic pulmonary fibrosis. *Exp Lung Res*, 36, 373-80.
- TU, H., BARR, M., DONG, D. L. & WIGLER, M. 1997. Multiple regulatory domains on the Byr2 protein kinase. *Mol Cell Biol*, 17, 5876-87.
- TU, L. N., MOROHAKU, K., MANNA, P. R., PELTON, S. H., BUTLER, W. R., STOCCO, D. M. & SELVARAJ, V. 2014. Peripheral benzodiazepine receptor/translocator protein global knock-out mice are viable with no effects on steroid hormone biosynthesis. *J Biol Chem*, 289, 27444-54.
- TU, L. N., ZHAO, A. H., STOCCO, D. M. & SELVARAJ, V. 2015. PK11195 effect on steroidogenesis is not mediated through the translocator protein (TSPO). *Endocrinology*, 156, 1033-9.
- TUMMALA, P., MALI, R. S., GUZMAN, E., ZHANG, X. & MITTON, K. P. 2010. Temporal ChIP-on-Chip of RNA-Polymerase-II to detect novel gene activation events during photoreceptor maturation. *Mol Vis*, 16, 252-71.
- VAN SCHIL, K., KARLSTETTER, M., ASLANIDIS, A., LEROY, B., COPPIETERS, F., DEPASSE, F., LANGMANN, T. & DE BAERE, E. 2015. Recessive RHO mutation

- E150K and SAMD7 regulatory variants in a consanguineous family with retinitis pigmentosa *Investigative Ophthalmology & Visual Science* June 2015, Vol.56,.
- VASIREDDY, V., CHAVALI, V. R., JOSEPH, V. T., KADAM, R., LIN, J. H., JAMISON, J. A., KOMPPELLA, U. B., REDDY, G. B. & AYYAGARI, R. 2011. Rescue of photoreceptor degeneration by curcumin in transgenic rats with P23H rhodopsin mutation. *PLoS One*, 6, e21193.
- VECINO, E., RODRIGUEZ, F. D., RUZAFRA, N., PEREIRO, X. & SHARMA, S. C. 2015. Glia-neuron interactions in the mammalian retina. *Prog Retin Eye Res*.
- VEIGA, S., AZCOITIA, I. & GARCIA-SEGURA, L. M. 2005. Ro5-4864, a peripheral benzodiazepine receptor ligand, reduces reactive gliosis and protects hippocampal hilar neurons from kainic acid excitotoxicity. *J Neurosci Res*, 80, 129-37.
- VENNETI, S., LOPRESTI, B. J. & WILEY, C. A. 2013. Molecular imaging of microglia/macrophages in the brain. *Glia*, 61, 10-23.
- VENNETI, S., WANG, G. & WILEY, C. A. 2007. Activated macrophages in HIV encephalitis and a macaque model show increased [3H](R)-PK11195 binding in a PI3-kinase-dependent manner. *Neurosci Lett*, 426, 117-22.
- VERLEYE, M., AKWA, Y., LIERE, P., LADURELLE, N., PIANOS, A., EYCHENNE, B., SCHUMACHER, M. & GILLARDIN, J. M. 2005. The anxiolytic etifoxine activates the peripheral benzodiazepine receptor and increases the neurosteroid levels in rat brain. *Pharmacol Biochem Behav*, 82, 712-20.
- VISEL, A., BRISTOW, J. & PENNACCHIO, L. A. 2007. Enhancer identification through comparative genomics. *Semin Cell Dev Biol*, 18, 140-52.
- WAGNER, A. H., TAYLOR, K. R., DELUCA, A. P., CASAVANT, T. L., MULLINS, R. F., STONE, E. M., SCHEETZ, T. E. & BRAUN, T. A. 2013. Prioritization of retinal disease genes: an integrative approach. *Hum Mutat*, 34, 853-9.
- WANG, H., ZHANG, K., ZHAO, L., TANG, J., GAO, L. & WEI, Z. 2014a. Anti-inflammatory effects of vinpocetine on the functional expression of nuclear factor-kappa B and tumor necrosis factor-alpha in a rat model of cerebral ischemia-reperfusion injury. *Neurosci Lett*, 566, 247-51.
- WANG, L., CHEN, K., LIU, K., ZHOU, Y., ZHANG, T., WANG, B. & MI, M. 2015. DHA inhibited AGEs-induced retinal microglia activation via suppression of the PPARgamma/NFkappaB pathway and reduction of signal transducers in the AGEs/RAGE axis recruitment into lipid rafts. *Neurochem Res*, 40, 713-22.
- WANG, M., WANG, X., ZHAO, L., MA, W., RODRIGUEZ, I. R., FARISS, R. N. & WONG, W. T. 2014b. Macrogliia-microglia interactions via TSPO signaling regulates microglial activation in the mouse retina. *J Neurosci*, 34, 3793-806.
- WANG, X., LI, X., XU, L., ZHAN, Y., YAISH-OHAD, S., ERHARDT, J. A., BARONE, F. C. & FEUERSTEIN, G. Z. 2003. Up-regulation of secretory leukocyte protease inhibitor (SLPI) in the brain after ischemic stroke: adenoviral expression of SLPI protects brain from ischemic injury. *Mol Pharmacol*, 64, 833-40.
- WANG, Y. & NEUMANN, H. 2010. Alleviation of neurotoxicity by microglial human Siglec-11. *J Neurosci*, 30, 3482-8.
- WEBER, B. H., SCHREWE, H., MOLDAY, L. L., GEHRIG, A., WHITE, K. L., SEELIGER, M. W., JAISSE, G. B., FRIEDBURG, C., TAMM, E. & MOLDAY, R. S. 2002. Inactivation of the murine X-linked juvenile retinoschisis gene, Rs1h, suggests a role of retinoschisin in retinal cell layer organization and synaptic structure. *Proc Natl Acad Sci U S A*, 99, 6222-7.
- WEI, X. H., WEI, X., CHEN, F. Y., ZANG, Y., XIN, W. J., PANG, R. P., CHEN, Y., WANG, J., LI, Y. Y., SHEN, K. F., ZHOU, L. J. & LIU, X. G. 2013. The upregulation of translocator protein (18 kDa) promotes recovery from neuropathic pain in rats. *J Neurosci*, 33, 1540-51.
- WILLIAMS, S. E., BROWN, T. I., ROGHANIAN, A. & SALLENAVE, J. M. 2006. SLPI and elafin: one glove, many fingers. *Clin Sci (Lond)*, 110, 21-35.
- XU, H., CHEN, M., MAYER, E. J., FORRESTER, J. V. & DICK, A. D. 2007. Turnover of resident retinal microglia in the normal adult mouse. *Glia*, 55, 1189-98.

- YANAGI, Y., TAKEZAWA, S. & KATO, S. 2002. Distinct functions of photoreceptor cell-specific nuclear receptor, thyroid hormone receptor beta2 and CRX in one photoreceptor development. *Invest Ophthalmol Vis Sci*, 43, 3489-94.
- YANG, J., ZHU, J., SUN, D. & DING, A. 2005. Suppression of macrophage responses to bacterial lipopolysaccharide (LPS) by secretory leukocyte protease inhibitor (SLPI) is independent of its anti-protease function. *Biochim Biophys Acta*, 1745, 310-7.
- YANG, Z., ZHAO, T., ZOU, Y., ZHANG, J. H. & FENG, H. 2014. Curcumin inhibits microglia inflammation and confers neuroprotection in intracerebral hemorrhage. *Immunol Lett*, 160, 89-95.
- YASUNO, F., OTA, M., KOSAKA, J., ITO, H., HIGUCHI, M., DORONBEKOV, T. K., NOZAKI, S., FUJIMURA, Y., KOEDA, M., ASADA, T. & SUHARA, T. 2008. Increased binding of peripheral benzodiazepine receptor in Alzheimer's disease measured by positron emission tomography with [<sup>11</sup>C]DAA1106. *Biol Psychiatry*, 64, 835-41.
- YEE, J. & CHRISTOU, N. V. 1993. Neutrophil priming by lipopolysaccharide involves heterogeneity in calcium-mediated signal transduction. Studies using fluo-3 and flow cytometry. *J Immunol*, 150, 1988-97.
- YOSHIDA, N., IKEDA, Y., NOTOMI, S., ISHIKAWA, K., MURAKAMI, Y., HISATOMI, T., ENAIDA, H. & ISHIBASHI, T. 2013. Laboratory evidence of sustained chronic inflammatory reaction in retinitis pigmentosa. *Ophthalmology*, 120, e5-12.
- ZASSLER, B., SCHERMER, C. & HUMPEL, C. 2003. Protein kinase C and phosphoinositol-3-kinase mediate differentiation or proliferation of slice-derived rat microglia. *Pharmacology*, 67, 211-5.
- ZEISS, C. J. & JOHNSON, E. A. 2004. Proliferation of microglia, but not photoreceptors, in the outer nuclear layer of the rd-1 mouse. *Invest Ophthalmol Vis Sci*, 45, 971-6.
- ZENG, H. Y., ZHU, X. A., ZHANG, C., YANG, L. P., WU, L. M. & TSO, M. O. 2005. Identification of sequential events and factors associated with microglial activation, migration, and cytotoxicity in retinal degeneration in rd mice. *Invest Ophthalmol Vis Sci*, 46, 2992-9.
- ZHANG, M. R., KUMATA, K., MAEDA, J., YANAMOTO, K., HATORI, A., OKADA, M., HIGUCHI, M., OBAYASHI, S., SUHARA, T. & SUZUKI, K. 2007. 11C-AC-5216: a novel PET ligand for peripheral benzodiazepine receptors in the primate brain. *J Nucl Med*, 48, 1853-61.
- ZHAO, L., ZABEL, M. K., WANG, X., MA, W., SHAH, P., FARISS, R. N., QIAN, H., PARKHURST, C. N., GAN, W. B. & WONG, W. T. 2015. Microglial phagocytosis of living photoreceptors contributes to inherited retinal degeneration. *EMBO Mol Med*.
- ZHAO, Y. Y., YU, J. Z., LI, Q. Y., MA, C. G., LU, C. Z. & XIAO, B. G. 2011. TSP0-specific ligand vinpocetine exerts a neuroprotective effect by suppressing microglial inflammation. *Neuron Glia Biol*, 7, 187-97.
- ZHU, H. T., BIAN, C., YUAN, J. C., CHU, W. H., XIANG, X., CHEN, F., WANG, C. S., FENG, H. & LIN, J. K. 2014a. Curcumin attenuates acute inflammatory injury by inhibiting the TLR4/MyD88/NF-kappaB signaling pathway in experimental traumatic brain injury. *J Neuroinflammation*, 11, 59.
- ZHU, L., BI, W., LU, D., ZHANG, C., SHU, X. & LU, D. 2014b. Luteolin inhibits SH-SY5Y cell apoptosis through suppression of the nuclear transcription factor-kappaB, mitogen-activated protein kinase and protein kinase B pathways in lipopolysaccharide-stimulated cocultured BV2 cells. *Exp Ther Med*, 7, 1065-1070.
- ZHU, L. H., BI, W., QI, R. B., WANG, H. D., WANG, Z. G., ZENG, Q., ZHAO, Y. R. & LU, D. X. 2011. Luteolin reduces primary hippocampal neurons death induced by neuroinflammation. *Neurol Res*, 33, 927-34.

## Acknowledgements

A PhD thesis is never the sole work of an individual, many people got significantly involved during these years and this is the time to express my heartfelt gratitude towards them.

First and foremost, I want to thank **Prof. Thomas Langmann**, my long-term supervisor and mentor. I consider myself incredibly blessed that our paths crossed already early on in my scientific journey and ignited a spark in myself. Thomas is a brilliant scientist and role model and provides so many opportunities for professional and personal growth, something I want to thank him for especially. I am also very grateful for his trust, support and the opportunity to follow him to Cologne as part of his new lab. Whoever gets to work with Thomas in the future, consider yourself lucky! Danke Thomas!

I also want to thank **Prof. Sabine Eming** and **Prof. Peter Kloppenburg** for being my IPMM Tutors, engaging in fruitful discussions and being part of my thesis revision committee.

A big thank you to the IPMM officials **Dr. Debora Grosskopf-Kroiher**, **Dr. Daniela Mutschler** and **Prof. Hildegard Büning**. It was a pleasure being part of the program and having had the opportunity to contribute to and represent the IPMM also abroad.

I want to thank **Prof. Claus Cursiefen**, **Prof. Bernd Kirchhof** and the **Hans und Marlies Stock Stiftung** for making our lab relocation from Regensburg to beautiful Cologne possible and giving us a warm welcome.

A huge thank you goes to **Dr. Marcus Karlstetter**, an outstanding scientist and incredible human being, who grew from a colleague to a good friend over these years. It is fair to say that his suggestions and honest words always helped my professional and, more importantly, personal growth. I wish him only the best for his future endeavours and hope that we will still find opportunities to get together for a lad talk from time to time. Merce Marcus!

Wonderful bench colleagues make science even more fun, therefore my heartfelt thank you goes to all current and former members of the Langmann lab, namely: **Isha Akhtar**, **Nadine Bremicker**, **Katharina Dannhausen**, **Jenny Fleischmann**, **Felicitas Horn**, **Anika Lückhoff**, **Rodica Maniu**, **Myriam Mirza**, **Katharina Möller**, **Christopher Nebel**, **Khalid Rashid**, **Viktoria Salz**, **Eva Scheiffert**, **Rebecca Scholz**, **Markus Sobotka**, **Anja Volkmann**, **Yana Walczak**, **Anne Wolf** and anyone I might have forgotten. I also want to thank **Dr. Markus Pietsch** and his whole lab for our fruitful collaboration and discussions.

I want to thank the **Pro Retina Germany foundation** for their everlasting support of my research. A big thank you especially to **Franz Badura**, a true companion who taught me that it doesn't necessarily take vision to see the beauty in life.

A heartfelt thank you goes to **Renáta**, for always supporting me during the rollercoaster ride a PhD thesis can sometimes become. Köszönöm szépen!

Most importantly, I want to thank **my beloved parents and family** for their unconditional support from day one. This thesis is entirely dedicated to them as I would not be here without them.

## Erklärung

Ich versichere, dass ich die von mir vorgelegte Dissertation selbständig angefertigt, die benutzten Quellen und Hilfsmittel vollständig angegeben und die Stellen der Arbeit – einschließlich Tabellen, Karten, und Abbildungen - , die anderen Werken im Wortlaut oder dem Sinn nach entnommen sind, in jedem Einzelfall als Entlehnung kenntlich gemacht habe; dass diese Dissertation noch keiner anderen Fakultät oder Universität zur Prüfung vorgelegen hat; dass sie abgesehen von unten angegebenen Teilpublikationen in wissenschaftlichen Fachzeitschriften noch nicht veröffentlicht worden ist sowie, dass ich eine solche Veröffentlichung vor Abschluss des Promotionsverfahrens nicht vornehmen werde. Die Bestimmungen dieser Promotionsordnung sind mir bekannt. Die von mir vorgelegte Dissertation ist von Prof. Dr. rer. nat. Thomas Langmann betreut worden.

### Publikationen:

Sterile alpha motif containing 7 (SAMD7) is a novel CRX-regulated transcriptional repressor in the retina.

Hlawatsch J\*, Karlstetter M\*, Aslanidis A\*, Lückoff A, Walczak Y, Plank M, Böck J, Langmann T.

*PLoS One*. 2013;8(4):e60633. doi: 10.1371/journal.pone.0060633.

Activated microglia/macrophage whey acidic protein (AMWAP) inhibits NFκB signaling and induces a neuroprotective phenotype in microglia.

Aslanidis A, Karlstetter M, Scholz R, Fauser S, Neumann H, Fried C, Pietsch M\*, Langmann T\*.

*J Neuroinflammation*. 2015 Apr 19;12:77. doi: 10.1186/s12974-015-0296-6.

Translocator protein (18 kDa) (TSPO) is expressed in reactive retinal microglia and modulates microglial inflammation and phagocytosis.

Karlstetter M\*, Nothdurfter C\*, Aslanidis A, Moeller K, Horn F, Scholz R, Neumann H, Weber BH, Rupprecht R\*, Langmann T\*.

*J Neuroinflammation*. 2014 Jan 8;11:3. doi: 10.1186/1742-2094-11-3.

Ich versichere, dass ich alle Angaben wahrheitsgemäß nach bestem Wissen und Gewissen gemacht habe und verpflichte mich, jedmögliche, die obigen Angaben betreffenden Veränderungen, dem Promotionsausschuss unverzüglich mitzuteilen.

Köln, den 28.07.2015

Alexander Aslanidis

# Sterile Alpha Motif Containing 7 (Samd7) Is a Novel Crx-Regulated Transcriptional Repressor in the Retina

Julia Hlawatsch<sup>1</sup>\*, Marcus Karlstetter<sup>1,2</sup>\*, Alexander Aslanidis<sup>1,2</sup>\*, Anika Lückhoff<sup>2</sup>, Yana Walczak<sup>1,2</sup>, Michael Plank<sup>1</sup>, Julia Böck<sup>1</sup>, Thomas Langmann<sup>1,2\*</sup>

**1** Institute of Human Genetics, University of Regensburg, Regensburg, Germany, **2** Department of Ophthalmology, University of Cologne, Cologne, Germany

## Abstract

Inherited retinal diseases are mainly caused by mutations in genes that are highly expressed in photoreceptors of the retina. The majority of these genes is under the control of the transcription factor Cone rod homeobox (Crx), that acts as a master transcription factor in photoreceptors. Using a genome-wide chromatin immunoprecipitation dataset that highlights all potential *in vivo* targets of Crx, we have identified a novel sterile alpha motif (SAM) domain containing protein, Samd7. mRNA Expression of Samd7 was confined to the late postnatal and adult mouse retina as well as the pineal gland. Using immunohistochemistry and Western blot, we could detect Samd7 protein in the outer nuclear layer of adult mouse retina. Ectopic over-expression in HEK293 cells demonstrated that Samd7 resides in the cytoplasm as well as the nucleus. *In vitro* electroporation of fluorescent reporters into living mouse retinal cultures revealed that transcription of the Samd7 gene depends on evolutionary conserved Crx motifs located in the first intron enhancer. Moreover, Crx knock-down with shRNA strongly reduced Samd7 reporter activity and endogenous Samd7 protein, indicating that Crx is required for retinal expression of Samd7. Finally, using co-transfections in luciferase reporter assays we found that Samd7 interferes with Crx-dependent transcription. Samd7 suppressed luciferase activity from a reporter plasmid with five Crx consensus repeats in a dose dependent manner and reduced Crx-mediated transactivation of regulatory sequences in the retinoschisin gene and the Samd7 gene itself. Taken together, we have identified a novel retinal SAM domain protein, Samd7, which could act as a transcriptional repressor involved in fine-tuning of Crx-regulated gene expression.

**Citation:** Hlawatsch J, Karlstetter M, Aslanidis A, Lückhoff A, Walczak Y, et al. (2013) Sterile Alpha Motif Containing 7 (Samd7) Is a Novel Crx-Regulated Transcriptional Repressor in the Retina. PLoS ONE 8(4): e60633. doi:10.1371/journal.pone.0060633

**Editor:** Karl-Wilhelm Koch, University of Oldenburg, Germany

**Received:** May 18, 2012; **Accepted:** March 1, 2013; **Published:** April 2, 2013

**Copyright:** © 2013 Hlawatsch et al. This is an open-access article distributed under the terms of the Creative Commons Attribution License, which permits unrestricted use, distribution, and reproduction in any medium, provided the original author and source are credited.

**Funding:** Funds were provided by the Deutsche Forschungsgemeinschaft (LA1203/6-2, LA1203/8-1), the Pro Retina Stiftung and the Hans und Marliese Stock-Stiftung. The funders had no role in study design, data collection and analysis, decision to publish, or preparation of the manuscript.

**Competing Interests:** TL is academic editor of PLOS ONE. This does not alter the authors' adherence to all the PLOS ONE policies on sharing data and materials.

\* E-mail: thomas.langmann@uk-koeln.de

☞ These authors contributed equally to this work.

## Introduction

Rods and cones of the retina are highly specialized cells required for phototransduction, the biochemical key step of visual perception. Up to now, mutations in more than 170 inherited retinal disease genes have been identified, which often lead to malfunction of retinal cells and progressive retinal degeneration (Retnet database, <http://www.sph.uth.tmc.edu/Retnet/>). Within this large group of causative genes, defects in retina-specific genes and key transcription factors are frequently associated with inherited retinal dystrophies [1]. There is a strong correlation between high transcript levels of a gene in photoreceptors and a dysfunction of the corresponding protein, which can subsequently lead to retinal disease [2]. Therefore, the identification of abundantly expressed genes in the retina and knowledge about their regulation may help to find yet unknown genetic causes for retinopathies.

Photoreceptor-specific gene regulation is controlled by a hierarchical network of transcription factors including orthodenticle homeobox 2 (Otx2) [3], cone rod homeobox (Crx) [4,5], neural retina leucine zipper (Nrl) [6], nuclear receptor subfamily 2 group E member 3 (Nr2e3) [7], thyroid hormone receptor beta 2 (Thrb2) [8], and retinoid related orphan receptor beta (Rorb) [9].

Crx is present in developing as well as adult rod and cone photoreceptors, where it critically influences the transcription of most photoreceptor-specific genes [10]. Accordingly, Crx acts like a classical terminal selector gene, which maintains and controls the terminally differentiated state of rods and cones [11]. ChIP-seq experiments in the mouse retina revealed that Crx coordinates the expression of several hundreds of photoreceptor genes including most retinal disease genes [12]. In a candidate-gene prioritization strategy based on these Crx ChIP-seq data, two novel retinitis pigmentosa genes, FAM161A and MAK, were recently identified [13,14]. Thus, the Crx ChIP-seq dataset is highly useful to identify novel retina-specific genes and define novel targets for genetic analyses.

Sterile alpha motif (SAM) domains are 70 amino acid long protein-protein interaction domains, which are present in a variety of proteins from different functional classes [15]. These proteins often self-associate via their SAM domains and some form polymeric complexes, which is required for modulation of functional activity [16]. SAM proteins can act as kinases [17], regulatory enzymes [18], scaffolding proteins [19], RNA-binding proteins [20,21], and transcriptional regulators [22,23]. The Ets transcription factor Yan contains a SAM domain and is a negative regulator of photoreceptor development [24]. Major retinal SAM

domain protein (Mr-s, alias Samd11) was identified as the first SAM domain protein predominantly expressed in rod photoreceptor cells and the pineal gland [25]. Mr-s, which contains an isolated SAM domain, is regulated by Crx and likely functions as a transcriptional repressor involved in photoreceptor development [25].

In this study, we cloned and characterized Samd7, the hitherto second SAM domain containing protein specifically expressed in the mammalian retina and pineal gland. Samd7 is confined to the outer nuclear layer of the developing and adult mouse retina and its transcription is controlled by Crx-bound *cis*-regulatory elements. We found that Samd7 is mainly localized in the nucleus, where it blocks Crx-dependent transcription from retina-specific promoters including those from the retinoschisin gene and the Samd7 gene itself. These findings propose a novel role for Samd7 in transcriptional regulation of retina-specific genes.

## Materials and Methods

### Mouse husbandry

CD1 and C57BL/6 mice were purchased from Charles River Laboratories (Sulzfeld, Germany) and maintained on a 12 hour light/dark schedule at 22°C with free access to water and food. The health of the animals was regularly monitored, and all procedures were approved by the University of Regensburg animal rights committee and complied with the German Law on Animal Protection and the Institute for Laboratory Animal Research Guide for the Care and Use of Laboratory Animals, 1999.

### DNA constructs

Mouse retinal cDNA was used to amplify the full-length Samd7 open reading frame using forward primer 5'-ccaagcttatgacaaacc-caatgatctctgag-3' and reverse primer 5'-cccgaattcttaattctca-taacgtcttctcag-3'. The PCR-product was cloned into the pFLAG-CMV-4 vector (Sigma Aldrich) at restriction sites *HindIII* and *EcoRI*. The clone was validated by cycle sequencing with vector-specific and internal primers. The pCAG-GFP and No-basal/Rho-basal dsRed vectors have been described previously [12]. The RNAi vector pBS/U6-Crx-shRNA has been described previously [26] and the plasmid pLKO.1 scramble shRNA was purchased from Addgene.

To create the Samd7-CBR1-dsRed construct, PCR was used to amplify a 495 bp region of the mouse Samd7 promoter region using forward primer 5'-tccccgaattcgcattctcacctagagca-3' and reverse primer 5'-ttcgggtaccgccttctgacagctctt-3'. The promoter fragment was subcloned upstream of dsRed in the no-basal reporter vector using *EcoRI* and *KpnI* restriction enzymes. The 581 bp insert of the Samd7-CBR2-dsRed construct was amplified from mouse genomic DNA with forward primer 5'-tccccttagagatgtggg-caactcaaacct-3' and reverse primer 5'-tccccgaattcagaccactctg-gatggt-3'. The intron fragment was subcloned in the Rho-basal reporter vector at *XbaI* and *EcoRI* restriction sites. Site-directed mutagenesis was performed to replace the central core motif of Crx binding sites within Crx-bound region 2 (CBR2) using the QuikChange Multi Site-Directed Mutagenesis Kit (Stratagene, La Jolla, CA, USA). In general, the TAAT site was substituted by CCCC nucleotides. The following primers were used for mutagenesis: CBR2/CBS1, forward 5'-cgtctgaaggcagcgcaccag-gcatctcat-3', reverse 5'-aggatgaagatgctggggcctgctcag-3', CBR2/CBS2, forward 5'-catctctcatctgccccctgctgcccacag-3', reverse 5'-ggatggccagcacggggcaggatgaagatgcc-3', CBR2/CBS3, forward 5'-ggccatccagccccagctctgggtcagag-3', reverse 5'-accag-gactcggggcctggatgccagcac-3', CBR2/CBS4, forward 5'-

ctctgtttgagccccagacacactctaca-3', reverse 5'-gagtgtctctgggggct-caaacagagagg-3'.

To clone the Samd7-CBR1-Luciferase construct, PCR was used to amplify a 495 bp region of the mouse Samd7 promoter region using forward primer 5'-ttcgggtaccgcattctcacctagagca-3' and reverse primer 5'-ggtagcctcagggccttctgacagctctt-3'. The promoter fragment was subcloned upstream of luciferase in the pGL4.10 reporter vector using *KpnI* and *XhoI* restriction enzymes. The Rs1 luciferase construct has been described previously [27]. Design and cloning of the p5xCrx-tk-Luc plasmid was published recently [28].

### Immunohistochemistry

For retinal immunofluorescence studies, cryo-sections were fixed with 4% paraformaldehyde and rinsed with PBS. Sections were then rehydrated in PBS and preincubated with 1% dried milk in PBS and 0.01% Tween 20 to reduce nonspecific staining. Overnight incubation with the primary anti-Samd7 antibody (Q-12, Sc100141, Santa Cruz Biotechnology, Santa Cruz, CA, USA) was performed at 4°C in PBS containing 2% BSA, 0.02% NaN<sub>3</sub> and 0.1% Triton X-100. After washing in PBS, samples were labeled for 1h at room temperature with the secondary goat anti-rabbit antibody conjugated to Alexa594 (red) (Dianova, Hamburg, Germany). Nuclei counter-staining was performed with 0.1 µg/ml 4',6-diamidino-2-phenylindol in PBS (Molecular Probes, Life Technologies, Frankfurt, Germany) for 10 min at room temperature. The cryo-sections were mounted with fluorescent mounting medium (Dako Cytomation, Hamburg, Germany) and viewed with a Zeiss Axio Imager fluorescence microscope equipped with ApoTome.2 (Carl Zeiss, Jena, Germany). Microscopic pictures were analyzed with ZEN software (Carl Zeiss, Jena, Germany).

### Immunocytochemistry

HEK293 cells were seeded on glass coverslips and transfected with the Flag-Samd7 expression plasmid for 48 hours. Slides were fixed with 4% paraformaldehyde, washed with PBS and incubated in blocking buffer containing 10% goat serum and 0.3% Triton X-100. Cells were then incubated with the anti-Samd7 antibody (Q-12, Sc100141, Santa Cruz Biotechnology, Santa Cruz, CA, USA) or the anti-Flag antibody (#2368, Cell Signaling technology, Cambridge, UK) in a solution containing 2.5% goat serum and 0.1% Triton X-100 for 1 hour at room temperature. After 30 min incubation with the secondary antibody conjugated to Alexa594 (red), slides were washed with PBS and counterstained with DAPI in PBS. Labeled cells were viewed with a Zeiss Axio Imager fluorescence microscope equipped with ApoTome.2 (Carl Zeiss, Jena, Germany). Microscopic pictures were analyzed with ZEN software (Carl Zeiss, Jena, Germany).

### Western blot analysis

Mouse retinal tissue was homogenized in cold RIPA buffer (50 mM Tris/HCl pH 7.4, 150 mM NaCl, 1% Triton X-100, 0.5% sodium deoxycholate, 0.1% SDS, and protease inhibitors) using a TissueLyser (Qjagen, Hilden, Germany). Insoluble debris was removed by centrifugation for 5 min at 5000 g. HEK293 cells transfected with Flag-Samd7 and mock vectors were directly lysed in RIPA buffer. Nuclear and cytoplasmic extracts were prepared using the NE-PER nuclear protein extraction kit according to the instructions of the manufacturer (Thermo Scientific, Schwerte, Germany). Protein concentrations were determined by Bradford assay (Roti-quant, Roth, Karlsruhe, Germany). 30 µg of proteins were separated by SDS-PAGE on 10% gels with PageRuler prestained protein ladder (Thermo Scientific, Waltham, MA, USA). Proteins were then transferred to 0.45 µm nitrocellulose

membranes (Biorad, Munich, Germany). After blocking in PBS containing 3.5% nonfat dry milk, membranes were incubated with primary antibodies against Samd7 (Q-12, Sc100141, Santa Cruz Biotechnology, Santa Cruz, CA, USA), Flag tag (#2368, Cell Signaling technology, Cambridge, UK), or beta-actin (mAbcam 8224, Cambridge, UK). Blots were then incubated with secondary goat anti-rabbit IgG antibodies conjugated to horseradish peroxidase. Western blot signals were visualized with the Multi-image II system (Alpha Innotech, Santa Clara, CA, USA).

### *In vitro* electroporation and culture of explanted retinas

*In vitro* electroporation of explanted retinas was performed as described previously [12]. Briefly, retinas from P0 wild-type CD1 mouse pups were dissected and placed into a microslide chamber containing a mixture of pCAG-GFP as loading control and the reporter construct driving dsRed expression. Retinas were subjected to five 30 V pulses with 50 ms in length and 950 ms apart using an ECM 830 square-wave electroporator (BTX Harvard Apparatus, Holliston, MA, USA). Each construct was electroporated into three different retinas and three independent electroporations were performed. The retinas were then rinsed in medium and placed on circular Nucleopore filters (25 mm, 0.2 mm; VWR, Darmstadt, Germany) with the lens facing the membrane. After eight days of *in vitro* culture, retinas were fixed and imaged in both flat-mounts and cross-sections. For quantification of promoter activities, dsRed fluorescence was determined and normalized to GFP control fluorescence as described before [29]. Briefly, retinal flat-mount images were captured for the red and the green channels using a fluorescence microscope (Axioskop2 MOT Plus, Zeiss, Jena, Germany). Five regions of interest within each retina and three regions outside each retina were defined using ImageJ software (National Institutes of Health, Bethesda, <http://rsbweb.nih.gov/ij/>). Then, the mean background-subtracted pixel intensity of the experimental red channel was divided by the mean pixel intensity of the green control channel for normalization.

### Transient transfections, luciferase and beta-Gal assays

HEK293 cells were cultured in DMEM containing 10% FCS, 100 U/ml penicillin/streptomycin at 37°C in a 5% CO<sub>2</sub> atmosphere. Cells in 12-well plates were transfected with 0.2 µg of reporter plasmid using the TransIT-LT1 Transfection Reagent (Mirus, Madison, WI, USA) following the manufacturer's instructions. For co-transfections, 0.2 µg luciferase plasmid were used together with various concentrations of pcDNA4/HisMax-Crx, pcDNA4/-Samd7, or empty expression vector. 0.4 µg pSV beta-galactosidase vector (Promega) were co-transfected in each reaction to control for transfection efficiency. Cells were harvested 24h after transfection by scraping in 1x lysis buffer (Promega, Madison, WI, USA). For luciferase assays, 20 µl of cytosolic extract and 100 µl of luciferase assay reagent were mixed and light emission was measured with a Tecan Infinite F200 pro reader (Tecan, Crailsheim, Germany). All data were normalized for beta-galactosidase activity using the Promega beta-galactosidase enzyme assay (Promega), calculating the absorbance at 420 nm. Fold activation was calculated relative to control transfected cells. For each construct, at least six independent experiments were performed. Statistical significance was determined using One-way Analysis of Variance and Tukey's Post Hoc Test.

### RNA-Isolation, RT-PCR and quantitative (real-time) RT-PCR

Total RNA was isolated from different mouse tissues and retinas at different postnatal ages using the RNeasy Mini Kit (Qiagen, Hilden, Germany). RNA quality was assessed on the Agilent 2100 Bioanalyzer with the RNA 6000 Nano LabChip reagent kit (Agilent Technologies, Palo Alto, CA). Reverse transcription was performed using the RevertAid H Minus First Strand cDNA Synthesis kit (Fermentas, St. Leon-Rot, Germany).

RT-PCR to amplify 563 bp of mouse Samd7 from stomach, lung, liver, testis, kidney, spleen, brain, retina, heart, muscle, and pineal gland was performed with 50 ng cDNA and primers forward, 5'-tcacttactactcaggctgggca-3' and reverse, 5'-gttcccggtggggtggcg-3'. A 293 bp product of Samd11 was amplified from pineal gland cDNA using primers forward, 5'-tgtccagcccgaacccaag-3' and reverse, 5'-tgtgtctctcatcagtggaaga-3'. A 292 bp fragment of β-actin was amplified as reference with primers forward, 5'-accacactgtgccatca-3' and reverse, 5'-cggaaccgctcattgcc-3' using the Taq Core kit (Qiagen, Hilden, Germany) and standard PCR conditions with 25 cycles.

qRT-PCR was carried out with the TaqMan 7900HT PCR detection system (Invitrogen Life Technologies, San Diego, CA) in 10 µl reaction mixture containing 1x TaqMan Gene Expression Master Mix (Invitrogen Life Technologies), 200 nM primers and 0.25 µl dual-labeled probe (Roche Universal Probe Library, Roche Diagnostics, Mannheim, Germany). For the detection of mouse Samd7 transcripts, intron-spanning primers forward, 5'-tgatggaagaatggggttt-3' and reverse, 5'-tctgagtcaacctgctcat-3' were combined with universal probe # 34. Atp5b was amplified as stable reference gene using primers forward, 5'-ggcacaatgcaggaaagg-3' and reverse, 5'-tcagcaggcacatagatagcc-3' together with probe # 77. The PCR reaction parameters were as follows: 40 s at 95°C melting, 1 min at 60°C annealing, and 2 min at 72°C extension. Each run was performed for 40 cycles and each measurement was performed in biological triplicates. PCR efficiencies of both products were determined with serial dilutions of mouse retinal cDNA and were shown to be >90% (Figure S1). Results were analyzed with the ABI sequence detector software version 2.3 using the ΔΔCt method for relative quantitation.

## Results

### Cloning of mouse Samd7

We have recently analyzed the targetome of the retinal transcription factor Crx using chromatin immunoprecipitation with massively parallel sequencing (ChIP-seq) [12]. Using this dataset, we have now identified a previously uncharacterized SAM domain containing protein, Samd7. In the ChIP-seq dataset, Samd7 was the gene locus with most Crx ChIP-seq reads (data not shown), indicating high expression and a putative important function in the mouse retina. To clone the 445 amino acid open reading frame (ORF) of the mouse Samd7 gene, we carried out RT-PCR with cDNA from 2 month old mouse retina. The Samd7 ORF contains an isolated SAM domain in the C-terminal part (Figure 1A), which exhibits high homology with SAM domains of the known proteins Samd4, Epha4, Ephb2, Tel, Samd11, Phc2, Mph1, and Phc1 (Figure 1B). Phylogenetic analysis indicated that the closest relative of Samd7 is Samd11, which also lacks further known protein domains (Figure 1C). Samd11 has been recently characterized as *major retinal SAM domain protein* (Mr-s), which may function as a transcriptional repressor in photoreceptor cells [25]. The mouse Samd7 ORF and especially its SAM domain is highly conserved in rat, human, chicken and zebrafish (Figure 1D). Samd7 maps to mouse chromosome 3A3. The human ortholog



**Figure 1. Samd7 is a novel phylogenetically conserved SAM-domain protein.** A: The full-length Samd7 protein comprises 445 amino acids including a 67 aa SAM domain, which is indicated by a box. B: Amino acid alignment of selected SAM domain sequences using Clustal W Blosum 62. The level of similarity is indicated by shading ranging from 100% (black) to less than 60% (light gray). C: Phylogenetic conservation of SAM-domain containing proteins. The branch length represents the number of substitutions that have occurred in that branch and the distance scale represents the number of differences between sequences, with 0.1 meaning 10% difference between two sequences. D: Amino acid sequence similarities of mouse, rat, human, chicken, and zebrafish Samd7 proteins. The percentage of similarity is shown for the full-length protein as well as for individual regions of the protein, respectively.

doi:10.1371/journal.pone.0060633.g001

resides at 3q26.2, which does not harbor a retinal disease candidate locus so far.

### Samd7 is expressed in the mouse retina and pineal gland

To compare retinal mRNA expression of Samd7 with other SAM domain proteins that lack additional functional domains, a DNA-microarray dataset that was previously published by our group was screened [30]. Seven SAM domain only proteins were present on the microarray and Samd11 (alias Mr-s) showed highest expression levels in the postnatal day (P) 7 retina (Figure 2A). Samd7 and Samd14 were also significantly expressed in the retina, whereas Samd4, Samd5, Samd10, and Samd12 were only weakly expressed (Figure 2A). To analyze the tissue specificity of Samd7 expression, transcript levels were amplified in various adult mouse tissues using RT-PCR. We observed that Samd7 was highly expressed in the retina but was not found in stomach, lung, liver, testis, kidney, spleen, brain, heart, or muscle (Figure 2B). As many photoreceptor-specific genes, including the related Samd11 gene, are expressed in the pineal gland [25,31], we next analyzed Samd7 transcripts in this tissue. RT-PCR amplification verified the previously described weak Samd11 expression [25] and showed a strong band specific for Samd7 (Figure 2C). We then investigated the temporal expression of Samd7 mRNA in the late stages of mouse retinal development using real-time qRT-PCR. Weak transcript levels were detected at birth and between P1 and P3 (Figure 2D). At P5, Samd7 showed a peak of expression, which slowly declined to intermediate levels at higher mouse ages (Figure 2D). The early expression pattern of Samd7 clearly parallels the maturation of photoreceptors and we thus speculate that the protein functions mainly in terminally differentiated photoreceptors.

### Samd7 is localized to the outer nuclear layer of the retina and resides in the cytoplasm and nucleus of transfected cells

Given the high mRNA expression in the retina, our next goal was to determine the localization of the Samd7 protein in the mouse retina. We first performed immunohistochemistry of adult mouse retinal sections using a commercial anti-Samd7 antibody. These experiments showed that Samd7 was predominantly expressed in the outer nuclear layer, where rod and cone photoreceptors reside (Figure 3A). We then performed Western blot analysis to confirm specificity of the antibody. The 49 kDa Samd7 protein was detected as a specific band in retinal extracts from adult mice (Figure 3B). To further corroborate antibody specificity, we cloned and expressed a recombinant Flag-tagged Samd7 protein in HEK293 cells. A specific band of 51 kDa was detected with both, the anti-Flag antibody and the anti-Samd7 antibody (Figure 3C). This result confirms that the anti-Samd7 antibody specifically recognizes Samd7.

To study the subcellular localization of Samd7 in mammalian cells, we again analyzed HEK293 cells transiently transfected with a full-length Flag-tagged Samd7 expression construct. Cell lysates were separated into cytoplasmic and nuclear fractions and Western blots were performed. Using the anti-Flag and the anti-

Samd7 antibody, corresponding Samd7 bands were identified in the cytoplasm as well as the nuclear fractions. Stronger signals were detected in the nuclear fractions which were often seen as double bands with slightly different molecular weights at an approximate size of 51 kDa (Figure 3D). We next analyzed mock-transfected and Samd7 transfected cells with immunocytochemistry using anti-Flag and anti-Samd7 antibodies (Figure 3E-P). Fluorescence microscopy of immunostained cells which were counter-stained with DAPI showed a predominant nuclear localization of Samd7 (Figure 3H-J, N-P). These data suggest that a significant portion of Samd7 protein resides in the nucleus. Interestingly, its closest relative Samd11 also shows a predominant distribution in the nucleus when transfected into HEK293 cells [25].

### Samd7 transcription is controlled by Crx

The identification of Samd7 as *in vivo* target of Crx in the Crx ChIP-seq study [12] and its retina-specific expression suggests that Samd7 transcription is directly regulated by Crx. We inspected the location of retinal Crx ChIP-seq reads at the Samd7 locus and identified two Crx-bound regions (CBRs) in the promoter region and the first intron, respectively (Figure 4A). Sequence analysis of a recently published RNA Polymerase II ChIP-chip dataset [32] also showed a significant Pol II association with the promoter region of Samd7 at postnatal day 2 (Figure 4A). At postnatal day 25, when the retina is fully developed, Pol II peaks were identified at the promoter as well as in the first intron. These Pol II bound regions fully overlap with both CBRs (Figure 4A), indicating that these regulatory sites indeed function as initiation and elongation sites of Samd7 transcription in the adult retina.

Bioinformatic sequence analysis using MatInspector then showed that CBR1 contains three canonical Crx binding sequences (CBS1–3), whereas CBR2 contains four CBS (Figure 4A). A nearly perfect phylogenetic conservation of Crx sites was found in CBS1 and CBS3 residing within CBR2 (Figure 4B). To test whether CBR1 and CBR2 represent active *cis*-regulatory regions, CBR-dsRed reporter fusions were electroporated into living mouse retinas. CBR1 located in the proximal promoter region of the Samd7 gene failed to drive detectable dsRed expression in the retina (Figure 4C). In contrast, intronic CBR2 upstream of a minimal rhodopsin promoter, which by itself is not active, drove strong expression with a predominant fluorescence signal in the outer nuclear layer, where photoreceptors are localized (Figure 4C). To evaluate the contribution of individual Crx binding sites to the strong activity of CBR2, site-directed mutagenesis was performed in the critical Crx core motifs. Mutations in all four CBS of CBR2 simultaneously resulted in a complete loss of activity in electroporated retinal explants (Figure 4C). Electroporations with four constructs that eliminated each CBS independently were then performed and fluorescence levels were quantified. Mutation of CBS1 and CBS3 nearly abolished enhancer activity, whereas mutagenesis of CBS2 and CBS4 had no major effect (Figure 4D). To analyze whether the same sites of intronic CBR2 also enhance activity of its own promoter, mutant CBR2 fragments were cloned upstream of CBR1 and the reporter

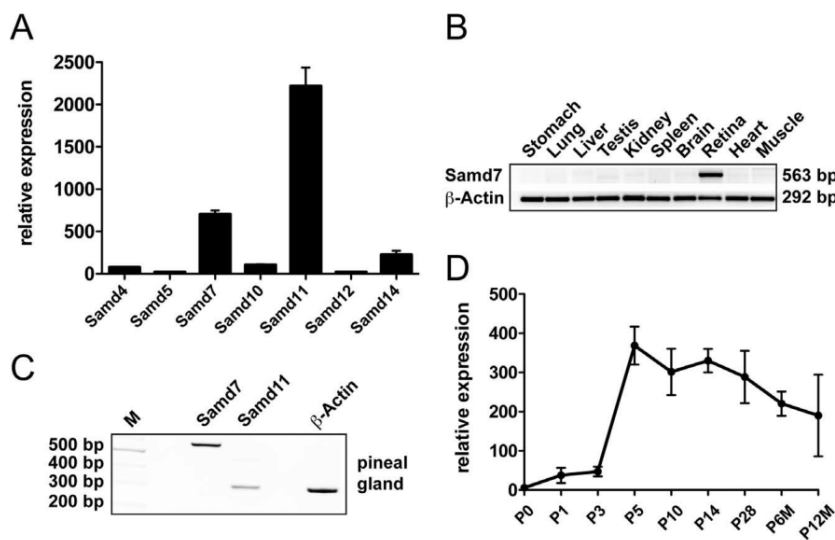


**Figure 2. Samd7 is expressed in the mouse retina and pineal gland.** A: Relative mRNA expression of all SAM-domain containing proteins with isolated SAM domains in postnatal day 7 mouse retinas. Mean signal intensities of three independent Affymetrix mouse expression 430A arrays (GEO accession number GSE5581) show that Samd7 is the second most abundant transcript in the retina. B: RT-PCR analysis of total RNAs extracted from mouse stomach, lung, liver, testis, kidney, spleen, brain, retina, heart, and muscle reveals retina-specific mRNA expression of Samd7. C: RT-PCR analysis of total RNA extracted from mouse pineal gland. Primer pairs specific for Samd7, Samd11 and beta-actin were used for PCR. D: Real-time qRT-PCR analysis of early postnatal and adult retina demonstrates that Samd7 expression peaks at postnatal day 5 and then stays at intermediate levels. doi:10.1371/journal.pone.0060633.g002

activity was determined. In accordance with the data from CBR2 electroporations alone, mutagenesis of CBS1 and CBS3 reduced dsRed expression, whereas nucleotide changes in CBS2 and CBS4 had no effect on reporter activity (Figure 4E). Thus, CBS1 and CBS3 in the intronic enhancer CBR2 are indispensable for Crx-regulated expression of Samd7 in the retina.

To further examine whether Crx is essential for Samd7 gene activity, we performed Crx knock-down experiments in explanted mouse retinas. Therefore, electroporations of Crx shRNA plasmids or scrambled shRNA negative controls together with the Samd7 CBR2 reporter construct were carried out. These experiments revealed a complete loss of dsRed fluorescence in flat-mount Crx knock-down retinas compared to scrambled shRNA retinas (Figure 5A). This indicates that the Crx-bound sequences in CBR2 are critically dependent on Crx. As a next step, we investigated endogenous Samd7 protein expression in the same Crx knock-down system using immunohistochemistry. In the postnatal day 8 retina co-electroporated with scrambled shRNA control, Samd7 protein was present at the border of the inner nuclear layer and the outer nuclear layer (Figure 5B, upper panel). This specific staining of Samd7 almost completely disappeared in Crx knock-down retinas (Figure 5B, lower panel), suggesting that endogenous Samd7 expression requires the presence of Crx.

### Samd7 functions as a transcriptional repressor

Samd7 is localized in the ONL of the adult retina and is present in the nucleus of transfected cells. Thus, we hypothesized that the protein could be a transcriptional regulator. In the absence of an obvious DNA-binding domain, we speculated that Samd7 may interfere with the activity of retinal transcription factors like Crx. To test this hypothesis, the effect of Samd7 co-transfection on Crx-dependent promoter activity was studied with luciferase reporter assays. In the first series of experiments, we used a previously published Crx-dependent luciferase reporter which contains five repeats of Crx consensus sites under the control of a thymidine kinase minimal promoter [28]. As expected, this construct showed

a five-fold increase when Crx was co-transfected (Figure 6A). Samd7 exerted a significant dose-dependent suppressive effect on this universal Crx reporter construct (Figure 6B). We selected the most effective concentration from these titration experiments and then analyzed specific regulatory sequences. The retinal expression of the murine and human retinoschisin (RS1) gene is under the control of Crx and thus represents a bona fide Crx target gene [27]. Therefore, this promoter was selected for Crx-specific transactivation assays in the absence or presence of Samd7 expression plasmid (Figure 6C). We could confirm the results from the universal 5xCrx-tk-Luc construct and showed that Crx co-transfection strongly increased luciferase activity of a RS1 reporter construct in HEK293 cells (Figure 6C). The increased luciferase level controlled by Crx was significantly suppressed by Samd7 (Figure 6C). As the Samd7 gene itself is regulated by Crx, we next studied the effects of Samd7 co-transfection on its own promoter construct. As expected, Crx-transfection markedly increased luciferase activity of the proximal Samd7 promoter (Figure 6D). In analogy to the retinoschisin gene, Samd7 co-transfection strongly diminished reporter activity of the Samd7 gene itself (Figure 6D). These experiments suggest that Samd7 functions as a negative regulator of Crx-controlled photoreceptor-specific gene expression.

### Discussion

In this study, we have cloned a novel SAM domain protein, Samd7, which is expressed in the retina and the pineal gland. The peak level of Samd7 expression is at P5, when photoreceptor cells differentiate into their functional form. Immunohistochemistry of mouse retinal sections showed that the Samd7 protein is mainly present in the outer nuclear layer. Ectopic expression of Samd7 in cultured cells revealed a distribution in the cytoplasm and the nucleus. The retinal expression and *cis*-regulatory activity of the Samd7 locus is critically controlled by a phylogenetically conserved Crx-bound enhancer region in the first intron as shown

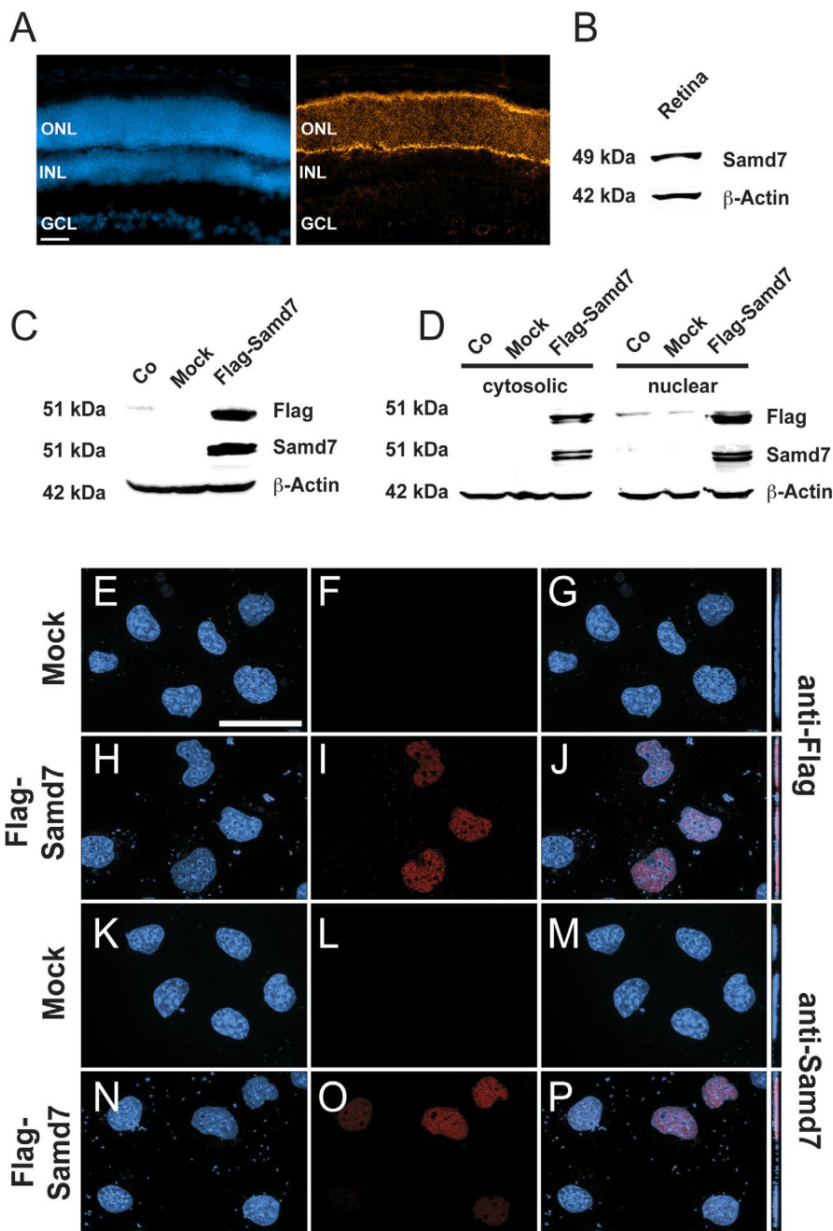


**Figure 3. Samd7 is expressed in the outer nuclear layer of the mouse retina and localizes to the nucleus of transfected cells.** A: Immunohistochemical analysis shows that Samd7 localizes to the outer nuclear layer in the adult mouse retina. Left panel: DAPI staining, right panel: anti-Samd7 antibody staining, ONL: outer nuclear layer, INL: inner nuclear layer, GCL: ganglion cell layer. Scale bar, 50  $\mu$ m. B: Western blot performed with retinal lysates detecting Samd7 at a molecular weight of 49 kDa and beta-actin as loading control. C: Western blot performed with protein lysates from naive HEK293 cells (Co) or HEK293 cells transfected with mock plasmid or Flag-Samd7 expression plasmid. Anti-Samd7 antibody, anti-flag antibody, and anti-beta-actin antibody were used. The Flag-Samd7 band had a molecular weight of approximately 51 kDa. D: Western blot of cytosolic and nuclear fractions of HEK293 cells transfected with mock plasmid or Flag-Samd7 expression vector. Samd7 was detected in both the cytosolic and nuclear fractions at a molecular weight of 51 kDa. (E–P): Subcellular localization of Samd7 in HEK293 cells transfected with Flag-Samd7 expression vector shown in fluorescent Z-stacked optical images. Mock transfected cells did not show a specific red signal with either the anti-Flag (F) or the anti-Samd7 (L) antibody. The anti-Flag antibody (I, J) as well as the anti-Samd7 antibody (O, P) showed a specific nuclear staining in Flag-Samd7 transfected cells when counter-stained with DAPI. doi:10.1371/journal.pone.0060633.g003

by explant electroporation and knock-down experiments. The potential function of Samd7 was further evaluated in luciferase co-transfection assays. These experiments showed that Samd7 inhibits synthetic Crx-regulatory sequences and specific promoter activities of Crx target genes and thus may function as a novel transcriptional regulator in the retina.

A major conclusion from our mRNA expression data is that Samd7 is now a second SAM domain protein with high expression levels in the retina and the pineal gland. The previously described Mr-s protein (alias Samd11) is the closest phylogenetic relative of Samd7 with a very similar expression profile [25]. Mr-s molecules can self-associate and share a relatively similar protein and SAM

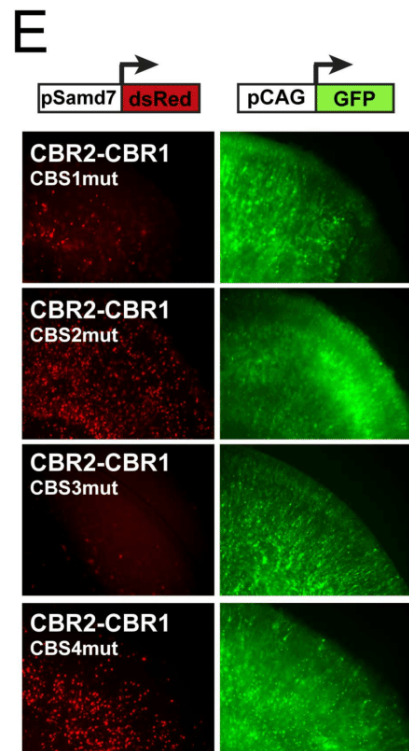
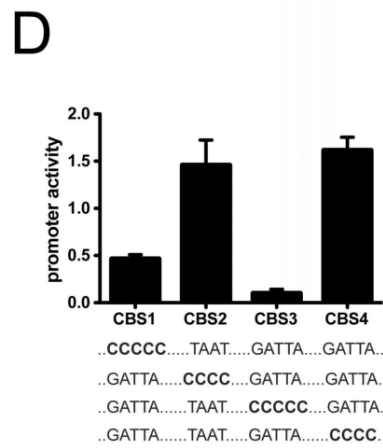
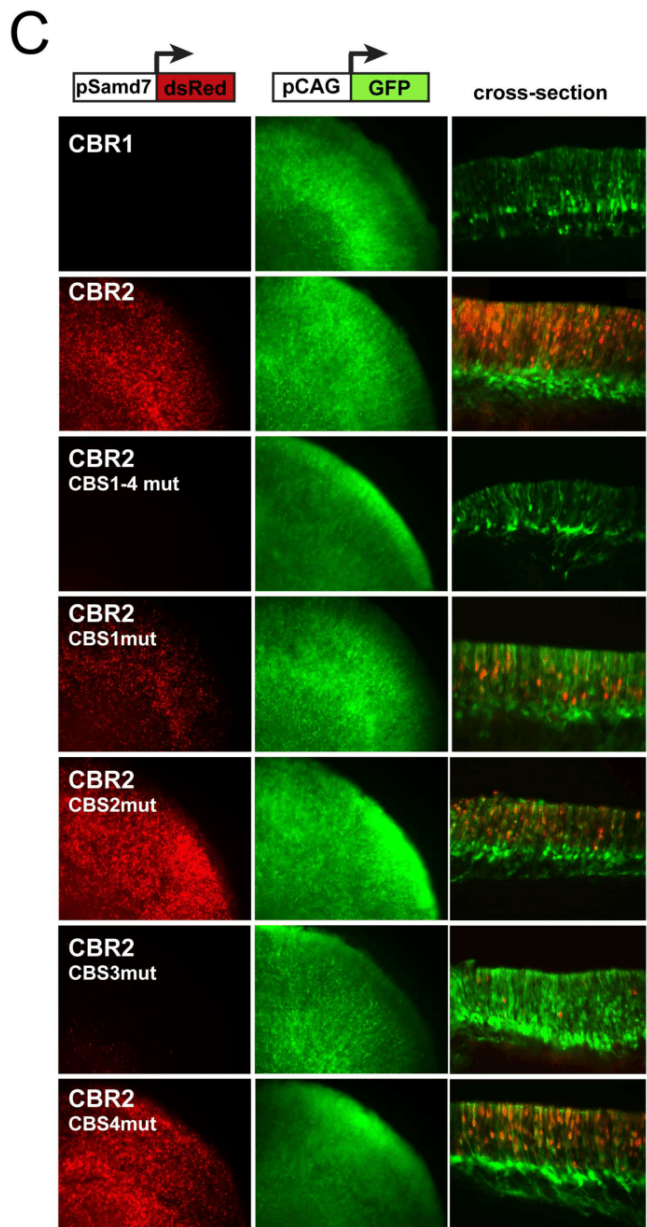
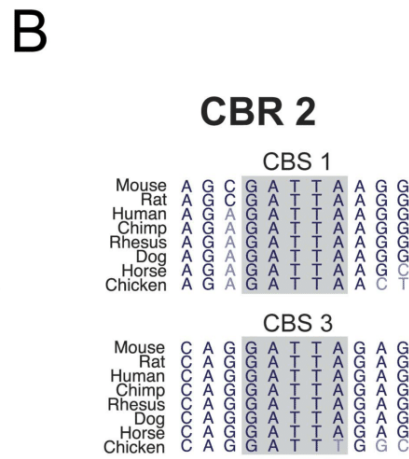
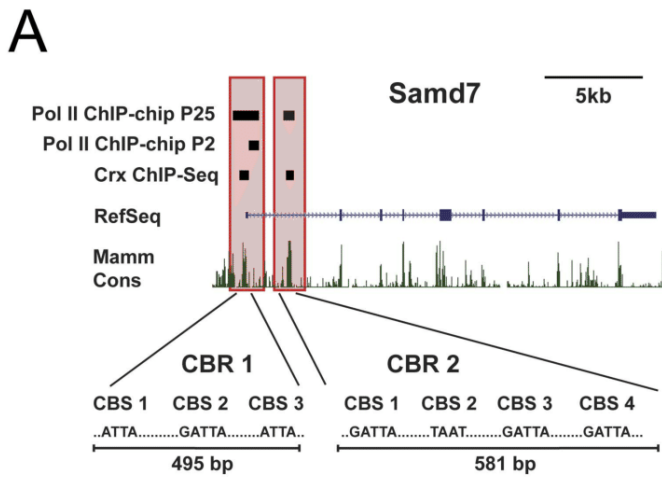


**Figure 4. Samd7 transcription is regulated by Crx.** A: Identification of two Crx-bound regions (CBR1 and CBR2) at the mouse Samd7 locus. Enriched Crx ChIP-seq regions are shown in the proximal promoter and first intron of Samd7 [12]. RNA polymerase II ChIP-Chip peaks at P2 and P25 [32] overlap with the Crx ChIP-Seq regions. The degree of mammalian conservation is indicated at the bottom. The nucleotide sequences of canonical Crx binding sequences (CBS) within CBR1 and CBR2 are depicted. B: The phylogenetic conservation of CBS1 and CBS2 within CBR2 is shown for several species. C-E: Activity of wild-type and mutant Samd7 CBRs in explanted mouse retinas. Co-electroporations were performed with pCAG-eGFP as control and the indicated Samd7 regulatory elements fused to dsRed. All constructs were electroporated at postnatal day 0 and the cultured explants were harvested at postnatal day 8. C: CBR1 is not active when fused to a promoterless dsRed reporter cassette. In contrast, CBR2 drives strong dsRed expression when fused to the minimal Rhodopsin promoter, which is *per se* not active. The cross-sections show that dsRed signals driven by Samd7 CBR2 were localized in the ONL, whereas the GFP signals by the ubiquitous control promoter were localized in the ONL, INL and GCL. ONL: outer nuclear layer, INL: inner nuclear layer, GCL: ganglion cell layer. D: Quantitative analysis of mutant constructs demonstrates that CBS1 and CBS3 are mandatory for high reporter expression of the intronic CBR2. E: Enhancer activity of CBR2 upstream of CBR1 also requires intact nucleotide sequences at CBS1 and CBS3.  
doi:10.1371/journal.pone.0060633.g004

domain structure with Samd7 [25]. It is currently not possible to assign interactions or functions to uncharacterized SAM domains via simple computational approaches [33]. However, both Samd7 and Samd11 have an isolated SAM domain in their C-terminal part and lack further known motifs. All other family members with isolated SAM domains, namely Samd1, Samd4, Samd5, Samd10, Samd12, and Samd14 are very weakly expressed in the retina and thus are unlikely to interact with Samd7 or Samd11. Therefore, it will be very interesting to determine in the future whether the retina-specific Samd7 and Samd11 proteins can interact with each other.

Crx-dependent regulation of Samd7 in the mouse retina has been implicated by a previous ChIP-seq study, which showed two significantly enriched Crx peaks around the Samd7 locus [12]. We now could pinpoint the two relevant *cis*-regulatory regions in the promoter and the first intron of the gene using *in vitro* electroporation of reporters into mouse retinas. CBR1, which contains three Crx sites was not active alone and required interaction with the intronic enhancer elements of CBR2 to drive dsRed reporter expression. Mutagenesis of individual Crx motifs in CBR2 revealed two critical binding sites, CBS1 and CBS3, which are almost perfectly conserved among various species. The GATTA core sequence of CBS1 and CBS3 also represents a perfect matrix as deduced from bioinformatic prediction and sequence analysis of more than 5000 Crx ChIP-seq regions [10,12]. In accordance with this, the previously published Pol II-ChIP-chip dataset revealed that the promoter region and first

intron of Samd7 are actively bound by RNA-polymerase II complexes and thus initiate transcription in the adult retina [32]. Our findings define Samd7 as a bona fide Crx-regulated target gene and hence corroborate the assumption that many photoreceptor genes are surrounded by a spatially distributed network of CBRs [34]. Crx often co-regulates photoreceptor genes together with Nr1 [35]. However, inspection of published datasets of Nr1<sup>-/-</sup> retinas revealed no aberrant expression of Samd7 [36]. In contrast, expression profiling of the Otx2-deficient retina revealed a significant down-regulation of Samd7 mRNA levels at P12 [37]. It remains to be explored whether Samd7 is indeed a direct Otx2 target gene, or, whether the loss of Samd7 expression may have been indirectly caused by a reduced Crx expression in Otx2<sup>-/-</sup> retinas.

Its site of expression in the retina, the nuclear localization, and the domain features shared with the Mr-s protein indicated that Samd7 could be a transcriptional regulator. Indeed, our *in vitro* assays showed that Samd7 interferes with Crx-mediated gene expression at synthetic consensus Crx sites and at two different retina-specific promoters. It is noteworthy that Samd7 exerted this effect without an obvious DNA binding domain. The *Drosophila* SAM protein Mae also contains solely a SAM domain and lacks DNA-binding activity [38]. Mae interacts with and facilitates phosphorylation of the transcriptional repressor Yan via direct interaction with its SAM domain [39]. Phosphorylation of Yan then results in abrogation of its repressor function and induces translocation to the cytoplasm [39]. Therefore, it is possible that

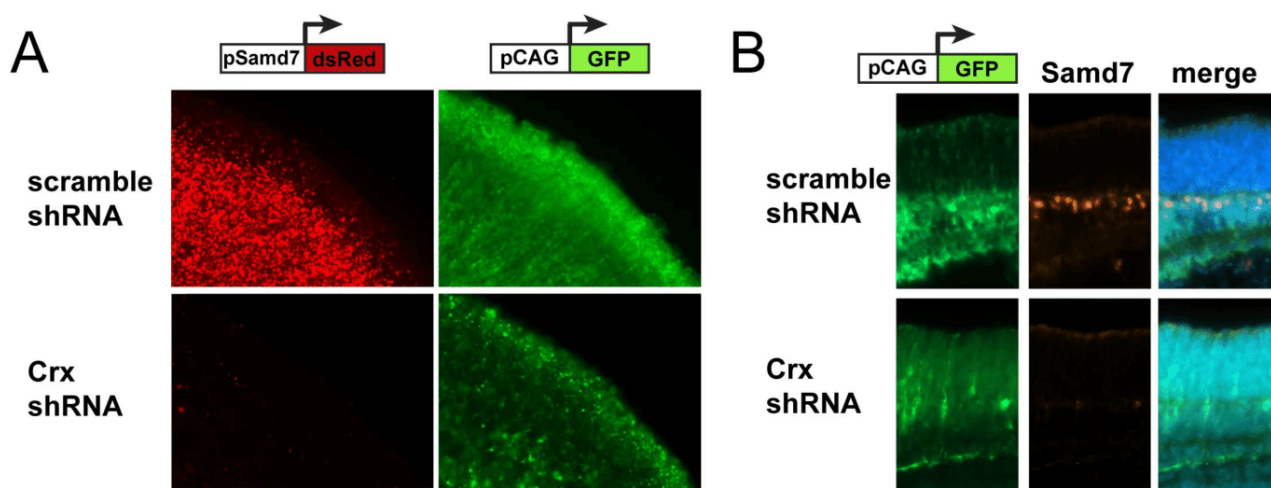


**Figure 5. Samd7 expression is reduced in Crx knock-down retinas.** A: Activity of wild-type Samd7 CBR2 fused to dsRed was strongly reduced in explanted P8 mouse retinas co-electroporated with Crx shRNA. B: Reduced staining of endogenous Samd7 with anti-Samd7 antibody in P8 mouse retinas electroporated with Crx shRNA compared to scramble shRNA control. pCAG-eGFP was used as electroporation control and scramble shRNA vector served as negative control for knock-down experiments. DAPI staining was performed in merged images.  
doi:10.1371/journal.pone.0060633.g005

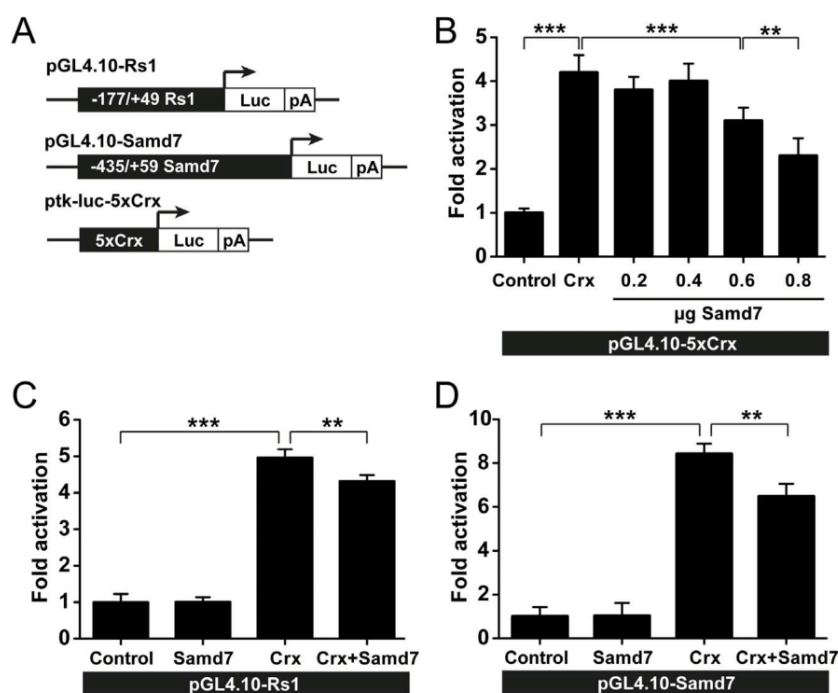


**Figure 6. Samd7-dependent suppression of Crx-activated promoters.** A: Schematic drawing of retinoschisin, Samd7, and 5xCrx tk Luc reporter constructs used for luciferase assays in HEK293 cells. B: The 5xCrx-tk-Luc construct was co-transfected with Crx and various concentrations of Samd7 expression plasmids. C: Samd7 expression plasmid was co-transfected in the absence or presence of Crx vector and the retinoschisin promoter activity was determined. pSV  $\beta$ -galactosidase vector was co-transfected in each reaction to control for transfection efficiency. Error bars represent standard deviation of the mean (n = 6). \*\* $P < 0.01$  and \*\*\* $P < 0.001$  One-way Analysis of Variance and Tukey's Post Hoc Test. doi:10.1371/journal.pone.0060633.g006

Samd7 elicits its repressor function by sequestration of Crx to non-active protein complexes. *In vitro* interaction studies like pull-down assays could further clarify this question. Another possibility could be that Samd7 is part of silencing complexes involving chromatin remodeling enzymes such as histone deacetylases (HDACs). Reporter assays in the presence or absence of HDAC inhibitors like trichostatin A could help to elucidate this mechanism of repression. Samd7 could also act independently from HDACs like the SAM domain containing polycomb complex PRC2, which functions as a methyl transferase and organizes chromatin loops at target genes in their repressed states [40].

Although we have shown that Samd7 can repress transcription from Crx-dependent promoters, the *in vivo* targets of Samd7 are currently unknown. It is obvious that fine-tuning of gene expression in the retina involves activating transcription factors like Crx. However, the role of transcriptional repressors in the control of this Crx-dominated gene regulatory network is poorly understood. Recently, Panky, a photoreceptor-specific ankyrin repeat protein was identified as another transcriptional cofactor that suppresses Crx-regulated photoreceptor genes [28]. We speculate that Samd7 could have a similar function but future studies will be required to precisely clarify the role of Samd7 in retinal gene expression. Mice with targeted disruption or knock-down experiments via *in vivo* electroporation of mouse retinas will be especially helpful to answer these questions.

## References

- Rattner A, Sun H, Nathans J (1999) Molecular genetics of human retinal disease. *Annu Rev Genet* 33: 89-131.
- Blackshaw S, Fraioli RE, Furukawa T, Cepko CL (2001) Comprehensive analysis of photoreceptor gene expression and the identification of candidate retinal disease genes. *Cell* 107: 579-589.

## Supporting Information

**Figure S1 PCR efficiencies of Samd7 and Atp5b real-time qRT-PCR amplifications.** (TIF)

## Acknowledgments

We thank Dr. Anand Swaroop (Neurobiology Neurodegeneration & Repair Laboratory, National Eye Institute) for providing the pcDNA4.1-CRX plasmid and Dr. Joseph Corbo (Department of Pathology and Immunology, Washington University School of Medicine) for sharing the pCAG-GFP plasmid, the No-basal/Rho-basal dsRed reporter vectors, and the pBS/U6-Crx-shRNA vector. We also thank Dr. Kenneth Mitton (Control of Gene Expression Laboratory, Eye Research Institute, Oakland University) for sharing retina-specific RNA-Pol II ChIP-Chip data and Dr. Takahisa Furukawa (Laboratory for Molecular and Developmental Biology, Institute for Protein Research, Osaka University) for providing the p5xCrx-tk-Luc plasmid.

## Author Contributions

Conceived and designed the experiments: MK TL. Performed the experiments: JH MK AA AL YW MP JB. Analyzed the data: JH MK AA MP. Wrote the paper: TL.

3. Nishida A, Furukawa A, Koike C, Tano Y, Aizawa S, et al. (2003) Otx2 homeobox gene controls retinal photoreceptor cell fate and pineal gland development. *Nat Neurosci* 6: 1255-1263.
4. Chen S, Wang QL, Nie Z, Sun H, Lennon G, et al. (1997) Crx, a novel Otx-like paired-homeodomain protein, binds to and transactivates photoreceptor cell-specific genes. *Neuron* 19: 1017-1030.
5. Furukawa T, Morrow EM, Cepko CL (1997) Crx, a novel otx-like homeobox gene, shows photoreceptor-specific expression and regulates photoreceptor differentiation. *Cell* 91: 531-541.
6. Mears AJ, Kondo M, Swain PK, Takada Y, Bush RA, et al. (2001) Nrl is required for rod photoreceptor development. *Nat Genet* 29: 447-452.
7. Milam AH, Rose L, Cideciyan AV, Barakat MR, Tang WX, et al. (2002) The nuclear receptor NR2E3 plays a role in human retinal photoreceptor differentiation and degeneration. *Proc Natl Acad Sci U S A* 99: 473-478.
8. Ng L, Hurley JB, Dierks B, Srinivas M, Salto C, et al. (2001) A thyroid hormone receptor that is required for the development of green cone photoreceptors. *Nat Genet* 27: 94-98.
9. Jia L, Oh EC, Ng L, Srinivas M, Brooks M, et al. (2009) Retinoid-related orphan nuclear receptor RORbeta is an early-acting factor in rod photoreceptor development. *Proc Natl Acad Sci U S A* 106: 17534-17539.
10. Hsiao TH, Diaconu C, Myers CA, Lee J, Cepko CL, et al. (2007) The cis-regulatory logic of the mammalian photoreceptor transcriptional network. *PLoS One* 2: e643.
11. Hobert O (2011) Regulation of terminal differentiation programs in the nervous system. *Annu Rev Cell Dev Biol* 27: 681-696.
12. Corbo JC, Lawrence KA, Karlstetter M, Myers CA, Abdelaziz M, et al. (2010) CRX ChIP-seq reveals the cis-regulatory architecture of mouse photoreceptors. *Genome Res* 20: 1512-1525.
13. Langmann T, Di Gioia SA, Rau I, Stohr H, Maksimovic NS, et al. (2010) Nonsense mutations in FAM161A cause RP28-associated recessive retinitis pigmentosa. *Am J Hum Genet* 87: 376-381.
14. Ozgul RK, Siemiatkowska AM, Yucel D, Myers CA, Collin RW, et al. (2011) Exome sequencing and cis-regulatory mapping identify mutations in MAK, a gene encoding a regulator of ciliary length, as a cause of retinitis pigmentosa. *Am J Hum Genet* 89: 253-264.
15. Qiao F, Bowie JU (2005) The many faces of SAM. *Sci STKE* 2005: re7.
16. Robinson AK, Leal BZ, Chadwell LV, Wang R, Ilangovan U, et al. (2012) The Growth-Suppressive Function of the Polycomb Group Protein Polyhomeotic Is Mediated by Polymerization of Its Sterile Alpha Motif (SAM) Domain. *J Biol Chem* 287: 8702-8713.
17. Tu H, Barr M, Dong DL, Wigler M (1997) Multiple regulatory domains on the Byr2 protein kinase. *Mol Cell Biol* 17: 5876-5887.
18. Harada BT, Knight MJ, Imai S, Qiao F, Ramachander R, et al. (2008) Regulation of enzyme localization by polymerization: polymer formation by the SAM domain of diacylglycerol kinase delta1. *Structure* 16: 380-387.
19. Baron MK, Boeckers TM, Vaida B, Faham S, Gingery M, et al. (2006) An architectural framework that may lie at the core of the postsynaptic density. *Science* 311: 531-535.
20. Aviv T, Lin Z, Lau S, Rendl LM, Sicheri F, et al. (2003) The RNA-binding SAM domain of Smaug defines a new family of post-transcriptional regulators. *Nat Struct Biol* 10: 614-621.
21. Green JB, Gardner CD, Wharton RP, Aggarwal AK (2003) RNA recognition via the SAM domain of Smaug. *Mol Cell* 11: 1537-1548.
22. Slupsky CM, Gentile LN, Donaldson LW, Mackereth CD, Seidel JJ, et al. (1998) Structure of the Ets-1 pointed domain and mitogen-activated protein kinase phosphorylation site. *Proc Natl Acad Sci U S A* 95: 12129-12134.
23. Jousset C, Carron C, Boureux A, Quang CT, Oury C, et al. (1997) A domain of TEL conserved in a subset of ETS proteins defines a specific oligomerization interface essential to the mitogenic properties of the TEL-PDGFR beta oncoprotein. *Embo J* 16: 69-82.
24. Lai ZC, Rubin GM (1992) Negative control of photoreceptor development in *Drosophila* by the product of the yan gene, an ETS domain protein. *Cell* 70: 609-620.
25. Inoue T, Terada K, Furukawa A, Koike C, Tamaki Y, et al. (2006) Cloning and characterization of mr-s, a novel SAM domain protein, predominantly expressed in retinal photoreceptor cells. *BMC Dev Biol* 6: 15.
26. Matsuda T, Cepko CL (2004) Electroporation and RNA interference in the rodent retina in vivo and in vitro. *Proc Natl Acad Sci U S A* 101: 16-22.
27. Langmann T, Lai CC, Weigelt K, Tam BM, Warneke-Wittstock R, et al. (2008) CRX controls retinal expression of the X-linked juvenile retinoschisis (RS1) gene. *Nucleic Acids Res* 36: 6523-6534.
28. Sanuki R, Omori Y, Koike C, Sato S, Furukawa T (2010) Panky, a novel photoreceptor-specific ankyrin repeat protein, is a transcriptional cofactor that suppresses CRX-regulated photoreceptor genes. *FEBS Lett* 584: 753-758.
29. Kraus D, Karlstetter M, Walczak Y, Hilfinger D, Langmann T, et al. (2011) Retinal expression of the X-linked juvenile retinoschisis (RS1) gene is controlled by an upstream CpG island and two opposing CRX-bound regions. *Biochim Biophys Acta* 1809: 245-254.
30. Gehrig A, Langmann T, Horling F, Janssen A, Bonin M, et al. (2007) Genome-wide expression profiling of the retinoschisin-deficient retina in early postnatal mouse development. *Invest Ophthalmol Vis Sci* 48: 891-900.
31. Blackshaw S, Snyder SH (1997) Developmental expression pattern of phototransduction components in mammalian pineal implies a light-sensing function. *J Neurosci* 17: 8074-8082.
32. Tummala P, Mali RS, Guzman E, Zhang X, Mitton KP (2010) Temporal ChIP-on-Chip of RNA-Polymerase-II to detect novel gene activation events during photoreceptor maturation. *Mol Vis* 16: 252-271.
33. Meruelo AD, Bowie JU (2009) Identifying polymer-forming SAM domains. *Proteins* 74: 1-5.
34. Montana CL, Lawrence KA, Williams NL, Tran NM, Peng GH, et al. (2011) Transcriptional regulation of neural retina leucine zipper (Nrl), a photoreceptor cell fate determinant. *J Biol Chem* 286: 36921-36931.
35. Hao H, Kim DS, Klocke B, Johnson KR, Cui K, et al. (2012) Transcriptional Regulation of Rod Photoreceptor Homeostasis Revealed by In Vivo NRL Targetome Analysis. *PLoS Genet* 8: e1002649.
36. Yoshida S, Mears AJ, Friedman JS, Carter T, He S, et al. (2004) Expression profiling of the developing and mature Nrl-/- mouse retina: identification of retinal disease candidates and transcriptional regulatory targets of Nrl. *Hum Mol Genet* 13: 1487-1503.
37. Omori Y, Katoh K, Sato S, Muranishi Y, Chaya T, et al. (2011) Analysis of transcriptional regulatory pathways of photoreceptor genes by expression profiling of the Otx2-deficient retina. *PLoS One* 6: e19685.
38. Baker DA, Mille-Baker B, Wainwright SM, Ish-Horowitz D, Dibb NJ (2001) Mae mediates MAP kinase phosphorylation of Ets transcription factors in *Drosophila*. *Nature* 411: 330-334.
39. Qiao F, Song H, Kim CA, Sawaya MR, Hunter JB, et al. (2004) Derepression by depolymerization; structural insights into the regulation of Yan by Mae. *Cell* 118: 163-173.
40. Aldiri I, Vetter ML (2012) PRC2 during vertebrate organogenesis: a complex in transition. *Dev Biol* 367: 91-99.

RESEARCH

Open Access

# Activated microglia/macrophage whey acidic protein (AMWAP) inhibits NFκB signaling and induces a neuroprotective phenotype in microglia

Alexander Aslanidis<sup>1</sup>, Marcus Karlstetter<sup>1</sup>, Rebecca Scholz<sup>1</sup>, Sascha Fauser<sup>1</sup>, Harald Neumann<sup>2</sup>, Cora Fried<sup>3</sup>, Markus Pietsch<sup>3†</sup> and Thomas Langmann<sup>1\*†</sup>

## Abstract

**Background:** Microglia reactivity is a hallmark of neurodegenerative diseases. We have previously identified activated microglia/macrophage whey acidic protein (AMWAP) as a counter-regulator of pro-inflammatory response. Here, we studied its mechanisms of action with a focus on toll-like receptor (TLR) and nuclear factor κB (NFκB) signaling.

**Methods:** Recombinant AMWAP was produced in *Escherichia coli* and HEK293 EBNA cells and purified by affinity chromatography. AMWAP uptake was identified by fluorescent labeling, and pro-inflammatory microglia markers were measured by qRT-PCR after stimulation with TLR ligands. NFκB pathway proteins were assessed by immunocytochemistry, Western blot, and immunoprecipitation. A 20S proteasome activity assay was used to investigate the anti-peptidase activity of AMWAP. Microglial neurotoxicity was estimated by nitrite measurement and quantification of caspase 3/7 levels in 661W photoreceptors cultured in the presence of microglia-conditioned medium. Microglial proliferation was investigated using flow cytometry, and their phagocytosis was monitored by the uptake of 661W photoreceptor debris.

**Results:** AMWAP was secreted from lipopolysaccharide (LPS)-activated microglia and recombinant AMWAP reduced gene transcription of IL6, iNOS, CCL2, CASP11, and TNFα in BV-2 microglia treated with LPS as TLR4 ligand. This effect was replicated with murine embryonic stem cell-derived microglia (ESdM) and primary brain microglia. AMWAP also diminished pro-inflammatory markers in microglia activated with the TLR2 ligand zymosan but had no effects on IL6, iNOS, and CCL2 transcription in cells treated with CpG oligodeoxynucleotides as TLR9 ligand. Microglial uptake of AMWAP effectively inhibited TLR4-dependent NFκB activation by preventing IRAK-1 and IκBα proteolysis. No inhibition of IκBα phosphorylation or ubiquitination and no influence on overall 20S proteasome activity were observed. Functionally, both microglial nitric oxide (NO) secretion and 661W photoreceptor apoptosis were significantly reduced after AMWAP treatment. AMWAP promoted the filopodia formation of microglia and increased the phagocytic uptake of apoptotic 661W photoreceptor cells.

**Conclusions:** AMWAP is secreted from reactive microglia and acts in a paracrine fashion to counter-balance TLR2/TLR4-induced reactivity through NFκB inhibition. AMWAP also induces a neuroprotective microglial phenotype with reduced neurotoxicity and increased phagocytosis. We therefore hypothesize that anti-inflammatory whey acidic proteins could have a therapeutic potential in neurodegenerative diseases of the brain and the retina.

**Keywords:** Activated microglia/macrophage whey acidic protein (AMWAP), Microglia, NFκB, Photoreceptors, Neurodegeneration

\* Correspondence: thomas.langmann@uk-koeln.de

†Equal contributors

<sup>1</sup>Laboratory for Experimental Immunology of the Eye, Department of Ophthalmology, University of Cologne, Kerpener Strasse 62, D-50931 Cologne, Germany

Full list of author information is available at the end of the article

## Background

Microglial cells are the resident macrophages of the central nervous system (CNS), including the retina, and play a pivotal role in innate immune responses and regulation of homeostasis in the healthy and degenerating CNS [1,2]. Despite being cells of the mononuclear phagocyte lineage, their CNS-specific location and morphology clearly distinguishes them from other macrophage populations [3]. While actively scanning the microenvironment with their long protrusions [4,5], loss of inhibitory signals and the recognition of damage-associated molecular patterns from degenerating neurons lead to the activation of microglia [6-8]. Therefore, reactive microgliosis is a common hallmark of various neurodegenerative diseases including Alzheimer's disease [9], Parkinson's disease [10], multiple sclerosis [11], inherited retinal degenerations [12], and several other retinal diseases [13].

We have previously identified activated microglia/macrophage whey acidic protein (AMWAP) as a novel marker of retinal microglial reactivity that is broadly upregulated in several prototypic mouse models of retinal degeneration including retinoschisin-deficient and Fam161a mutant animals [14,15]. AMWAP consists of a 76 aa polypeptide with a cleavable N-terminal 19 aa signal sequence for cellular export and a single 57 aa four-disulfide core domain that is characteristic for all whey acidic proteins [16]. AMWAP overexpression in microglia elicits several immunoregulatory effects including reduction of both pro-inflammatory marker gene expression and migration [14].

The whey acidic protein family is characterized by a highly conserved whey acidic protein domain which is named after the most abundantly expressed protein WAP from rodent milk [17]. AMWAP is closely related to secretory leukocyte protease inhibitor (SLPI), which is the best studied whey acidic protein [18,19]. In contrast to AMWAP, SLPI contains two consecutive WAP domains and is produced at mucosal surfaces as well as by neutrophils and macrophages [20]. SLPI was recently identified as a biomarker for amyotrophic lateral sclerosis [21] and its application has beneficial therapeutic effects after spinal cord injury and optic nerve damage in rodents [22-24].

Toll-like receptor (TLR)-mediated NF $\kappa$ B signaling is a major pathway of pro-inflammatory microglia reactivity that may contribute to chronic neuroinflammation [25,26]. NF $\kappa$ B is tightly regulated via inhibitory  $\kappa$ B (I $\kappa$ B) proteins (predominantly I $\kappa$ B $\alpha$ ) which mask the nuclear translocation signal of NF $\kappa$ B [27]. TLR ligands including damage-associated molecular patterns from apoptotic retinal neurons [28] and bacterial lipopolysaccharide induce rapid phosphorylation of I $\kappa$ B $\alpha$  by I $\kappa$ B kinase (IKK) followed by ubiquitination and proteasomal degradation within minutes [29,30]. Upon translocation to the nucleus, NF $\kappa$ B rapidly activates the transcription of pro-inflammatory genes. The whey acidic proteins SLPI and

elafin both inhibit NF $\kappa$ B activation in monocytes by interfering with degradation of I $\kappa$ B $\alpha$  and IRAK-1, an upstream mediator of NF $\kappa$ B signaling [31,32].

In this study, we used microglial cells and several biochemical and immunological assays to elucidate whether AMWAP also influences NF $\kappa$ B signaling and thereby triggers an anti-inflammatory and neuroprotective phenotype in microglia.

## Methods

### Reagents

*Escherichia coli* 0111:B4 lipopolysaccharide (LPS), zymosan from *Saccharomyces cerevisiae*, Z-Leu-Leu-Leu-al (MG-132), and D-desthiobiotin were purchased from Sigma-Aldrich (St. Louis, MO, USA). CpG oligodeoxynucleotides were purchased from Invivogen (Toulouse, France). N-Acetyl-Leu-Leu-Norleu-al (ALLN) was purchased from Santa Cruz Biotechnology (Dallas, TX, USA). Puromycin dihydrochloride was purchased from Gold Biotechnology (St. Louis, MO, USA).

### Cell culture

BV-2 microglia were cultured in RPMI1640 with 5% fetal calf serum (FCS) supplemented with 2 mM L-glutamine and 195 nM  $\beta$ -mercaptoethanol at 37°C in a humidified atmosphere of 5% CO<sub>2</sub> as previously described [33]. BV-2 cells were preincubated for 24 h with 10  $\mu$ g/ml recombinant AMWAP or PBS as vehicle control, unless stated otherwise. BV-2 cells were stimulated with 50 ng/ml LPS, 50  $\mu$ g/ml zymosan, or 4  $\mu$ g/ml CpG oligodeoxynucleotides. BV-2 cells were preincubated with the proteasome inhibitor ALLN (100  $\mu$ g/ml) for 30 min before LPS stimulation to allow for accumulation of phosphorylated proteins. Generation and culture conditions of embryonic stem cell-derived microglia (ESdM) and mouse brain microglia have been described previously [34,35]. ESdM and primary microglia were preincubated for 24 h with 10  $\mu$ g/ml recombinant AMWAP or PBS as vehicle control and stimulated with 500 ng/ml and 50 ng/ml LPS, respectively. 661W photoreceptor-like cells were a kind gift from Prof. Muayyad Al-Ubaidi (Department of Cell Biology, University of Oklahoma Health Sciences Center, Oklahoma City, OK, USA), and the culture conditions have been described elsewhere [36]. HEK293 EBNA cells were cultured in DMEM low glucose with 1 mM sodium pyruvate and 10% FCS. All media were supplemented with 1% penicillin/streptomycin.

### Recombinant protein expression

Recombinant expression and purification of C-terminally His-tagged AMWAP in *E. coli* was carried out as described previously [14]. For eukaryotic expression of C-terminally Strep(II)-tagged AMWAP, the AMWAP ORF was amplified from BV-2 microglial cDNA with primers

forward 5'-cccctagccacatgtagtgcttggccc-3' and reverse 5'-cccctcgagaagacaggagtttgcaga-3' and subcloned into the pCEP-Pu plasmid at restriction sites *NheI* and *XhoI*. This plasmid includes the BM-40 signaling peptide which leads to secretion and is then cleaved off from the recombinant protein. The clone was validated by DNA sequencing. HEK293 EBNA cells were transfected with the expression plasmid using the Turbofect™ reagent (Thermo Scientific, Waltham, MA, USA). After 24 h, 3 µg/ml puromycin was added to select for plasmid-positive cells. After expansion of the cells, FCS-free supernatants containing secreted AMWAP were collected every 48 h, centrifuged for 7 min at 3,500 rpm at 4°C and 1 mM PMSF was added. For affinity chromatography, a Strep-Tactin® Sepharose (Iba Life Sciences, Goettingen, Germany) column was prepared and the supernatant loaded onto and passed through the column at a velocity of 0.25 ml/min at 4°C using a peristaltic pump P-1 (GE Healthcare, Little Chalfont, UK). Thereafter, the column was washed with PBS (pH 7.8) and recombinant AMWAP eluted with PBS containing 2.5 mM D-desithiobiotin. Protein-containing fractions were identified using a NanoDrop 2000 (Thermo Scientific), and protein concentration was determined by Bradford assay (Roti®-Quant, Roth, Karlsruhe, Germany) and BCA assay (Roti®-Quant universal, Roth). Recombinant protein was then stored at -20°C until further use.

#### Generation of an AMWAP antiserum and Western blot analysis

Rabbit antibodies were raised against an N-terminally GST-tagged recombinant AMWAP peptide. The AMWAP ORF was cloned into a pGEX-4-T1 vector system to express an N-terminally GST-tagged AMWAP protein in prokaryotic cells. The AMWAP ORF was PCR amplified from a plasmid that was described previously [14]. GST-tagged AMWAP protein was expressed and purified as described above. Immunization of rabbits, isolation of serum, and affinity purification was performed by Davids Biotechnologie GmbH (Neutraubling, Germany). For extraction of total cellular protein, BV-2 cells were lysed in cold RIPA buffer (20 mM Na-phosphate buffer, 150 mM NaCl, 5 mM EDTA, 1% Triton X-100, and protease inhibitors) and insoluble debris was removed by centrifugation for 15 min at 13,200 rpm. Nuclear and cytosolic protein extraction was carried out using the NE-PER kit (Thermo Scientific) according to the manufacturer's instructions. Serum-free microglial supernatants were concentrated 50-fold using Amicon® Ultra-4 centrifugal filter units with a molecular weight cut-off at 3 kDa (Merck-Millipore, Billerica, MA, USA). Protein concentrations were determined by Bradford assay (Roti®-Quant, Roth). A 10 to 20 µg of protein was separated by SDS-PAGE on 10% to 15% gels with PageRuler pre-stained protein ladder (Thermo Scientific). Proteins were then transferred to 0.45 µm nitrocellulose

membranes (Bio-Rad, Munich, Germany). After blocking in TBS-T containing 5% nonfat dry milk or bovine serum albumin, membranes were incubated with primary antibodies against AMWAP, NFκB p65 (sc-372, Santa Cruz Biotechnology), phosphorylated NFκB p65 (sc-33020, Santa Cruz Biotechnology), IRAK-1 (sc-7883, Santa Cruz Biotechnology), IκBα (sc-371, Santa Cruz Biotechnology), phosphorylated IκBα (sc-101713, Santa Cruz Biotechnology), ubiquitin (ab7780, Abcam, Cambridge, UK), actin (sc-1616, Santa Cruz Biotechnology), or GAPDH (sc-48166, Santa Cruz Biotechnology). Blots were then incubated with secondary goat anti-rabbit IgG-HRP or rabbit anti-goat IgG-HRP antibodies (sc-2004, sc-2768, Santa Cruz Biotechnology). Enhanced chemiluminescence signals were visualized and imaged with the MultiImage II system (Alpha Innotech, Santa Clara, CA, USA). Total protein visualization was done by Ponceau S staining.

#### RNA isolation and reverse transcription

Total RNA was extracted from microglia cells according to the manufacturer's instructions using the NucleoSpin® RNA Mini Kit (Macherey-Nagel, Dueren, Germany). RNA was quantified spectrophotometrically using a NanoDrop 2000 (Thermo Scientific) and then stored at -80°C. First-strand cDNA synthesis was performed with the RevertAid™ H Minus First strand cDNA Synthesis Kit (Thermo Scientific).

#### Quantitative real-time RT-PCR

Amplifications of 50 ng cDNA were performed with an ABI7900HT machine (Applied Biosystems, Carlsbad, CA, USA) in 10 µl reaction mixtures containing 1× TaqMan Universal PCR Master Mix (Applied Biosystems), 200 nM of primers, and 0.125 µl of dual-labeled UPL probe (Roche Applied Science, Basel, Switzerland). The reaction parameters were as follows: 2 min 50°C hold, 30 min 60°C hold, and 5 min 95°C hold, followed by 40 cycles of 20 s 94°C melt and 1 min 60°C anneal/extension. Primer sequences and UPL probe numbers were as follows: IL6, forward primer 5'-gatggatgctaccaactggat-3', reverse primer 5'-ccagtagctatggtactccaga-3', probe #6; iNOS, forward primer 5'-ctttgccacggacgagac-3', reverse primer 5'-tcattgtactctgagggtga-3', probe #13; CCL2, forward primer 5'-catccactgttggtca-3', reverse primer 5'-gatcatctgctgtgtaagt-3', probe #62; CASP11, forward primer 5'-gatcgggcaacctgaca-3', reverse primer 5'-tgagattcagttgctgttg-3', probe #72; TNFα, forward primer 5'-ctgtagcccacgtctagc-3', reverse primer 5'-ttgagatccatgcgctt-3', probe #78; ATP5B, forward primer 5'-ggcacaatgcaggaagg-3', reverse primer 5'-tcagcaggcacatagatagc-3', probe #77. ATP5B expression was used as the most stable reference gene. Measurements were performed in triplicates, and results were analyzed with the

ABI sequence detector software version 2.4 using the  $\Delta\Delta C_t$  method for relative quantification.

#### Fluorescence labeling of recombinant AMWAP

Recombinant AMWAP was fluorescently labeled using the Fluorescein-EX Protein Labeling Kit (Life Technologies, Carlsbad, CA, USA) according to the manufacturer's instructions. This dye has a seven-atom spacer between the succinimidyl ester group and the fluorophore to minimize unwanted interaction between the fluorophore and the labeled protein. After labeling, the protein solution was passed five times through an Amicon® Ultra-4 centrifugal filter unit with a molecular weight cut-off at 3 kDa (Merck-Millipore) at 4°C and extensively washed with PBS to get rid of excess fluorescent dye.

#### Immunocytochemistry

BV-2 cells were seeded on glass cover slips and incubated with 10 µg/ml fluorescently labeled AMWAP or vehicle for different time spans prior to stimulation with 50 ng/ml LPS for 1 h. Cells were then fixed with 4% formaldehyde, washed with PBS, and incubated in blocking buffer containing 10% goat serum and 0.3% Triton X-100. Subsequently, cells were incubated with antibodies against Iba1 or the p65 subunit of NFκB in a solution containing 2.5% goat serum and 0.1% Triton X-100 for 1 h at room temperature. After 30-min incubation with goat anti-rabbit Alexa-594 (A-11012, Life Technologies), slides were washed with PBS and stained with 4',6-diamidino-2-phenylindole (DAPI). Cover slips were mounted with fluorescent mounting medium (Dako Cytomation, Hamburg, Germany), and fluorescence photomicrographs were taken with an AxioImager.M2 plus ApoTome2 microscope (Carl Zeiss, Oberkochen, Germany). ImageJ software (National Institutes of Health, Bethesda, MD, USA) was used to determine the ratio of nuclear to cytosolic NFκB p65 after quantifying pixel intensities of both cellular compartments and subtracting background fluorescence.

#### Immunoprecipitation

In a total volume of 200 µl, cytosolic extracts (200 µg of protein), supplemented with 1× complete protease inhibitor mix (Roche Applied Science), were incubated with 30 µl Protein A-sepharose® 4B (Sigma-Aldrich) for 60 min at 4°C and subsequently centrifuged for 10 min at 2,000 g. The pre-cleared samples were then incubated at 4°C overnight with 2 µg of anti-IκBα antibody (sc-371, Santa Cruz Biotechnology). Thereafter, 30 µl fresh Protein A-sepharose® 4B was added and the mixture was incubated overnight at 4°C to allow for immunoprecipitation. The beads were then pelleted by centrifugation at 2,000 g and the pellet washed five times with PBS. Beads were then incubated in SDS-PAGE sample buffer at 95°C for

5 min and electrophoresed on a 10% SDS-PAGE. The gel was blotted and the membrane incubated with an anti-ubiquitin antibody at 4°C overnight followed by incubation with secondary goat anti-rabbit IgG-HRP at room temperature for 1 h. Enhanced chemiluminescence signals were then visualized and imaged with the MultiImage II system (Alpha Innotech).

#### 20S proteasome activity assay

Trypsin-, chymotrypsin-, and caspase-like peptidase activities associated with the 20S proteasome were measured using the Proteasome-Glo™ Assay System (Promega, Madison, WI, USA). A 1 µg/ml of purified 20S proteasome (Enzo Life Sciences, Farmingdale, NY, USA) was incubated at room temperature for 30 min with vehicle, 20 µg/ml AMWAP or 1 µM MG-132 peptidase inhibitor positive control in a 96-well plate containing the substrate for one specific peptidase. Luminescence was then measured with an Infinite F200 Pro plate reader (Tecan, Crailsheim, Germany). A blank reaction without 20S proteasome was used to determine background luminescence associated with the vehicle and Proteasome-Glo™ reagent. The values of the blank reactions were subtracted from all experimental values. Relative luciferase units (RLUs) correspond to the levels of peptidase activity.

#### Nitrite measurement

Nitric oxide concentrations were determined by measurement of nitrite released into BV-2 culture supernatants using the Griess reagent system (Promega). Fifty microliter cell culture supernatants from control, 50 ng/ml LPS-, 10 µg/ml AMWAP-, or 50 ng/ml LPS + 10 µg/ml AMWAP-treated BV-2 microglia were incubated with 100 µl Griess reagent in each well of a translucent 96-well plate. After incubation for 30 min at room temperature, absorbance was measured at 540 nm on an Infinite F200 Pro plate reader (Tecan). Nitrite concentrations were calculated on the basis of a sodium nitrite reference curve.

#### 661W photoreceptor apoptosis assay

To investigate microglial neurotoxicity, 661W photoreceptor cells were incubated for 48 h with culture supernatants from control, 50 ng/ml LPS-, 10 µg/ml AMWAP-, or 50 ng/ml LPS + 10 µg/ml AMWAP-treated BV-2 microglia. Apoptotic cell death was determined using the Caspase-Glo® 3/7 Assay (Promega). Cells were lysed and incubated with a luminogenic caspase-3/7 substrate, which contains the tetrapeptide sequence DEVD. After incubation at room temperature for 1 h, the generated luminescence was measured on an Infinite F200 Pro plate reader (Tecan). A blank reaction without cells was used to determine background luminescence associated with the cell culture system and Caspase-Glo® 3/7 reagent.

The values of the blank reactions were subtracted from all experimental values. Negative control reactions were performed to determine the basal caspase activity of 661W cells. Relative luciferase units (RLUs) reflect the level of apoptotic cell death.

#### Phalloidin-TRITC staining

BV-2 cells were seeded on cover slips in six-well plates, and attachment was allowed overnight. Cells were then preincubated with 10 µg/ml AMWAP or vehicle for 24 h before incubation with 50 ng/ml LPS for 24 h. Thereafter, cells were fixed with 4% formaldehyde, permeabilized with 0.1% Triton X-100, and F-actin was fluorescently labeled using 0.1 µg/ml Phalloidin-TRITC (Sigma-Aldrich). Nuclei were stained using DAPI, and the cover slips were mounted with fluorescent mounting medium (Dako Cytomation). Photomicrographs were taken with an AxioImager.M2 plus ApoTome2 microscope (Carl Zeiss).

#### Proliferation assay

For carboxyfluorescein diacetate succinimidyl ester (CFSE) proliferation assay, BV-2 microglia were labeled with 5 µM CFSE (e-Bioscience, San Diego, CA, USA) and cultured in a six-well plate. After 24 h of AMWAP or vehicle pretreatment and subsequent 24 h of LPS treatment, cells were stained with a fixable viability dye (e-Bioscience) to exclude dead cells from the analysis. The fluorescence intensity of CFSE-labeled BV-2 cells was analyzed by flow cytometry on a FACS Canto II (BD Biosciences, San Jose, CA, USA). Analysis of cell division rate was performed using FlowJo software (Treestar Inc., Ashland, OR, USA).

#### Phagocytosis assay

661W photoreceptor cells were starved by serum deprivation and harvested and fluorescently labeled using CellTracker CM-DiI (Invitrogen, Carlsbad, CA, USA). For phagocytosis assay, BV-2 cells were seeded on cover slips in six-well plates and attachment was allowed overnight. After pretreatment with 10 µg/ml AMWAP for 24 h and subsequent stimulation with 50 ng/ml LPS for 24 h, 500 µl-stained apoptotic 661W cell suspension was added for 6 h. After extensive washing with PBS to get rid of remaining extracellular 661W debris, cells were fixed and nuclei were stained with DAPI. Fluorescence micrographs with constant exposure times were taken with an AxioImager.M2 plus ApoTome2 microscope (Carl Zeiss). ImageJ software (National Institutes of Health) was used to determine the ratio of phagocytosed apoptotic photoreceptor fragments (background-corrected red signal) relative to the total microglia cell number (background-corrected DAPI signal).

#### Statistical analysis

Quantitative real-time RT-PCR data were analyzed with the  $\Delta\Delta C_t$  method using an unpaired Student's *t*-test. Assays for NFκB localization, 20S proteasome inhibition, nitrite secretion, caspase 3/7, and phagocytic activity were analyzed with a Mann–Whitney U-test.  $P < 0.05$  was considered statistically significant.

#### Results

##### AMWAP is secreted from reactive microglia

To elucidate whether AMWAP is secreted from reactive microglia, we treated BV-2 microglial cells with 50 ng/ml LPS for 48 h and analyzed AMWAP in cell culture supernatants and cellular extracts using a newly generated anti-AMWAP antibody. The Western blot analysis detected a single specific band at approximately 12 kDa in culture supernatants of LPS-activated BV-2 microglia but not in unstimulated cells (Figure 1A). Anti-GAPDH immunoblotting and Ponceau S staining served as loading controls for intracellular and secreted proteins. Thus, we conclude that AMWAP can be actively secreted from microglia when stimulated with a pro-inflammatory trigger such as the TLR4 ligand LPS.

To analyze the paracrine effects of AMWAP, we next carried out recombinant expression of C-terminally His-tagged and C-terminally Strep(II)-tagged AMWAP using *E. coli* and HEK293 EBNA cells, respectively. After purification by affinity chromatography, recombinant proteins were immunoblotted and detected with the anti-AMWAP antibody. Specific single bands were present at approximately 11 kDa for AMWAP-His and approximately 13 kDa for AMWAP-Strep(II) (Figure 1B). These recombinant AMWAP proteins were then used for all further functional studies.

##### AMWAP reduces the TLR-mediated pro-inflammatory microglia response through NFκB inhibition

Next, we investigated whether exogenous stimulation with AMWAP influences pro-inflammatory microglia reactivity in BV-2 cells. We tested the effects of different AMWAP concentrations ranging from 0.1 to 10 µg/ml on TLR4/LPS-induced mRNA expression of the pro-inflammatory mediators IL6, iNOS, CCL2, and CASP11 using quantitative real-time RT-PCR. These specific transcripts were selected as surrogate markers for the key microglia pathways pro-inflammatory cytokines, radical production, chemotaxis, and inflammatory caspases. AMWAP strongly and dose-dependently suppressed mRNA levels of IL6 and iNOS and had a less pronounced but significant effect on CCL2 and CASP11 gene expression (Figure 2).

Since BV-2 is a microglial cell line, we then validated these findings in embryonic stem cell-derived microglia (ESdM), a recently established model system which exhibits

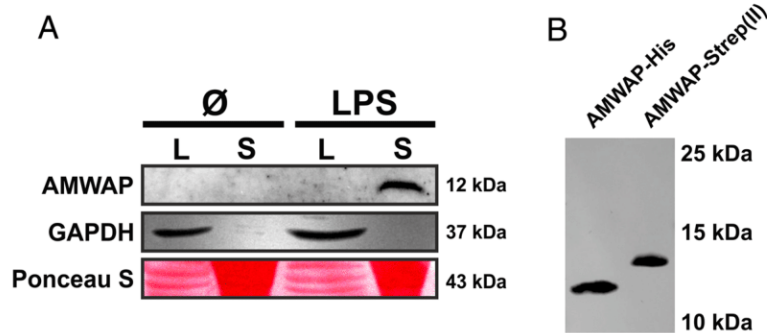


**Figure 1** AMWAP is secreted from reactive BV-2 microglia. **(A)** BV-2 microglial cells were treated with 50 ng/ml LPS for 48 h before obtaining cellular protein lysates (L) as well as concentrated culture supernatants (S). Anti-AMWAP immunoblot analysis revealed a band of approximately 12 kDa only present in the supernatant of LPS-activated microglia. GAPDH and Ponceau S served as loading controls. **(B)** Anti-AMWAP immunoblot analysis of recombinantly expressed and purified AMWAP from *E. coli* (AMWAP-His) and HEK293 EBNA cells (AMWAP-Strep(II)) shows single bands at approximately 11 to 13 kDa.

many properties of primary microglia [35,37]. ESdM pretreated with 10 µg/ml AMWAP showed significantly reduced mRNA expression of the pro-inflammatory mediators IL6, iNOS, CCL2, CASP11, and TNFα after LPS activation (Figure 3A-E). These results were also fully

replicated in primary mouse brain microglia (Figure 3F-J), indicating that BV-2 microglia are a suitable model to study the effects of AMWAP on microglia.

We next investigated a potential anti-inflammatory effect of AMWAP on microglial cells that were activated with

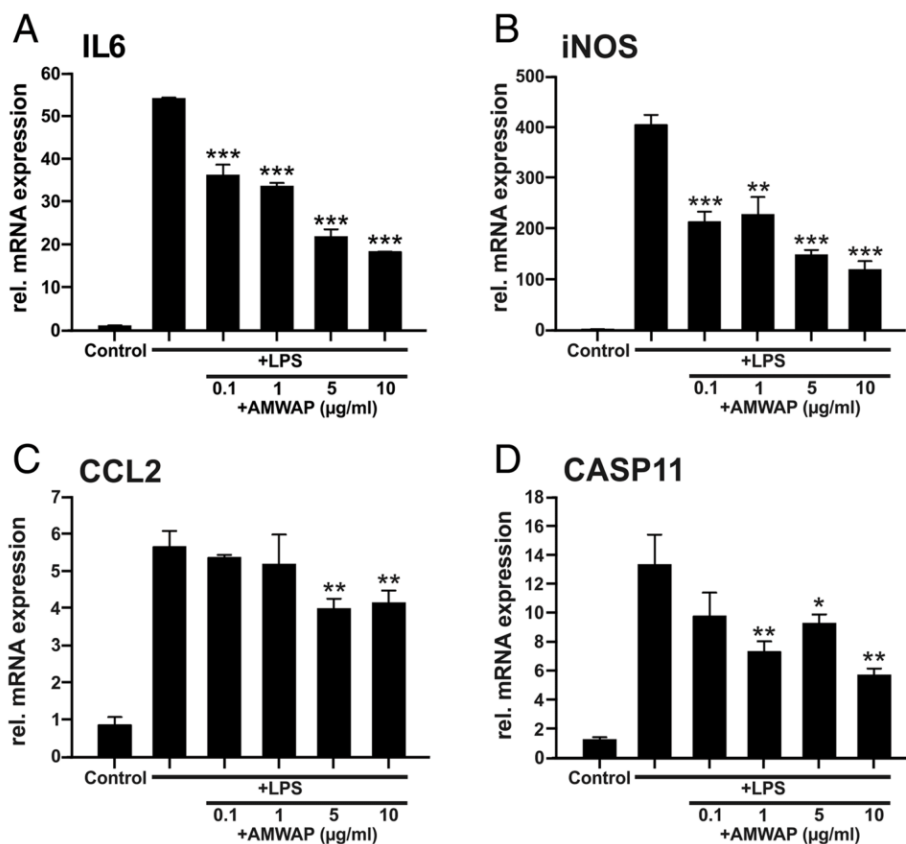
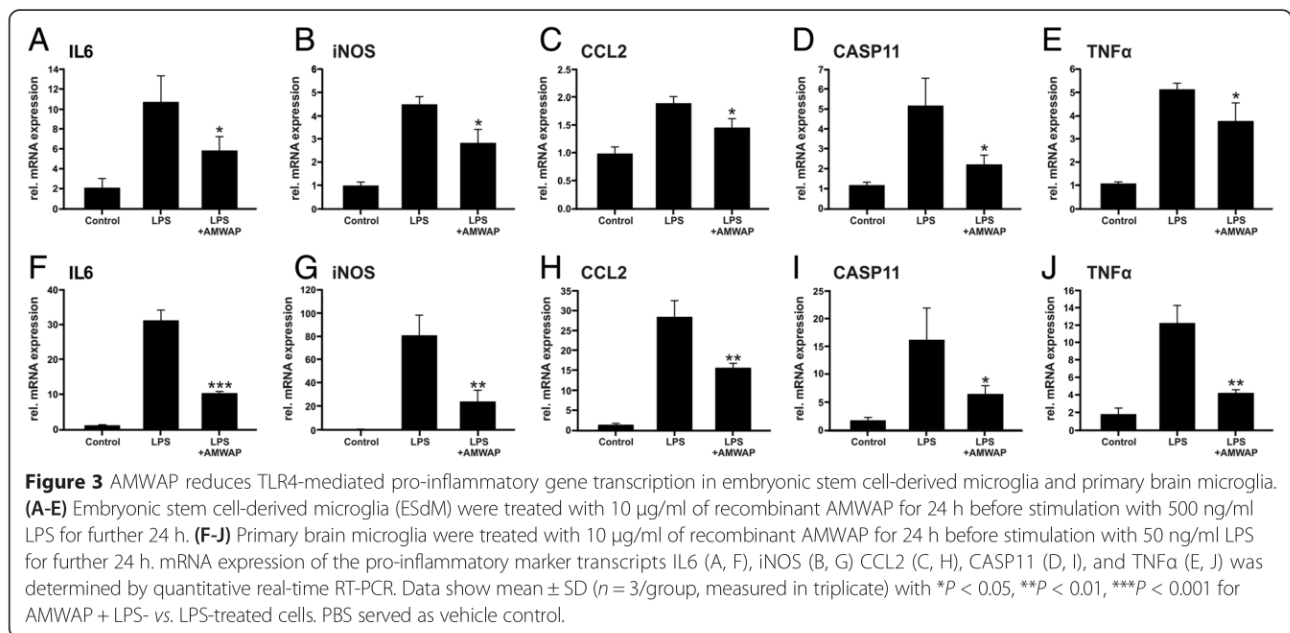


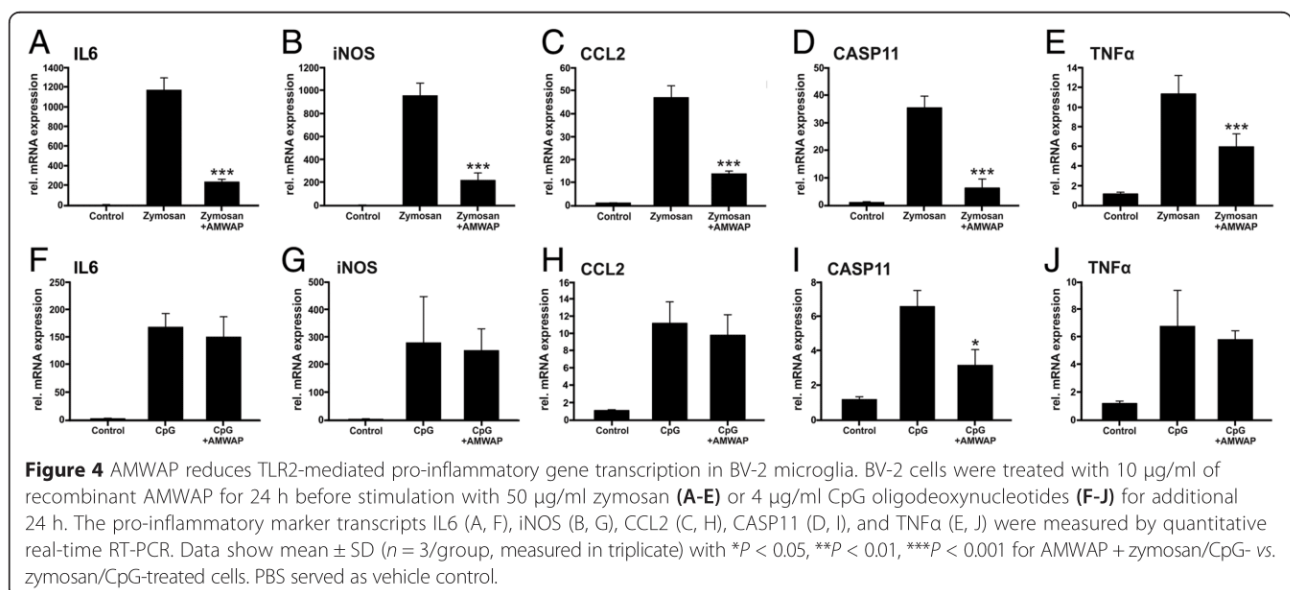
**Figure 2** AMWAP reduces pro-inflammatory marker gene transcription in BV-2 microglia. BV-2 cells were treated with various concentrations of recombinant AMWAP for 24 h before further stimulation with 50 ng/ml LPS for 12 h. Transcript levels of the pro-inflammatory markers IL6 **(A)**, iNOS **(B)**, CCL2 **(C)**, and CASP11 **(D)** were determined by quantitative real-time PCR. Data show mean ± SD (*n* = 3/group, measured in triplicate) with \**P* < 0.05, \*\**P* < 0.01, \*\*\**P* < 0.001 for AMWAP + LPS- vs. LPS-treated cells. PBS served as vehicle control.

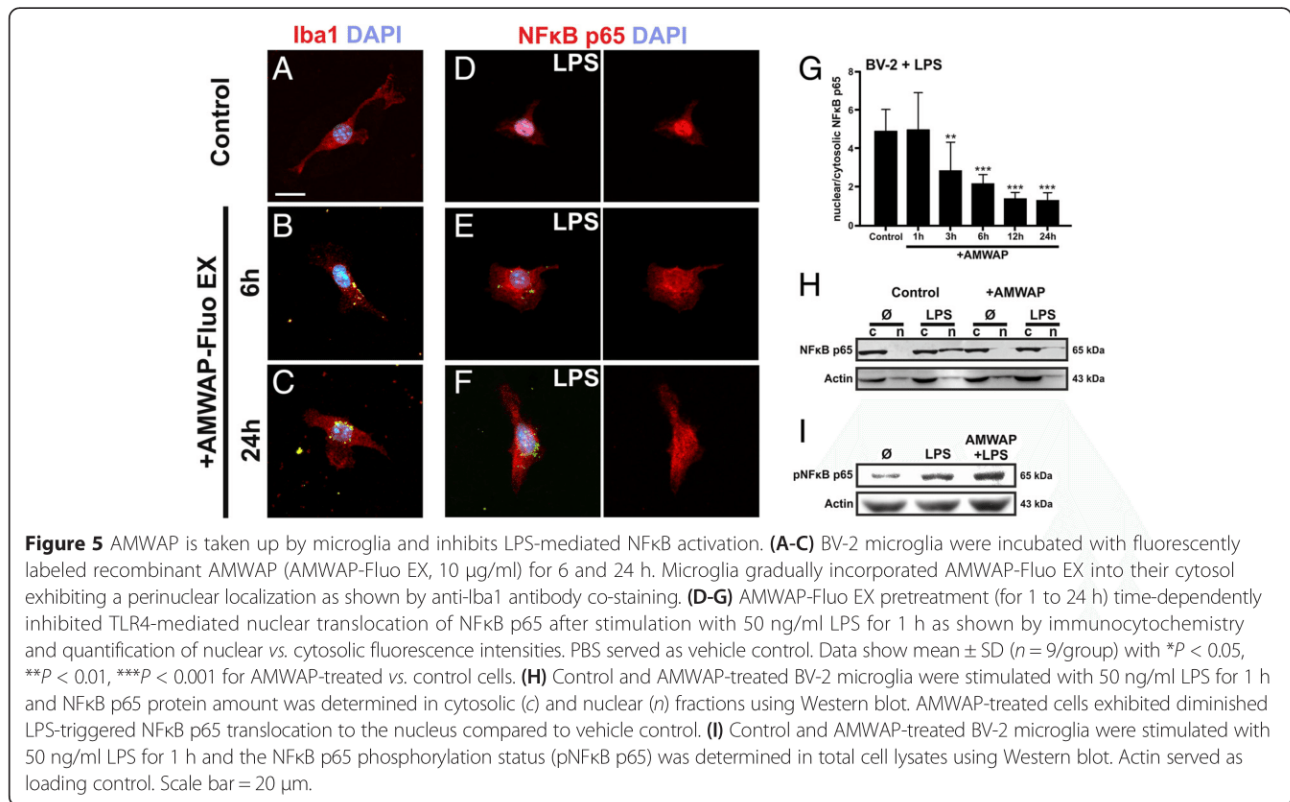


TLR2 and TLR9 ligands, respectively. TLR2, as does TLR4, acts on the cell surface and predominantly signals via NFκB, whereas intracellular TLR9 activation mainly stimulates interferon regulatory factors and has only a minor effect on NFκB targets [38]. BV-2 microglia pretreated with 10 µg/ml AMWAP showed strongly reduced mRNA expression of IL6, iNOS, CCL2, CASP11, and TNFα after activation with the TLR2 ligand zymosan (Figure 4A-E). In contrast, AMWAP only weakly influenced gene transcription of CASP11 triggered by CpG oligodeoxynucleotides as TLR9 ligands (Figure 4F-J).

To investigate whether exogenous AMWAP is taken up by microglia and potentially influences NFκB activation,

we treated BV-2 cells with 10 µg/ml fluorescently labeled AMWAP (AMWAP-Fluo EX) for different time periods. AMWAP-Fluo EX was gradually incorporated by microglia and ultimately localized to the cytosol in a perinuclear fashion (Figure 5A-C). Upon stimulation with 50 ng/ml LPS for 1 h, TLR4-mediated NFκB p65 translocation to the nucleus was effectively inhibited in AMWAP-positive cells as shown by quantitative immunocytochemistry (Figure 5D-G). These findings were confirmed by Western blot analysis of cytosolic vs. nuclear NFκB p65 levels for control and AMWAP-treated BV-2 microglia with or without stimulation with 50 ng/ml LPS for 1 h (Figure 5H). AMWAP did not interfere with LPS-induced





phosphorylation of NFκB p65 in BV-2 microglia (Figure 5I), indicating that AMWAP acts mainly through inhibition of nuclear NFκB p65 translocation rather than blocking NFκB p65 phosphorylation. These data are in agreement with observations from microglia overexpressing AMWAP-GFP, which showed diminished nuclear NFκB p65 translocation upon LPS-stimulation (Additional file 1: Figure S1).

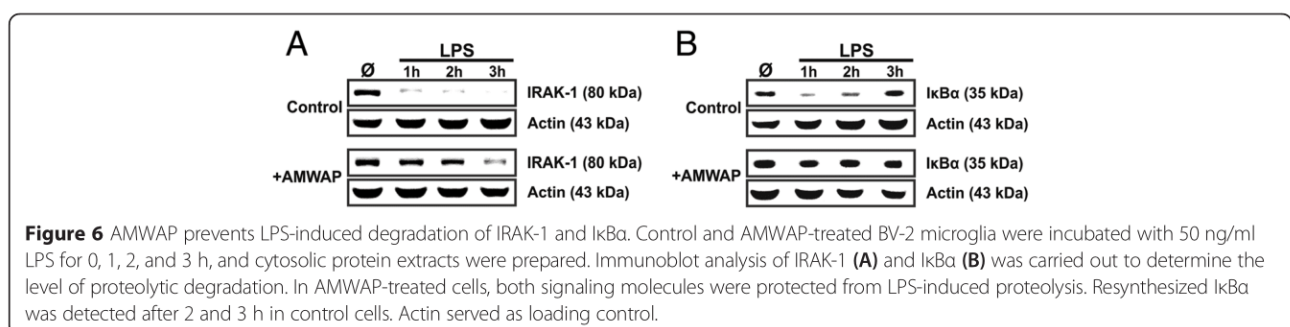
#### AMWAP prevents LPS-triggered degradation of IRAK-1 and IκBα

To further investigate the mechanisms of AMWAP on microglial NFκB signaling, we analyzed the protein levels of the NFκB pathway mediators IRAK-1 and IκBα in a short time course of LPS and AMWAP co-treatment. Western blot analysis of cytosolic fractions showed a rapid degradation of both signaling proteins as early as 1 h after

LPS stimulation of microglia (Figure 6), with apparent IκBα resynthesis starting after 2 h (Figure 6B). Treatment with AMWAP effectively protected IRAK-1 and particularly IκBα from rapid LPS-induced proteolysis.

#### AMWAP acts independent of IκBα phosphorylation, ubiquitination, or the 20S proteasome

We next assessed the effect of AMWAP on LPS-induced phosphorylation of IκBα. IκBα phosphorylation is an upstream event of NFκB p65 nuclear translocation and thus a critical event in NFκB signaling. BV-2 microglia were preincubated with the proteasome inhibitor ALLN (100 μg/ml) for 30 min to allow for accumulation of labile phosphorylated IκBα species. After stimulation with 50 ng/ml LPS for 30 min, the amount of phosphorylated IκBα in cytosolic extracts was analyzed using Western



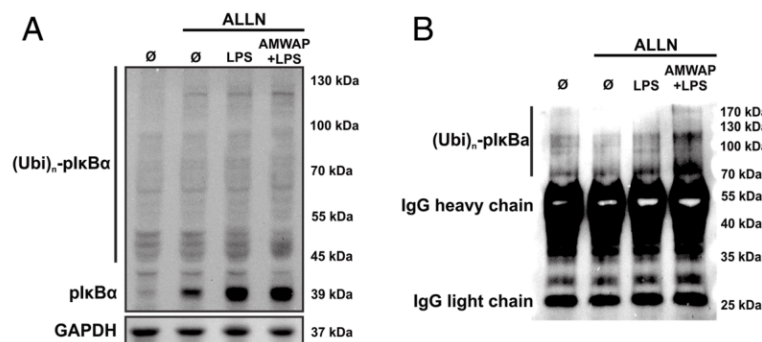


**Figure 7** AMWAP does not inhibit IκBα phosphorylation and ubiquitination. **(A)** Control and AMWAP-treated BV-2 microglia were preincubated with the proteasome inhibitor ALLN (100 μg/ml) for 30 min to allow for accumulation of phosphorylated IκBα before stimulation with LPS (50 ng/ml) for 30 min. Levels of phosphorylated IκBα were assessed in cytoplasmic extracts using Western blot analysis. AMWAP did not reduce LPS-induced IκBα phosphorylation. The presence of various high molecular weight bands was noticed, presumably representing polyubiquitinated, phosphorylated IκBα. **(B)** IκBα was immunoprecipitated from cytoplasmic samples of cells treated as in (A). Thereafter, anti-ubiquitin immunoblot revealed the presence of high molecular weight polyubiquitinated forms of phosphorylated IκBα, which were not diminished in AMWAP-positive cells. GAPDH served as loading control. (p)IκBα, (phosphorylated) inhibitor of kappa B alpha; Ubi, ubiquitin; IgG, immunoglobulin G; ALLN; N-acetyl-Leu-Leu-Norleu-al.

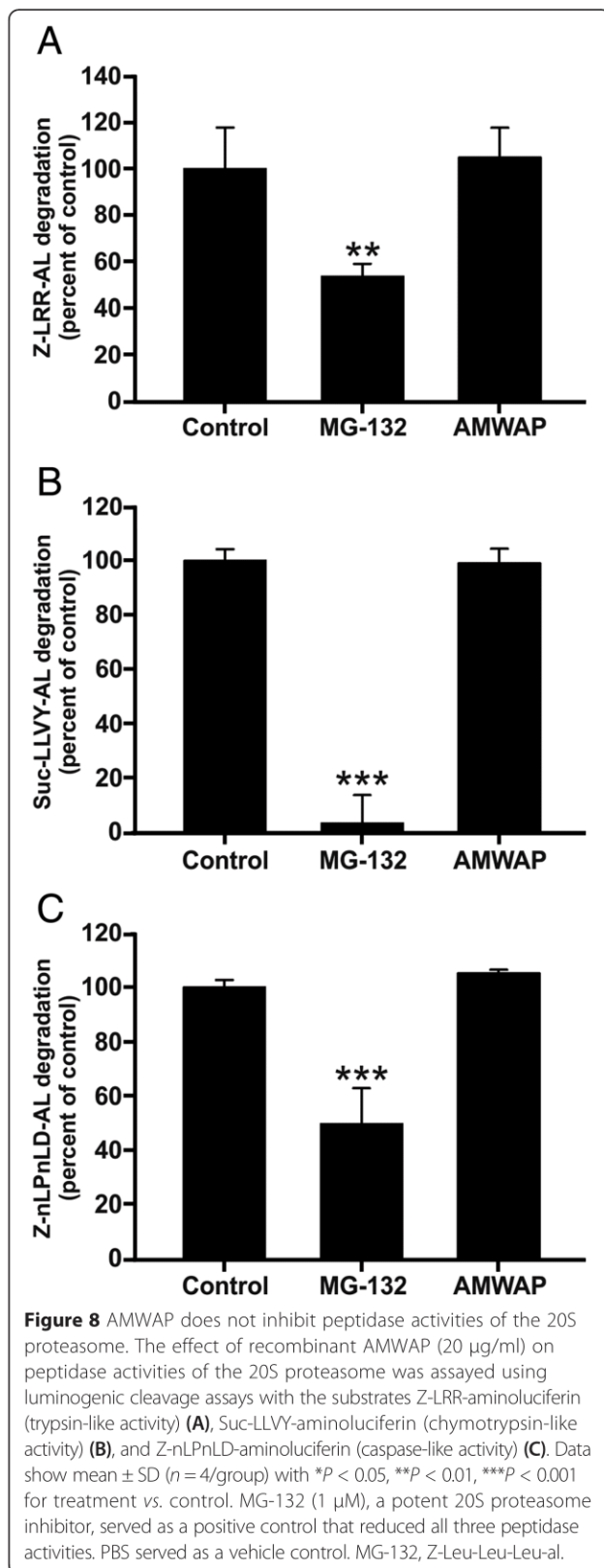
blot. Phosphorylated IκBα levels were significantly elevated in LPS-treated cells (Figure 7A). However, this rapid IκBα phosphorylation was not changed in AMWAP-treated cells (Figure 7A). In this Western blot, we noticed the presence of multiple high molecular weight bands, which presumably represent polyubiquitinated, phosphorylated IκBα-species. To verify this assumption, we immunoprecipitated IκBα from the cytoplasmic samples and carried out anti-ubiquitin immunoblot analysis. This experiment clearly revealed the presence of high molecular weight polyubiquitinated forms of phosphorylated IκBα between 70 and 130 kDa in LPS-treated microglia, which were not reduced by AMWAP treatment (Figure 7B).

Of note, we observed that AMWAP-treated BV-2 microglia accumulated phosphorylated IκBα after stimulation with 50 ng/ml LPS for 30 min even in the absence of the proteasome inhibitor ALLN and even slightly inhibited the basal turnover of (phosphorylated) IκBα under non-LPS-treated conditions (Additional file 2: Figure S2). These findings prompted us to investigate whether AMWAP reduces IκBα proteolysis due to direct inhibition of the 20S proteasome. A luminogenic cleavage assay using the substrates Z-LRR-aminoluciferin (for trypsin-like activity), Suc-LLVY-aminoluciferin (for chymotrypsin-like activity), and Z-nLPnLD-aminoluciferin (for caspase-like activity) was used to test the three different 20S peptidase activities. There was no influence on 20S peptidase activities by AMWAP in contrast to a strong reduction of all three activities by the proteasome inhibitor MG-132 (Figure 8). Based on these findings, we conclude that the AMWAP-triggered inhibition of IκBα degradation is not mediated by direct interference with 20S proteasome activity.

#### AMWAP induces a neuroprotective microglia phenotype

We next aimed to investigate the effects of recombinant AMWAP on pro-inflammatory microglial functions including the production of toxic oxygen radicals and direct effects on retinal neurons. As AMWAP significantly reduced iNOS gene expression in LPS-treated microglia (Figure 2A, Figure 3B,G), we also tested its influence on NO production. AMWAP effectively diminished the strong LPS-induced NO secretion into the microglia culture supernatant (Figure 9A). To further test the influence of AMWAP on microglial neurotoxicity, 661W photoreceptor cells were incubated for 48 h with conditioned media from BV-2 cells and caspase-related apoptotic cell death was monitored. 661W photoreceptors cultured in the presence of microglial supernatants derived from LPS-activated cells showed higher caspase 3/7 activity, which was effectively reduced when microglia were treated with AMWAP (Figure 9B). These data suggest that AMWAP limits microglial production of neurotoxic molecules and may potentially induce the release of neurotrophic factors.

As filopodia formation is a hallmark of homeostatic microglia, we investigated the effect of AMWAP on microglia morphology. LPS-activated or control BV-2 cells were cultured in the absence or presence of AMWAP, and their F-actin cytoskeleton was stained using Phalloidin-TRITC. AMWAP treatment induced filopodia formation in control microglia and even reversed the amoeboid phenotype observed after LPS activation (Figure 10A). CFSE labeling and FACS analysis demonstrated that AMWAP did not exert significant anti-mitotic effects on BV-2 cells, which could have been a potential bias in cell shape (Figure 10B). We finally analyzed phagocytosis of cellular debris as another parameter of the non-inflammatory housekeeping function of microglia. For this



purpose, CM-DiI-stained apoptotic 661W photoreceptor fragments were exposed to control and LPS-treated cells in the absence or presence of AMWAP and the amount of phagocytosed debris was monitored. AMWAP significantly increased the phagocytic uptake of 661W photoreceptor debris in the presence or absence of LPS, indicating its important regulatory activity on microglia (Figure 10C,D).

## Discussion

We have previously shown that AMWAP overexpression in microglia induces an anti-inflammatory counter-regulatory phenotype and that knockdown of AMWAP leads to higher intrinsic pro-inflammatory cytokine expression [14]. AMWAP expression and secretion are themselves controlled by NFκB as blockade of NFκB activation inhibits LPS-mediated induction of AMWAP expression [14]. In the present study, we show that AMWAP is a secreted protein of reactive microglia that acts in a paracrine fashion to prevent TLR4- and TLR2-triggered NFκB translocation. Furthermore, we demonstrate here that AMWAP interferes with the proteolytic degradation of the regulator proteins IRAK-1 and IκBα. This function of AMWAP in microglia is reminiscent of SLPI, another member of the WAP family, which is secreted from macrophages and acts as a suppressor of LPS responses [39].

To obtain larger amounts of recombinant protein for further exploration of the immunoregulatory role of AMWAP, we first generated prokaryotic AMWAP. Since previous studies on SLPI function demonstrated improved folding and disulfide bond formation when expressed in the yeast *Pichia pastoris* [40,41], we then also obtained AMWAP from a eukaryotic source. Despite the fact that both recombinant AMWAP forms used in our study exerted similar NFκB inhibitory and anti-inflammatory functions, the risk of LPS contamination is significantly reduced when using eukaryotic HEK293 EBNA cells for AMWAP expression.

We showed that AMWAP dampened the TLR4-induced expression of the bona fide NFκB target genes IL6, iNOS, CCL2, CASP11, and TNFα in BV-2 microglia, as well as in ESdM cells, which closely mimic primary microglia regarding their transcriptomic profile [37] and in mouse brain microglia. We also found that AMWAP effectively reduced TLR2-mediated pro-inflammatory gene expression but had only weak effects on TLR9 signaling. TLR2 signals mainly through NFκB, while TLR9 acts predominantly via interferon regulatory factors (IRFs) [38,42]. Therefore, a plausible explanation for the lack of AMWAP-mediated inhibition of IL6, iNOS, CCL2, and TNFα after CpG oligodeoxynucleotide treatment is that these genes are also IRF regulated [43-46]

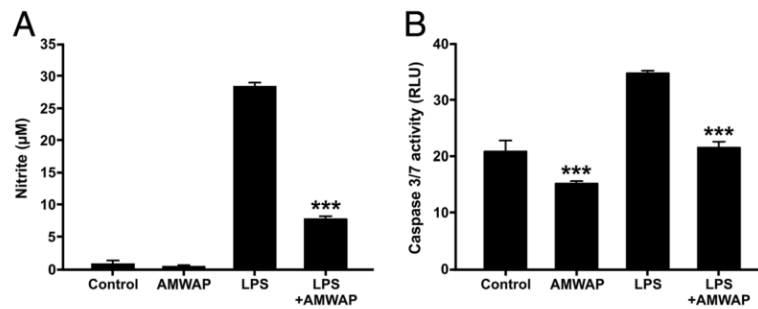


**Figure 9** AMWAP reduces pro-inflammatory microglial nitric oxide production and neurotoxicity on photoreceptor cells. **(A)** Production of nitric oxide (NO) as determined by detection of nitrite from BV-2 microglial cells pre-treated with 10 µg/ml AMWAP or vehicle for 24 h before stimulation with 50 ng/ml LPS for further 24 h. Data show mean ± SD ( $n = 6$ /group) with  $*P < 0.05$ ,  $**P < 0.01$ ,  $***P < 0.001$  for AMWAP + LPS vs. LPS-treated cells. **(B)** 661W photoreceptor cells were incubated with conditioned media from vehicle-, 10 µg/ml AMWAP-, 50 ng/ml LPS-, and 50 ng/ml LPS + 10 µg/ml AMWAP-treated BV-2 microglia for 48 h and apoptosis-related caspase 3/7 activity was determined. Data show mean ± SD ( $n = 5$ /group) with  $*P < 0.05$ ,  $**P < 0.01$ ,  $***P < 0.001$  for AMWAP-treated cells vs. control and AMWAP + LPS vs. LPS-treated cells, respectively. PBS served as a vehicle control. NO, nitric oxide; RLU, relative luciferase units.

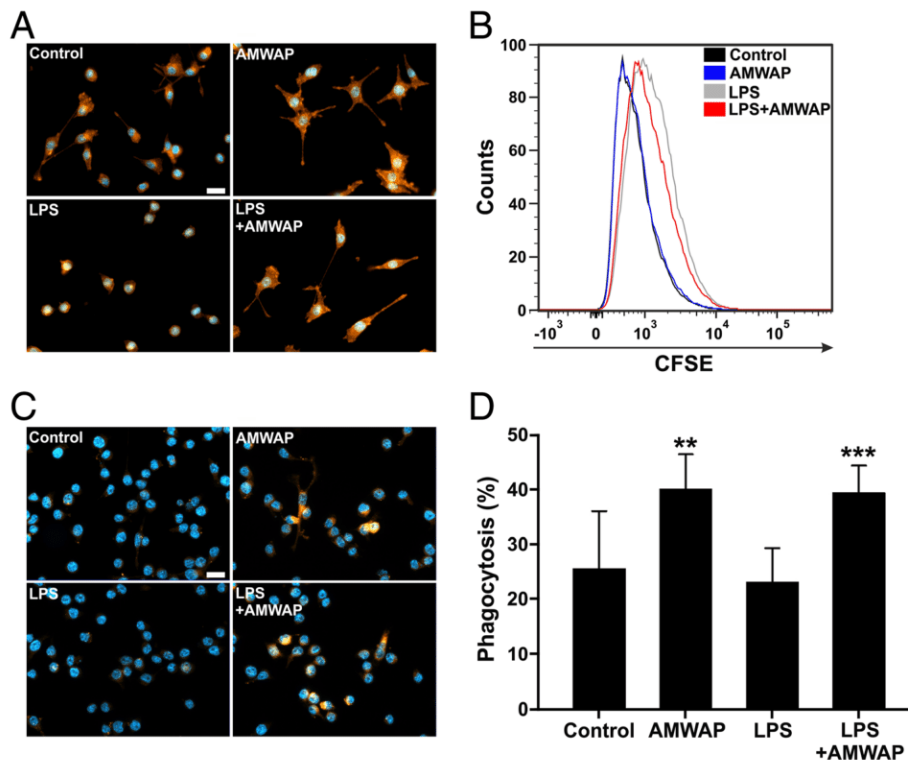


**Figure 10** AMWAP promotes microglial filopodia formation and phagocytosis. **(A)** Representative images of Phalloidin-TRITC labeled BV-2 microglial cells pre-treated with 10 µg/ml AMWAP or vehicle for 24 h in the absence or presence of 50 ng/ml LPS for 24 h. **(B)** CFSE-proliferation assay of BV-2 microglia treated with 10 µg/ml AMWAP or vehicle for 24 h in the absence or presence of 50 ng/ml LPS for 24 h. The proliferation rate was assessed 24 h after LPS treatment using flow cytometry and a representative graph out of three repetitions is shown. **(C, D)** Phagocytosis of CM-Dil-stained apoptotic 661W photoreceptor debris by BV-2 microglia was monitored and quantified after 6-h feeding time of AMWAP- vs. vehicle-treated cells in the absence or presence of 50 ng/ml LPS for 24 h. Data show mean ± SD ( $n = 9$ /group) with  $*P < 0.05$ ,  $**P < 0.01$ ,  $***P < 0.001$  for AMWAP-treated cells vs. control and AMWAP + LPS vs. LPS-treated cells, respectively. PBS served as a vehicle control. CFSE, carboxyfluorescein diacetate succinimidyl ester. Scale bar = 20 µm.

whereas TLR-induced CASP11 expression is mediated by NF $\kappa$ B and independent from IRFs [47]. These findings are also consistent with data from other whey acidic proteins as SLPI has been reported to inhibit TLR2- and TLR4-mediated NF $\kappa$ B activation in human monocytic U937 cells [48].

Together with our previous observation that AMWAP inhibits NF $\kappa$ B-dependent CCL2 promoter activity [14], these findings prompted us to study the direct influence of AMWAP on microglial NF $\kappa$ B activation. Exogenous AMWAP was taken up by microglia and effectively inhibited LPS-triggered nuclear NF $\kappa$ B p65 translocation. This effect very likely works in an autocrine and paracrine way as AMWAP is actively secreted from pro-inflammatory microglia. Upon LPS stimulation, NF $\kappa$ B p65 is rapidly phosphorylated at Ser536 by I $\kappa$ B kinases (IKKs) in the cytosol, increasing its transactivation potential once translocated into the nucleus [49]. We did not observe an inhibition of NF $\kappa$ B p65 phosphorylation through AMWAP, indicating that the anti-inflammatory effect of AMWAP is mainly due to cytosolic NF $\kappa$ B retention. We observed a 'patchy' perinuclear pattern of fluorescently labeled AMWAP in the cells, which raised the question of a possible localization in subcellular compartments. Interestingly, SLPI is located in cellular granules in neutrophils and can be released through exocytosis [50]. Another study reported that SLPI partially resides in the nucleus, where it competes with NF $\kappa$ B for binding sites at pro-inflammatory gene promoters [51]. However, in this study, we did not observe any nuclear translocation of fluorescently labeled AMWAP into microglia, even after prolonged incubation periods.

Our results showed that AMWAP effectively inhibited the rapid LPS-mediated proteolytic degradation of IRAK-1 and I $\kappa$ B $\alpha$ , concomitantly preventing nuclear NF $\kappa$ B translocation. Further experiments demonstrated that I $\kappa$ B $\alpha$  phosphorylation and ubiquitination were not influenced by AMWAP. This is in agreement with previous studies reporting similar observations for SLPI and elafin in monocytes [31,32]. Our experiments also revealed that AMWAP did not exert direct inhibitory effects on 20S proteasome activity. In accordance with our data, the LPS-inducible antibacterial peptide PR39 was shown to block degradation of I $\kappa$ B $\alpha$  without affecting its phosphorylation, ubiquitination, or overall proteasome activity [52]. The anti-bacterial and anti-protease functions of whey acidic proteins are mainly attributed to their WAP domains [53-55]. In contrast, the suppression of the LPS-induced pro-inflammatory macrophage response mediated by SLPI is independent of its anti-protease activity [56]. Further analysis will be required to determine which functional elements in AMWAP are responsible for its immunomodulatory function.

AMWAP significantly inhibited the LPS-triggered release of nitric oxide from microglia, an effect that has been observed in SLPI overexpressing macrophages [39,56]. AMWAP also reduced microglial neurotoxicity on 661W photoreceptor cells. In line with this, SLPI has been shown to reduce LPS-induced neutrophil apoptosis and a lack of SLPI resulted in increased apoptosis of myeloid cells [57,58].

Filopodia formation is a hallmark of homeostatic microglial cells that constantly survey their microenvironment with their branched protrusions [5]. Our experiments indeed showed that AMWAP promotes the formation of branched filopodia. High phagocytic clearance of apoptotic debris by microglia is also regarded as an important anti-inflammatory feature [59,60]. We observed an increased phagocytic uptake of apoptotic photoreceptor fragments by AMWAP-treated microglia, which was independent of further LPS stimulation as apoptotic cells *per se* represent an activating stimulus for microglia [8]. Along this line, macrophages show elevated secretion of SLPI during the ingestion of cellular debris, and a similar effect can be hypothesized for AMWAP and microglia [61]. Of note, elafin overexpression protects macrophages from neutrophil elastase-mediated degradation of their receptors for apoptotic cell recognition, effectively restoring phagocytic recognition and clearance in inflammatory settings [62].

Reactive microglia generally exhibit higher proliferation rates compared to regulatory microglia [9,60]. However, we were not able to detect any anti-mitotic effect of AMWAP in BV-2 microglia. It is noteworthy, that there is conflicting evidence in the literature regarding the anti-proliferative potential of whey acidic proteins. One report even observed a SLPI-induced increase of stem cell proliferation towards an oligodendroglial cell fate via induction of cyclin D1 [63].

## Conclusions

We have shown that AMWAP is a secreted anti-inflammatory protein of reactive microglia that acts in a paracrine fashion. Endocytosed AMWAP is localized in a perinuclear region where it prevents NF $\kappa$ B signaling via inhibition of IRAK-1 and I $\kappa$ B $\alpha$  proteolytic degradation. AMWAP does not affect phosphorylation or ubiquitination of these signaling proteins and has no influence on overall 20S proteasome activity. On a functional level, AMWAP inhibits pro-inflammatory gene expression, reduces microglial neurotoxicity, promotes filopodia formation, and increases phagocytic uptake of apoptotic debris. In conclusion, our data suggest that AMWAP triggers a neuroprotective phenotype in microglia and that whey acidic proteins may be potential therapeutics to inhibit a detrimental microglial phenotype in neurodegenerative diseases of the brain and retina.

## Additional files

**Additional file 1: Figure S1.** AMWAP overexpression reduces LPS-induced nuclear translocation of NFκB p65. (A) BV-2 microglia overexpressing AMWAP-GFP and MOCK-GFP control cells were incubated with 50 ng/ml LPS for 2 h before anti-NFκB immunocytochemistry. AMWAP-GFP overexpressing cells showed a reduced nuclear translocation of NFκB p65 as shown by quantification of nuclear and cytosolic fluorescence signals (B) Data show mean ± SD (n = 9/group) \*P < 0.05, \*\*P < 0.01, \*\*\*P < 0.001. Scale bar = 20 μm.

**Additional file 2: Figure S2.** AMWAP inhibits LPS-induced turnover of (phosphorylated) IκBα. Control and AMWAP-treated BV-2 microglia were incubated with 50 ng/ml LPS for 30 min, and cytosolic protein extracts were prepared before immunoblot analysis of phosphorylated IκBα. LPS-induced IκBα phosphorylation was observed in AMWAP-treated and control cells. However, AMWAP-treated cells accumulated phosphorylated IκBα, protecting it from proteasomal degradation and even inhibited the basal IκBα turnover in unstimulated cells. GAPDH served as loading control. plκBα, phosphorylated inhibitor of kappa B alpha.

### Competing interests

The authors declare that they have no competing interests.

### Authors' contributions

TL, AA, and MK designed the research; AA, RS, CF, MP, HN, and SF performed the research. AA, RS, and MK analyzed the data. TL obtained funding and designed the study. AA and TL wrote the manuscript. All authors read and approved the final manuscript.

### Acknowledgements

This work was supported by grants from the German Research Foundation (DFG LA1203/6-2 and FOR2240/LA1203/9-1), the Pro Retina Foundation, the Hans- und Marlies Stock-Stiftung, and the Bayer graduate program in pharmacology and experimental therapeutics. The authors thank Dr. Frank Zaucke for providing the pCEP-Pu plasmid and Prof. Muayyad Al Ubaidi for providing the 661W photoreceptor cell line.

### Author details

<sup>1</sup>Laboratory for Experimental Immunology of the Eye, Department of Ophthalmology, University of Cologne, Kerpener Strasse 62, D-50931 Cologne, Germany. <sup>2</sup>Institute of Reconstructive Neurobiology, University of Bonn, Sigmund-Freud-Straße 25, D-53127 Bonn, Germany. <sup>3</sup>Department of Pharmacology, University of Cologne, Gleueler Straße 24, D-50931 Cologne, Germany.

Received: 10 December 2014 Accepted: 7 April 2015

Published online: 19 April 2015

### References

- Hanisch UK, Kettenmann H. Microglia: active sensor and versatile effector cells in the normal and pathologic brain. *Nat Neurosci.* 2007;10:1387–94.
- Streit WJ. Microglia as neuroprotective, immunocompetent cells of the CNS. *Glia.* 2002;40:133–9.
- Giulian D, Li J, Bartel S, Broker J, Li X, Kirkpatrick JB. Cell surface morphology identifies microglia as a distinct class of mononuclear phagocyte. *J Neurosci.* 1995;15:7712–26.
- Davalos D, Grutzendler J, Yang G, Kim JV, Zuo Y, Jung S, et al. ATP mediates rapid microglial response to local brain injury in vivo. *Nat Neurosci.* 2005;8:752–8.
- Nimmerjahn A, Kirchhoff F, Helmchen F. Resting microglial cells are highly dynamic surveillants of brain parenchyma in vivo. *Science.* 2005;308:1314–8.
- Broderick C, Hoek RM, Forrester JV, Liversidge J, Sedgwick JD, Dick AD. Constitutive retinal CD200 expression regulates resident microglia and activation state of inflammatory cells during experimental autoimmune uveoretinitis. *Am J Pathol.* 2002;161:1669–77.
- Cardona AE, Pioro EP, Sasse ME, Kostenko V, Cardona SM, Dijkstra IM, et al. Control of microglial neurotoxicity by the fractalkine receptor. *Nat Neurosci.* 2006;9:917–24.
- Heneka MT, Kummer MP, Latz E. Innate immune activation in neurodegenerative disease. *Nat Rev Immunol.* 2014;14:463–77.
- Perry VH, Nicoll JA, Holmes C. Microglia in neurodegenerative disease. *Nat Rev Neurol.* 2010;6:193–201.
- Orr CF, Rowe DB, Halliday GM. An inflammatory review of Parkinson's disease. *Prog Neurobiol.* 2002;68:325–40.
- Raivich G, Banati R. Brain microglia and blood-derived macrophages: molecular profiles and functional roles in multiple sclerosis and animal models of autoimmune demyelinating disease. *Brain Res Brain Res Rev.* 2004;46:261–81.
- Langmann T. Microglia activation in retinal degeneration. *J Leukoc Biol.* 2007;81:1345–51.
- Karlstetter M, Scholz R, Rutar M, Wong WT, Provis JM, Langmann T. Retinal microglia: just bystander or target for therapy? *Prog Retin Eye Res.* 2015;45:30–57.
- Karlstetter M, Walczak Y, Weigelt K, Ebert S, Van den Brulle J, Schwer H, et al. The novel activated microglia/macrophage WAP domain protein, AMWAP, acts as a counter-regulator of proinflammatory response. *J Immunol.* 2010;185:3379–90.
- Karlstetter M, Sorusch N, Caramoy A, Dannhausen K, Aslanidis A, Fauser S, et al. Disruption of the retinitis pigmentosa 28 gene Fam161a in mice affects photoreceptor ciliary structure and leads to progressive retinal degeneration. *Hum Mol Genet.* 2014;23:5197–210.
- Simpson KJ, Nicholas KR. The comparative biology of whey proteins. *J Mammary Gland Biol Neoplasia.* 2002;7:313–26.
- Hennighausen LG, Sippel AE. Mouse whey acidic protein is a novel member of the family of 'four-disulfide core' proteins. *Nucleic Acids Res.* 1982;10:2677–84.
- Scott A, Weldon S, Taggart CC. SLPI and elafin: multifunctional antiproteases of the WFDC family. *Biochem Soc Trans.* 2011;39:1437–40.
- Bingle CD, Vyakarnam A. Novel innate immune functions of the whey acidic protein family. *Trends Immunol.* 2008;29:444–53.
- Doumas S, Kolokotronis A, Stefanopoulos P. Anti-inflammatory and antimicrobial roles of secretory leukocyte protease inhibitor. *Infect Immun.* 2005;73:1271–4.
- Lilo E, Wald-Altman S, Solmesky LJ, Ben Yaakov K, Gershoni-Emek N, Bulvik S, et al. Characterization of human sporadic ALS biomarkers in the familial ALS transgenic mSOD1(G93A) mouse model. *Hum Mol Genet.* 2013;22:4720–5.
- Ghasemlou N, Bouhy D, Yang J, Lopez-Vales R, Haber M, Thuraisingam T, et al. Beneficial effects of secretory leukocyte protease inhibitor after spinal cord injury. *Brain.* 2010;133:126–38.
- Hannila SS, Siddiq MM, Carmel JB, Hou J, Chaudhry N, Bradley PM, et al. Secretory leukocyte protease inhibitor reverses inhibition by CNS myelin, promotes regeneration in the optic nerve, and suppresses expression of the transforming growth factor-beta signaling protein Smad2. *J Neurosci.* 2013;33:5138–51.
- Hannila SS. Secretory leukocyte protease inhibitor (SLPI): emerging roles in CNS trauma and repair. *Neuroscientist.* Published online before print August 12, 2014, doi:10.1177/1073858414546000.
- Wulczyn FG, Krappmann D, Scheidereit C. The NF-kappa B/Rel and I kappa B gene families: mediators of immune response and inflammation. *J Mol Med (Berl).* 1996;74:749–69.
- Mattson MP, Camandola S. NF-kappaB in neuronal plasticity and neurodegenerative disorders. *J Clin Invest.* 2001;107:247–54.
- Krappmann D, Wulczyn FG, Scheidereit C. Different mechanisms control signal-induced degradation and basal turnover of the NF-kappaB inhibitor I kappa B alpha in vivo. *EMBO J.* 1996;15:6716–26.
- Kohno H, Chen Y, Kevany BM, Pearlman E, Miyagi M, Maeda T, et al. Photoreceptor proteins initiate microglial activation via toll-like receptor 4 in retinal degeneration mediated by all-trans-retinal. *J Biol Chem.* 2013;288:15326–41.
- Karin M, Ben-Neriah Y. Phosphorylation meets ubiquitination: the control of NF-[kappa]B activity. *Annu Rev Immunol.* 2000;18:621–63.
- Bhoj VG, Chen ZJ. Ubiquitylation in innate and adaptive immunity. *Nature.* 2009;458:430–7.
- Taggart CC, Greene CM, McElvaney NG, O'Neill S. Secretory leucoprotease inhibitor prevents lipopolysaccharide-induced I kappa Balpha degradation without affecting phosphorylation or ubiquitination. *J Biol Chem.* 2002;277:33648–53.
- Butler MW, Robertson I, Greene CM, O'Neill SJ, Taggart CC, McElvaney NG. Elafin prevents lipopolysaccharide-induced AP-1 and NF-kappaB activation via an effect on the ubiquitin-proteasome pathway. *J Biol Chem.* 2006;281:34730–5.

33. Dirscherl K, Karlstetter M, Ebert S, Kraus D, Hlawatsch J, Walczak Y, et al. Luteolin triggers global changes in the microglial transcriptome leading to a unique anti-inflammatory and neuroprotective phenotype. *J Neuroinflammation*. 2010;7:3.
34. Napoli I, Kierdorf K, Neumann H. Microglial precursors derived from mouse embryonic stem cells. *Glia*. 2009;57:1660–71.
35. Beutner C, Roy K, Linnartz B, Napoli I, Neumann H. Generation of microglial cells from mouse embryonic stem cells. *Nat Protoc*. 2010;5:1481–94.
36. Ebert S, Schoeberl T, Walczak Y, Stoecker K, Stempfl T, Moehle C, et al. Chondroitin sulfate disaccharide stimulates microglia to adopt a novel regulatory phenotype. *J Leukoc Biol*. 2008;84:736–40.
37. Beutner C, Linnartz-Gerlach B, Schmidt SV, Beyer M, Mallmann MR, Staratschek-Jox A, et al. Unique transcriptome signature of mouse microglia. *Glia*. 2013;61:1429–42.
38. O'Neill LA, Golenbock D, Bowie AG. The history of toll-like receptors - redefining innate immunity. *Nat Rev Immunol*. 2013;13:453–60.
39. Jin FY, Nathan C, Radzioch D, Ding A. Secretory leukocyte protease inhibitor: a macrophage product induced by and antagonistic to bacterial lipopolysaccharide. *Cell*. 1997;88:417–26.
40. Li Z, Moy A, Gomez SR, Franz AH, Lin-Cereghino J, Lin-Cereghino GP. An improved method for enhanced production and biological activity of human secretory leukocyte protease inhibitor (SLPI) in *Pichia pastoris*. *Biochem Biophys Res Commun*. 2010;402:519–24.
41. Li Z, Moy A, Sohal K, Dam C, Kuo P, Whittaker J, et al. Expression and characterization of recombinant human secretory leukocyte protease inhibitor (SLPI) protein from *Pichia pastoris*. *Protein Expr Purif*. 2009;67:175–81.
42. Honda K, Taniguchi T. IRFs: master regulators of signalling by toll-like receptors and cytosolic pattern-recognition receptors. *Nat Rev Immunol*. 2006;6:644–58.
43. Jin X, Kim SH, Jeon HM, Beck S, Sohn YW, Yin J, et al. Interferon regulatory factor 7 regulates glioma stem cells via interleukin-6 and Notch signalling. *Brain*. 2012;135:1055–69.
44. Kamijo R, Harada H, Matsuyama T, Bosland M, Gerecitano J, Shapiro D, et al. Requirement for transcription factor IRF-1 in NO synthase induction in macrophages. *Science*. 1994;263:1612–5.
45. Hamilton ST, Scott GM, Naing Z, Rawlinson WD. Human cytomegalovirus directly modulates expression of chemokine CCL2 (MCP-1) during viral replication. *J Gen Virol*. 2013;94:2495–503.
46. Vila-del Sol V, Punzon C, Fresno M. IFN-gamma-induced TNF-alpha expression is regulated by interferon regulatory factors 1 and 8 in mouse macrophages. *J Immunol*. 2008;181:4461–70.
47. Lee J, Hur J, Lee P, Kim JY, Cho N, Kim SY, et al. Dual role of inflammatory stimuli in activation-induced cell death of mouse microglial cells. Initiation of two separate apoptotic pathways via induction of interferon regulatory factor-1 and caspase-11. *J Biol Chem*. 2001;276:32956–65.
48. Greene CM, McElvaney NG, O'Neill SJ, Taggart CC. Secretory leucoprotease inhibitor impairs toll-like receptor 2- and 4-mediated responses in monocytic cells. *Infect Immun*. 2004;72:3684–7.
49. Viatour P, Merville MP, Bours V, Chariot A. Phosphorylation of NF-kappaB and I kappaB proteins: implications in cancer and inflammation. *Trends Biochem Sci*. 2005;30:43–52.
50. Jacobsen LC, Sorensen OE, Cowland JB, Borregaard N, Theilgaard-Monch K. The secretory leukocyte protease inhibitor (SLPI) and the secondary granule protein lactoferrin are synthesized in myelocytes, colocalize in subcellular fractions of neutrophils, and are coreleased by activated neutrophils. *J Leukoc Biol*. 2008;83:1155–64.
51. Taggart CC, Cryan SA, Weldon S, Gibbons A, Greene CM, Kelly E, et al. Secretory leucoprotease inhibitor binds to NF-kappaB binding sites in monocytes and inhibits p65 binding. *J Exp Med*. 2005;202:1659–68.
52. Gao Y, Lecker S, Post MJ, Hietaranta AJ, Li J, Volk R, et al. Inhibition of ubiquitin-proteasome pathway-mediated I kappa B alpha degradation by a naturally occurring antibacterial peptide. *J Clin Invest*. 2000;106:439–48.
53. Hiemstra PS, Maassen RJ, Stolk J, Heinzl-Wieland R, Steffens GJ, Dijkman JH. Antibacterial activity of antileukoprotease. *Infect Immun*. 1996;64:4520–4.
54. Ranganathan S, Simpson KJ, Shaw DC, Nicholas KR. The whey acidic protein family: a new signature motif and three-dimensional structure by comparative modeling. *J Mol Graph Model*. 1999;17:106–13.
55. Williams SE, Brown TI, Roghanian A, Sallenave JM. SLPI and elafin: one glove, many fingers. *Clin Sci (Lond)*. 2006;110:21–35.
56. Yang J, Zhu J, Sun D, Ding A. Suppression of macrophage responses to bacterial lipopolysaccharide (LPS) by secretory leukocyte protease inhibitor (SLPI) is independent of its anti-protease function. *Biochim Biophys Acta*. 2005;1745:310–7.
57. Subramaniam D, Hollander C, Westin U, Erjefalt J, Stevens T, Janciauskiene S. Secretory leukocyte protease inhibitor inhibits neutrophil apoptosis. *Respiology*. 2011;16:300–7.
58. Klimenkova O, Ellerbeck W, Klimiankou M, Unalan M, Kandabarau S, Gigina A, et al. A lack of secretory leukocyte protease inhibitor (SLPI) causes defects in granulocytic differentiation. *Blood*. 2014;123:1239–49.
59. Sierra A, Abiega O, Shahraz A, Neumann H. Janus-faced microglia: beneficial and detrimental consequences of microglial phagocytosis. *Front Cell Neurosci*. 2013;7:6.
60. Karlstetter M, Nothdurfter C, Aslanidis A, Moeller K, Horn F, Scholz R, et al. Translocator protein (18 kDa) (TSPO) is expressed in reactive retinal microglia and modulates microglial inflammation and phagocytosis. *J Neuroinflammation*. 2014;11:3.
61. Odaka C, Mizuuchi T, Yang J, Ding A. Murine macrophages produce secretory leukocyte protease inhibitor during clearance of apoptotic cells: implications for resolution of the inflammatory response. *J Immunol*. 2003;171:1507–14.
62. Henriksen PA, Devitt A, Kotelevtsev Y, Sallenave JM. Gene delivery of the elastase inhibitor elafin protects macrophages from neutrophil elastase-mediated impairment of apoptotic cell recognition. *FEBS Lett*. 2004;574:80–4.
63. Mueller AM, Pedré X, Stempfl T, Kleiter I, Couillard-Despres S, Aigner L, et al. Novel role for SLPI in MOG-induced EAE revealed by spinal cord expression analysis. *J Neuroinflammation*. 2008;5:20.

**Submit your next manuscript to BioMed Central and take full advantage of:**

- Convenient online submission
- Thorough peer review
- No space constraints or color figure charges
- Immediate publication on acceptance
- Inclusion in PubMed, CAS, Scopus and Google Scholar
- Research which is freely available for redistribution

Submit your manuscript at  
www.biomedcentral.com/submit



RESEARCH

Open Access

# Translocator protein (18 kDa) (TSPO) is expressed in reactive retinal microglia and modulates microglial inflammation and phagocytosis

Marcus Karlstetter<sup>1†</sup>, Caroline Nothdurfter<sup>2†</sup>, Alexander Aslanidis<sup>1</sup>, Katharina Moeller<sup>1</sup>, Felicitas Horn<sup>1</sup>, Rebecca Scholz<sup>1</sup>, Harald Neumann<sup>3</sup>, Bernhard H F Weber<sup>4</sup>, Rainer Rupprecht<sup>2\*†</sup> and Thomas Langmann<sup>1\*†</sup>

## Abstract

**Background:** The translocator protein (18 kDa) (TSPO) is a mitochondrial protein expressed on reactive glial cells and a biomarker for gliosis in the brain. TSPO ligands have been shown to reduce neuroinflammation in several mouse models of neurodegeneration. Here, we analyzed TSPO expression in mouse and human retinal microglia and studied the effects of the TSPO ligand XBD173 on microglial functions.

**Methods:** TSPO protein analyses were performed in retinoschisin-deficient mouse retinas and human retinas. Lipopolysaccharide (LPS)-challenged BV-2 microglial cells were treated with XBD173 and TSPO shRNAs *in vitro* and pro-inflammatory markers were determined by qRT-PCR. The migration potential of microglia was determined with wound healing assays and the proliferation was studied with Fluorescence Activated Cell Sorting (FACS) analysis. Microglial neurotoxicity was estimated by nitrite measurement and quantification of caspase 3/7 levels in 661 W photoreceptors cultured in the presence of microglia-conditioned medium. The effects of XBD173 on filopodia formation and phagocytosis were analyzed in BV-2 cells and human induced pluripotent stem (iPS) cell-derived microglia (iPSdM). The morphology of microglia was quantified in mouse retinal explants treated with XBD173.

**Results:** TSPO was strongly up-regulated in microglial cells of the dystrophic mouse retina and also co-localized with microglia in human retinas. Constitutive TSPO expression was high in the early postnatal Day 3 mouse retina and declined to low levels in the adult tissue. TSPO mRNA and protein were also strongly induced in LPS-challenged BV-2 microglia while the TSPO ligand XBD173 efficiently suppressed transcription of the pro-inflammatory marker genes chemokine (C-C motif) ligand 2 (CCL2), interleukin 6 (IL6) and inducible nitric oxide (NO)-synthase (iNOS). Moreover, treatment with XBD173 significantly reduced the migratory capacity and proliferation of microglia, their level of NO secretion and their neurotoxic activity on 661 W photoreceptor cells. Furthermore, XBD173 treatment of murine and human microglial cells promoted the formation of filopodia and increased their phagocytic capacity to ingest latex beads or photoreceptor debris. Finally, treatment with XBD173 reversed the amoeboid alerted phenotype of microglial cells in explanted organotypic mouse retinal cultures after challenge with LPS.

**Conclusions:** These findings suggest that TSPO is highly expressed in reactive retinal microglia and a promising target to control microglial reactivity during retinal degeneration.

**Keywords:** Translocator protein (18 kDa), Microglia, Retinal degeneration, Phagocytosis

\* Correspondence: rainer.rupprecht@medbo.de; thomas.langmann@uk-koeln.de

†Equal contributors

<sup>2</sup>Department of Psychiatry and Psychotherapy, University of Regensburg, D-93053 Regensburg, Germany

<sup>1</sup>Department of Ophthalmology, University of Cologne, D-50931 Cologne, Germany

Full list of author information is available at the end of the article

## Background

The translocator protein (18 kDa) (TSPO), previously known as the peripheral benzodiazepine receptor, is an integral part of the outer mitochondrial membrane [1] where it forms a complex with other mitochondrial proteins, such as the voltage-dependent anion channel (VDAC) and the adenine nucleotide transporter (ANT) [2]. TSPO mediates the transport of cholesterol into the inner mitochondrial membrane, where it serves as a precursor for steroids and neurosteroids [3]. Hence, the protein is constitutively expressed in steroidogenic tissues such as the adrenal gland, the gonads and the brain [4]. In the central nervous system TSPO is present both in neurons and activated glial cells [5-7]. Endogenous ligands of TSPO are cholesterol, porphyrins and active peptide fragments cleaved off from the diazepam binding inhibitor [8]. Glial up-regulation of TSPO is a major hallmark of neurodegenerative diseases [9] and various TSPO ligands have been developed as molecular markers to detect gliosis by means of Positron Emission Tomography (PET) imaging [10].

TSPO ligands are also under investigation as treatment options for a variety of neurological disorders, including Alzheimer's disease [11], multiple sclerosis [12], neuropathic pain [13], peripheral nerve injury [9] and anxiety disorders [14]. Classical synthetic TSPO ligands, such as the benzodiazepine derivative 4'-chlorodiazepam (Ro5-4864) and the isoquinoline carboxamide PK11195, directly enhance GABAergic neurotransmission [15]. TSPO ligands such as etifoxine and XBD173 (emapunil) stimulate the synthesis of neurosteroids and may exert anti-inflammatory and neuroprotective effects [16].

Inherited retinal degenerations are clinically and genetically heterogeneous diseases characterized by progressive vision loss [17]. Although the individual mechanisms of pathogenesis remain to be resolved, microglial activation is a common hallmark of retinal degeneration [18]. The retinoschisin-deficient (*Rs1h*<sup>-Y</sup>) mouse is a prototypic model for inherited retinal dystrophies with strong microglial reactivity [19,20]. Modulation of retinal microglia with docosahexaenoic acid could dampen microglial reactivity in *Rs1h*<sup>-Y</sup> mice and thereby reduced retinal degeneration [21]. TSPO ligands could potentially have a similar effect and may target the neurodegenerative cascade via their anti-inflammatory and microglia modulating effects.

In this study, we showed that TSPO expression is directly connected to retinal microgliosis in a mouse model of retinal degeneration and in human retinal sections. Moreover, we demonstrated that the TSPO ligand XBD173 induces an anti-inflammatory, neuroprotective and pro-phagocytic phenotype in microglia using cultures of murine and human microglial cell lines as well as mouse retinal explants.

## Methods

### Animals

MacGreen [22], *Rs1h*<sup>-Y</sup> [19] and wild-type mice were all on a pure C57BL/6 J background. Animals were maintained in an air-conditioned environment on a 12-hour light-dark schedule at 22°C, and had free access to food and water. The health of the animals was regularly monitored, and all procedures complied with the German Law on Animal Protection and the Institute for Laboratory Animal Research Guide for the Care and Use of Laboratory Animals, 2011.

### Human tissue

Retinal samples of donors were obtained from the Eye Bank of the Center of Ophthalmology, University of Cologne, Germany. The donor age ranged between 54 and 72 years. Postmortem time ranged between 5 and 36 h. After dissection of the anterior segment, the remaining tissue included the posterior pole. The research followed the tenets of the Declaration of Helsinki.

### Reagents

*E. coli* 0111:B4 lipopolysaccharide and aminoglutethimide were purchased from Sigma Aldrich (St. Louis, MO, USA). XBD173 (emapunil) was obtained by custom synthesis from APAC Pharmaceuticals (Ellicott City, MD, USA). XBD173 was dissolved in ethanol.

### Cell culture and retinal explants

BV-2 microglia-like cells were cultured in RPMI/5% fetal calf serum (FCS) supplemented with 2 mM L-Glutamine and 195 nM  $\beta$ -mercaptoethanol. Isolation and culture of primary retinal microglia has been described previously [21]. BV-2 cells were stimulated with 50 ng/ml lipopolysaccharide (LPS) and various concentrations of XBD173 or ethanol as vehicle control. 661 W photoreceptor-like cells were a gift from Prof. Muayyad Al-Ubaidi (Department of Cell Biology, University of Oklahoma Health Sciences Center, Oklahoma City, OK, USA) and the culture conditions have been described elsewhere [23]. Human microglial cell lines (iPSdM) were generated from induced pluripotent stem (iPS) cell lines obtained by reprogramming from skin fibroblasts as previously described [24,25]. These cells proliferate without addition of growth factors and they were passaged 1:3 twice a week. The microglial phenotype was confirmed by flow cytometry (CD11b, CD16/32, CD36, CD45, CX3CR1). Retinas from MacGreen mice were rinsed in DMEM/Ham's F12 medium supplemented with 1% FCS and placed on 25 mm circular Nucleopore filters (VWR, Darmstadt, Germany) with the photoreceptor side facing the membrane. After 24 h of *in vitro* culture with vehicle, 1  $\mu$ g/ml LPS, 20  $\mu$ M XBD173 or 1  $\mu$ g/ml LPS + 20  $\mu$ M XBD173, retinas were fixed and imaged in flat-mounts. Ramified and

amoeboid microglial cells were directly imaged by green fluorescent protein (GFP) fluorescence using the Axioskop2 MOT Plus Apotome microscope (Carl Zeiss, Jena, Germany) and counted.

#### Scratch wound-healing assay

A total of 400,000 BV-2 microglial cells were grown in six-well plates as 80% confluent monolayers and were wounded with a sterile 100  $\mu$ l pipette tip. Thereafter, the cells were stimulated with 50 ng/ml LPS, 50  $\mu$ M XBD173, 50 ng/ml LPS + 50  $\mu$ M XBD173, or ethanol as solvent control. Migration into the open scar was documented with microphotographs taken at different time points after wounding using a Nikon ECLIPSE TE2000 inverted microscope (Nikon, Tokyo, Japan). The number of migrating cells was quantified by counting all cells within a 0.4 mm<sup>2</sup> region in the center of each scratch. The number of migrated cells was then normalized to the average cell density to account for changes in proliferation. A minimum of five individual cultures was used to calculate the mean migratory capacity of each cell culture condition.

#### Proliferation assay

For carboxyfluorescein diacetate succinimidyl ester (CFSE) proliferation assays, BV-2 microglial cells were labeled with 1  $\mu$ M CFSE (e-Bioscience, San Diego, CA, USA) and cultured ( $1.5 \times 10^5$  per well) in a six-well plate. After 24 h of culture with vehicle, 100 ng/ml LPS, 50  $\mu$ M XBD173 or 100 ng/ml LPS + 50  $\mu$ M XBD173, cells were stained with a fixable viability dye (e-Bioscience), to exclude dead cells from the analysis. The fluorescence intensity of CFSE-labeled BV-2 cells was analyzed by flow cytometry (FACS Canto II). Analysis of cell division was performed using FlowJo software (Treestar Inc., Ashland, OR, USA).

#### shRNA knock-down of TSPO in BV-2 cells

For knockdown of endogenous TSPO in BV-2 cells, shRNA vectors were obtained from the RNAi consortium (TRC). Briefly, BV-2 cells were transfected with 2.5  $\mu$ g vector DNA using TransIT<sup>®</sup>-LT1 transfection reagent (Mirus Bio LLC, Madison, WI, USA) to express TSPO-specific or scrambled shRNAs. Twenty-four hours after transfection cells were stimulated with vehicle, 50 ng/ml LPS, 20  $\mu$ M XBD173 or 50 ng/ml LPS + 20  $\mu$ M XBD173 for 12 hours before cells were harvested for RNA isolation and mRNA expression analysis.

#### 661 W photoreceptor apoptosis assay

To test microglial neurotoxicity, a culture system of 661 W photoreceptors with microglia-conditioned medium was established. 661 W photoreceptor cells were incubated for 48 h either in their own medium or with culture supernatants from unstimulated, 50 ng/ml LPS, 50  $\mu$ M XBD173 or

50 ng/ml LPS + 50  $\mu$ M XBD173 treated microglial cells. The 661 W cell morphology was assessed by phase contrast microscopy and apoptotic cell death was determined with the Caspase-Glo<sup>®</sup> 3/7 Assay (Promega GmbH, Mannheim, Germany). Cells were lysed and incubated with a lumino-genic caspase-3/7 substrate, which contains the tetrapeptide sequence DEVD. Luminescence was then generated by addition of recombinant luciferase and was proportional to the amount of caspase activity present. The luminescent signal was read on an Infinite F200 pro plate reader (Tecan, Crailsheim, Germany). A blank reaction was used to measure background luminescence associated with the cell culture system and Caspase-Glo<sup>®</sup> 3/7 Reagent (Promega). The value for the blank reaction was subtracted from all experimental values. Negative control reactions were performed to determine the basal caspase activity of 661 W cells. Relative luciferase units (RLU) reflect the level of apoptotic cell death in the different 661 W cell cultures.

#### Nitrite measurement

Nitric oxide concentrations were determined by measuring the amount of nitrite produced by BV-2 microglial cells into the culture medium using the Griess reagent system (Promega). A 50  $\mu$ l cell culture supernatant was collected and an equal volume of Griess reagent was added to each well. After incubation for 15 minutes at room temperature, the absorbance was read at 540 nm on an Infinite F200 pro plate reader (Tecan). The concentration of nitrite for each sample was calculated from a sodium nitrite standard curve.

#### Phagocytosis assays

BV-2 microglial cells were pre-treated for 2 h with compounds before 4  $\mu$ l latex bead solution (Polystyrene microparticles, Sigma Aldrich, St. Louis, MO, USA) was added to the wells. Cells were incubated for 6 h and five micrographs per well were taken using an AxioVert.A1 inverted microscope (Carl Zeiss). The phagocytic activity was determined by calculating the number of cells which phagocytosed 10 or more latex beads compared to all cells per field. The conditions for human microglial cells (iPSdM) were the same with the modification that cells were pre-treated for 24 h, the incubation time with beads was 24 h and only fully saturated cells were counted as positive. To study the microglial uptake of apoptotic photoreceptor cell material, 661 W photoreceptor cells were starved with serum deprivation, harvested and fluorescently labeled using CellTracker CM-DiI (Invitrogen, Carlsbad, CA, USA). For phagocytosis, BV-2 microglial cells were pre-treated for 2 h with compounds before 400  $\mu$ l stained apoptotic 661 W solution was added for further 6 h. iPSdM cells were pre-treated for 24 h before 400  $\mu$ l stained apoptotic 661 W solution was added for further 24 h. Cells were then

fixed and nuclei were stained with 4',6-diamidino-2-phenylindole. Fluorescence micrographs were taken and ImageJ software (National Institutes of Health, Bethesda, MD, USA) was used to determine the ratio of phagocytosed apoptotic photoreceptor fragments (red signal) relative to the total microglia cell number (DAPI signal).

#### Phalloidin staining

BV-2 microglial cells or human microglial cells (iPSdM) were grown on cover slips in six-well plates and the indicated compounds were added for 24 h. Thereafter, the cells were fixed, permeabilized with 0.1% Triton X-100 and f-actin was fluorescently labeled using 0.1 µg/ml Phalloidin-TRITC (Sigma). The nuclei were stained using 4',6-diamidino-2-phenylindole and photomicrographs were taken with an Axioskop2 MOT Plus Apotome microscope (Carl Zeiss).

#### Immunohistochemistry

Immunohistochemical analyses were performed on 10 µm retinal sections embedded in optimal cutting temperature (OCT) compound (Hartenstein, Würzburg, Germany) or on retinal flat mounts. Samples were fixed in 4% paraformaldehyde, rinsed and rehydrated with PBS. Sections were blocked with a dried milk solution followed by an overnight incubation with primary antibodies at 4°C. Antibodies included rabbit anti-Iba1 antibody (Wako Chemicals, Neuss, Germany), rabbit anti-TSPO antibody (Abcam, Cambridge, UK), goat anti-MAP2 antibody (Santa Cruz Biotechnology, Santa Cruz, CA, USA), and goat anti-GFAP antibody (Santa Cruz Biotechnology). After washing, samples were labeled with a secondary antibody conjugated to Alexa488 (green) or Alexa594 (red) (Jackson Immuno-Research, West Grove, PA, USA) and counter-stained with DAPI. Sections and flat-mounts were mounted in DAKO fluorescent mounting medium (Dako Deutschland GmbH, Hamburg, Germany) and viewed with an Axioskop2 MOT Plus Apotome microscope (Carl Zeiss).

#### Western blot analysis

Mouse retinal tissue was homogenized in cold RIPA buffer (20 mM Na-phosphate buffer, 150 mM NaCl, 5 mM EDTA, 1% Triton X-100 and protease inhibitors) using a TissueLyser LT (Qiagen, Hilden, Germany). Insoluble debris was removed by centrifugation for 15 minutes at 16,000 g. LPS-treated and control BV-2 microglia were directly lysed in RIPA buffer. Protein concentrations were determined by Bradford assay (Roti-quant, Roth, Karlsruhe, Germany). A total of 10 µg of microglial or 30 µg of total-retina proteins were separated by SDS-PAGE on 15% gels with PageRuler pre-stained protein ladder (Thermo Scientific, Waltham, MA, USA). Proteins were then transferred to 0.45 µm nitrocellulose

membranes (Biorad, Munich, Germany). After blocking in TBS-T containing 5% nonfat dry milk, membranes were incubated with primary antibodies against TSPO (ab109497, Abcam,) or Actin (sc-1616, Santa Cruz Biotechnology). Blots were then incubated with secondary goat anti-rabbit IgG-HRP or rabbit anti-goat IgG-HRP antibodies (sc-2004, sc-2768, Santa Cruz Biotechnology). Enhanced chemiluminescence signals were then visualized and imaged with the MultiImage II system (Alpha Innotech, Santa Clara, CA, USA).

#### RNA isolation and reverse transcription

Total RNA was extracted from total retina, BV-2 microglial cells or isolated retinal microglia according to the manufacturer's instructions using the RNeasy Mini Kit (Qiagen). Purity and integrity of the RNA was assessed on the Agilent 2100 Bioanalyzer with the RNA 6000 Nano LabChip® reagent set (Agilent Technologies, Santa Clara, CA, USA). The RNA was quantified spectrophotometrically and then stored at -80°C. First-strand cDNA synthesis was performed with the RevertAid™ H Minus First Strand cDNA Synthesis Kit (Fermentas, Schwerte, Germany).

#### Quantitative real-time RT-PCR

Amplifications of 50 ng cDNA were performed with an ABI7900HT machine (Applied Biosystems, Carlsbad, CA, USA) in 10 µl reaction mixtures containing 1 × TaqMan Universal PCR Master Mix (Applied Biosystems), 200 nM of primers and 0.25 µl of dual-labeled probe (Roche ProbeLibrary, Roche Applied Science, Basel, Switzerland). The reaction parameters were as follows: 2 minutes 50°C hold, 30 minutes 60°C hold and 5 minutes 95°C hold, followed by 45 cycles of 20 s 94°C melt and 1 minute 60°C anneal/extension. Primer sequences and Roche Library Probe numbers were as follows: CCL2, forward primer 5'-catccacgtgttgctca-3', reverse primer 5'-gatcatcttgctggtgaatgagt-3', probe #62; IL6, forward primer 5'-gatggatgctacaaactggat-3', reverse primer 5'-ccaggtagctatggtactccaga-3', probe #6; iNOS, forward primer 5'-ctttgccacggacgagac-3', reverse primer 5'-tcattgtactctgagggtga-3', probe #13. Measurements were performed in triplicates and results were analyzed with an ABI sequence detector software version 2.3 using the  $\Delta\Delta C_t$  method for relative quantification.

#### Pregnenolone ELISA

BV-2 cells were seeded on 24-well plates in 1 ml/well of RPMI/5% FCS supplemented with 2 mM L-Glutamine and 195 nM β-mercaptoethanol. After cells had attached after 6 h, 50 ng/ml LPS and/or 20 µM XBD173 were added to each well. After 21 h, cells were washed twice with HEPES assay buffer (140 mM NaCl, 5 mM KCl, 1.8 mM CaCl<sub>2</sub>, 1 mM MgSO<sub>4</sub>, 10 mM glucose, 10 mM

HEPES/NaOH, pH 7.4) as described previously [26]. Then 1 ml of HEPES assay buffer supplemented with BSA (0.1%) and Trilostane (25  $\mu$ M) (Sigma-Aldrich) was added to each well. Again 50 ng/ml LPS and/or 20  $\mu$ M XBD173 were added. After 3 h the supernatants were removed to perform pregnenolone ELISA according to the manufacturer's recommendations (IBL International, Hamburg, Germany). In brief, 50  $\mu$ l of each sample were pipetted into a rabbit anti-pregnenolone antibody coated 96-microwell Plate. A total of 100  $\mu$ l of pregnenolone-HRP conjugate was then added. Ready-to-use-calibrators were provided by IBL international. After 1 h of incubation and washing 150  $\mu$ l of tetramethylbenzidine/hydrogen peroxide (TMB) substrate was added. Assays were read with a Tecan Spectra at 450 nm. Data were analyzed by Magellan Data Analysis Software (Tecan).

#### Statistical analyses

Real-time quantitative RT-PCR data were analyzed with the  $\Delta\Delta$ Ct method using an unpaired Student's *t*-test. Assays for nitrite secretion, microglial migration and pregnenolone ELISAs were analyzed with an unpaired Student's *t* test. Caspase 3/7 assays and phagocytosis assays were analyzed with a Mann-Whitney *U*-test. *P* < 0.05 was considered as statistically significant.

## Results

### Induction of TSPO expression in activated microglia of the retina

To identify genes regulated during activation of microglia, we have previously performed DNA microarray analysis of isolated retinal microglial cells from degenerating retinoschisin-deficient (Rs1h<sup>-Y</sup>) and control macrophage/microglia MacGreen reporter mice [21]. Among the differently expressed transcripts, a significantly increased mRNA expression of TSPO was detected in activated retinal microglia (data not shown). Therefore, we determined the protein expression of TSPO in the retina and found a weak expression in the MacGreen reporter mouse, which was present in ramified microglia of the plexiform layers and astrocytes of the ganglion cell layer (Figure 1A-C). However, there was a remarkable increase of TSPO expression specifically in microglia of MacGreen/Rs1h<sup>-Y</sup> retinas (Figure 1D-F). Notably, there was nearly a full overlap of TSPO signals with amoeboid microglial cells which migrated to the degenerating inner nuclear layer (Figure 1F). In the human retina, TSPO expression was also evident in inner plexiform layer microglial cells as demonstrated by Iba1 co-immunostaining as well as in astrocytes (Figure 1G-I). To exclude that TSPO is significantly expressed in Müller cells or retinal neurons, immunostainings for glial fibrillary acid protein (GFAP) and microtubule-associated protein 2 (MAP2) were performed. Neither wild-type retinas nor Rs1h<sup>-Y</sup> retinas

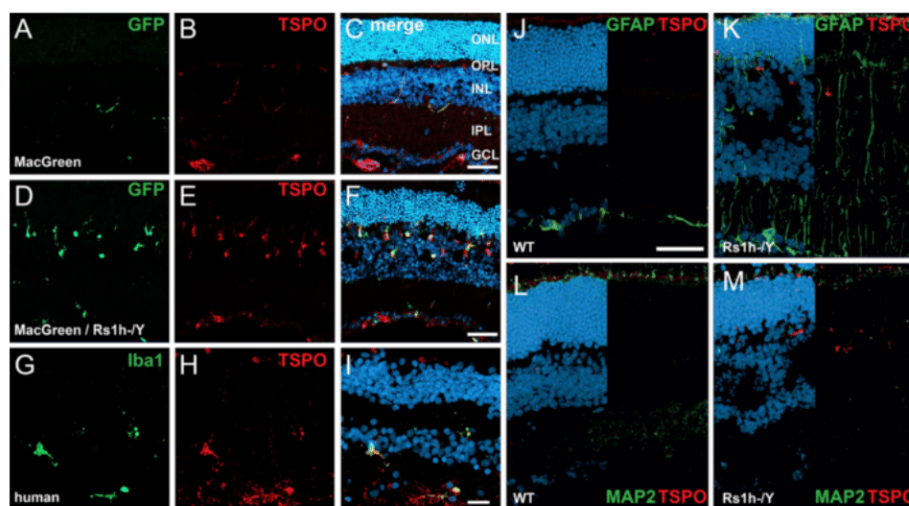


**Figure 1** TSPO expression as a marker for microgliosis in degenerating and aging retinas. In MacGreen mice, representative photomicrographs show low TSPO expression in retinal microglia (green GFP signal and red TSPO immunofluorescence) and constitutive expression in astrocytes (red TSPO immunofluorescence) (A-C) but strong up-regulation in retinal microglia from MacGreen/Rs1h<sup>-Y</sup> mice (D-F). The overlap of TSPO and Iba1 immunostaining also indicates co-expression in human retinal microglia (G-I). TSPO immunostaining staining does not co-localize with the Müller cell marker GFAP (J, K) or the neuronal microtubule marker MAP2 (L, M). ONL, outer nuclear layer; OPL, outer plexiform layer; INL, inner nuclear layer; IPL, inner plexiform layer; GCL, ganglion cell layer, GFP, green fluorescent protein (18 kDa); GFAP, glial fibrillary acid protein; MAP2, microtubule-associated protein 2. Scale bar, 50  $\mu$ m.

displayed an overlap of TSPO signals with GFAP (Figure 1J, K) or MAP2 (Figure 1L, M), respectively.

To further verify the steep TSPO expression in reactive microglia, mRNA analysis of isolated retinal microglia from MacGreen and MacGreen/Rs1h<sup>-Y</sup> retinas was performed. There was a strong and significant increase of TSPO mRNA in MacGreen/Rs1h<sup>-Y</sup> microglia ( $12.01 \pm 0.82$ ,  $P < 0.01$ ) compared to MacGreen microglia ( $1.0 \pm 1.07$ ) (Figure 2A). TSPO induction was also confirmed on the protein level when total retinas of MacGreen/Rs1h<sup>-Y</sup> mice compared to MacGreen mice were analyzed (Figure 2B). We next performed TSPO transcript analysis in early postnatal development of the mouse retina. TSPO was present at higher levels in early retinal development and turned to lower levels in the adult retina (Figure 2C). We then analyzed whether the induction of TSPO expression is also present in cultured BV-2 microglia, which were activated by LPS. Treatment of BV-2 cells with 50 ng/ml LPS elicited a highly significant increase in TSPO levels ( $4.11 \pm 0.31$ ,  $P < 0.001$ ) compared to vehicle-treated BV-2 cells ( $1.0 \pm 0.80$ ) (Figure 2D). The increase of TSPO in LPS-activated BV-2 microglia was also confirmed on the protein level using Western blot analysis (Figure 2E).

#### The selective TSPO ligand XBD173 dampens pro-inflammatory and neurotoxic microglial activation

We investigated whether stimulation of TSPO with the selective ligand XBD173 influences microglial reactivity. We first tested the mRNA expression of the chemo-attractant protein CCL2, the pro-inflammatory cytokine IL6 and iNOS in LPS-activated microglia upon treatment with three

different doses of XBD173. The TSPO ligand significantly and dose-dependently suppressed mRNA levels of CCL2 (Figure 3A,  $P = 0.0014$  for 20  $\mu$ M XBD173 and  $P = 0.0003$  for 50  $\mu$ M XBD173 versus vehicle control), IL6 (Figure 3B,  $P = 0.0004$  for 20  $\mu$ M XBD173 and  $P = 0.0001$  for 50  $\mu$ M XBD173 versus vehicle control), and iNOS (Figure 3C,  $P = 0.0104$  for 20  $\mu$ M XBD173 and  $P = 0.0004$  for 50  $\mu$ M XBD173 versus vehicle control).

To test whether the anti-inflammatory effect of XBD173 depends on TSPO expression, shRNA mediated knock-down of TSPO was performed. Transfection of BV-2 cells with two different TSPO-specific shRNAs showed a 50 to 60% knock-down of TSPO mRNA levels compared to a scramble control (data not shown). The mRNA expression levels of CCL2 (Figure 3D), IL6 (Figure 3E) and iNOS (Figure 3F) were no longer suppressed by XBD173 treatment when either shRNA1 or shRNA2 that specifically target TSPO were present. This clearly implicates that the suppressing effect of XBD173 acts via TSPO in BV-2 cells.

When co-administered together with 50 ng/ml LPS, 50  $\mu$ M XBD173 also strongly diminished NO-production from BV-2 microglial cells compared to vehicle-treated cells (Figure 3G,  $P < 0.0001$ ). We then performed an apoptosis assay of 661 W photoreceptor cells incubated in the presence of microglia-conditioned medium. LPS-activated microglial cells incubated in the presence of 50  $\mu$ M XBD173 had a significantly lower pro-apoptotic effect on photoreceptor cells than microglia cultured with vehicle (Figure 3H,  $P < 0.0022$ ).

We then analyzed the effect of the TSPO ligand on microglial migration. Stimulation of BV-2 microglial cells

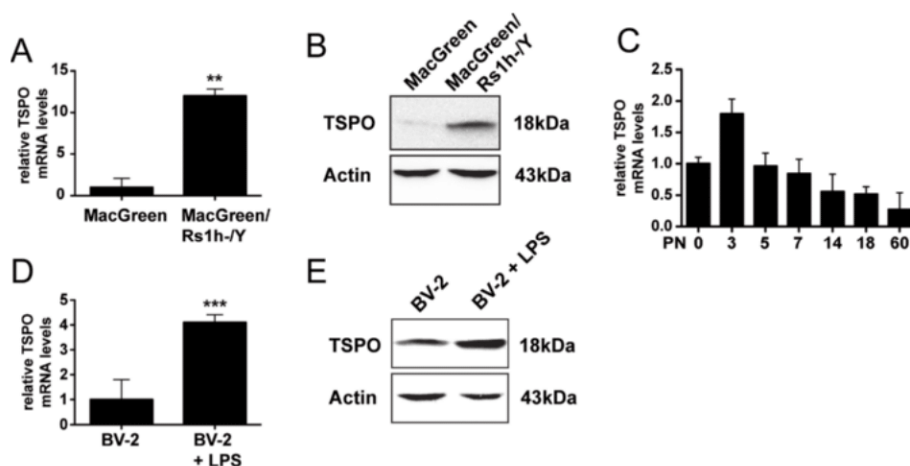


**Figure 2 TSPO mRNA and protein expression in reactive microglia.** (A) Strong induction of TSPO mRNA levels in isolated microglial cells from MacGreen/Rs1h<sup>-Y</sup> mice compared to MacGreen mice. (B) TSPO protein induction in total retinas from MacGreen/Rs1h<sup>-Y</sup> mice compared to MacGreen mice. (C) Temporal TSPO mRNA expression profiling shows a high early postnatal expression level and continuous decline to low levels in adult mouse retinas. (D, E) LPS activation of BV-2 microglial cells leads to the induction of TSPO transcripts (D) and protein (E). Data show mean  $\pm$  SD (n = 3/group, measured in triplicates) \*\* $P < 0.01$  MacGreen/Rs1h<sup>-Y</sup> versus MacGreen; \*\*\* $P < 0.001$  BV-2 + 50 ng/ml LPS versus BV-2. LPS, lipopolysaccharide; TSPO, translocator protein (18 kDa).

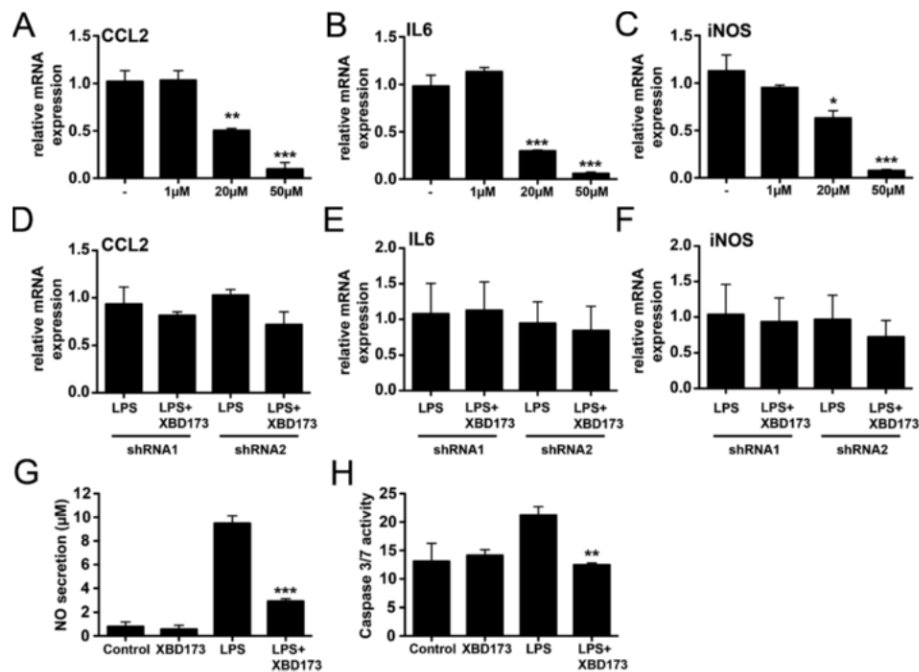


**Figure 3** The TSPO agonist XBD173 dampens gene transcription of pro-inflammatory markers and reduces microglial neurotoxicity.

LPS-activated BV-2 microglial cells were cultured in the presence of various concentrations of XBD173 for 24 h and the pro-inflammatory transcript markers CCL2 (A), IL6 (B), iNOS (C) were determined by *real time* qRT-PCR. Data show mean  $\pm$  SD (n = 3/group, measured in triplicates) \**P* < 0.05, \*\**P* < 0.01, \*\*\**P* < 0.001 XBD173 + LPS versus LPS-treated cells. (D-F), Knock-down of TSPO with two independent shRNAs abrogates the suppressing effects of XBD173 on CCL2 (D), IL6 (E) and iNOS (F) gene expression in BV-2 cells. (G), Production of NO as determined by detection of nitrite from BV-2 microglial cells treated with 50 µM XBD173 in the absence or presence of 50 ng/ml LPS. Data show mean  $\pm$  SD (n = 9/group) \*\*\**P* < 0.001 XBD173 + LPS versus LPS-treated cells. (H), 661 W photoreceptor cell cultures were treated with conditioned media from BV-2 microglial cells for 48 hours. The supernatant from control-stimulated, 20 µM XBD173-treated, 50 ng/ml LPS-treated, or 20 µM XBD173 + 50 ng/ml LPS-treated cells was added to 661 W photoreceptor cells and apoptosis-related caspase 3/7 activation was determined. Data show mean  $\pm$  SD (n = 6/group) \*\**P* < 0.01 XBD173 + LPS versus LPS-treated cells. CCL2, (C-C motif) ligand 2; IL6, interleukin-6; iNOS, inducible nitric oxide synthase; LPS, lipopolysaccharide; NO, nitric oxide.

with 50 µM XBD173 strongly reduced the migration of BV-2 cells in a wound-healing scratch assay (Figure 4A). This effect was quantified and significant in non-activated microglia (Figure 4B, *P* < 0.0008) as well as LPS-primed BV-2 cells (Figure 4B, *P* < 0.0406). We

constantly noticed a reduced cell number in our culture assays and, therefore, tested a potential anti-mitotic effect of XBD173. CFSE labeling and FACS analyses clearly demonstrated that XBD173 reduced the proliferation rate of both unstimulated and LPS-treated BV-2 cells (Figure 4C).

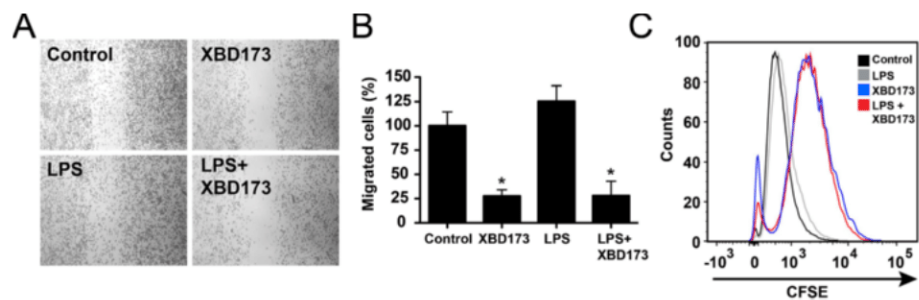


**Figure 4** The TSPO agonist XBD173 reduces microglial migration and proliferation. (A) Scratch assay to mimic wound-healing in cultured BV-2 microglia treated with vehicle, 50 ng/ml LPS, 50 µM XBD173 or both. Microphotographs from scratched areas were quantified 8 h after treatment (B). Data show mean  $\pm$  SEM (n = 5/group) \**P* < 0.05 XBD173 versus control, \**P* < 0.001 XBD173 + LPS versus LPS-treated cells. (C), CFSE-based proliferation assay of BV-2 microglial cells treated with vehicle, 100 ng/ml LPS, 50 µM XBD173 or 100 ng/ml LPS + 50 µM XBD173. The proliferation rate of BV-2 microglia was analyzed 24 hours after treatment using flow cytometry and a representative graph out of four repetitions is shown. CFSE, carboxyfluorescein diacetate succinimidyl ester; LPS, lipopolysaccharide; TSPO, translocator protein (18 kDa).

### XBD173 increases filopodia formation and phagocytosis in murine and human microglia

To investigate further functional consequences of treatment with the TSPO ligand, we tested the effects of TSPO activation on the morphology and phagocytosis of murine BV-2 microglia and human microglial cells (iPSdM) derived from human induced pluripotent stem cells. Staining of the f-actin cytoskeleton with phalloidin indicated that XBD173 caused a prominent formation of filopodia in murine BV-2 cells either in the absence or presence of LPS (Figure 5A-D). This effect was even more pronounced in human iPSdM, which showed a large rim of flattened filopodia (Figure 5E-H).

This striking phenomenon of XBD173-induced filopodia formation prompted us to analyze the phagocytic capacity in detail using latex beads and CM-Dil-stained apoptotic 661 W photoreceptor material as a more physiological trigger. BV-2 microglial cells stimulated with XBD173 showed a significantly higher phagocytosis rate of latex beads in non-activated cells (Figure 6A, B,  $P = 0.0013$ ) as well as LPS-primed cells (Figure 6A, B,  $P = 0.0029$ ). A similar effect of XBD173 was noticed with fluorescent apoptotic 661 W photoreceptors in non-activated (Figure 6C, D,  $P = 0.0192$ ) and LPS-primed BV-2 cells (Figure 6C, D,  $P = 0.0013$ ). XBD173 had a similar stimulating effect on the phagocytic potential of human microglial cells with strongly increased uptake of latex beads (Figure 6E, F,  $P < 0.0001$ ) and CM-Dil-stained apoptotic 661 W membranes (Figure 6G, H,  $P < 0.0001$ ).

To test whether the phenomenon of XBD173-induced phagocytosis is dependent on neurosteroid synthesis, we first quantified pregnenolone levels in BV-2 cells. Stimulation of BV-2 microglia with either 20  $\mu\text{M}$  XBD173 alone (Figure 7A,  $P < 0.0005$ ) or together with 50 ng/ml LPS (Figure 7A,  $P < 0.0074$ ) strongly increased pregnenolone levels measured in the cell culture supernatant. We next performed bead phagocytosis assays with BV-2 cells

stimulated with 20  $\mu\text{M}$  XBD173 in the presence or absence of the CYP11A1 inhibitor aminoglutethimide. As previously shown in Figure 6, BV-2 cells stimulated with XBD173 showed a higher phagocytosis potential than control cells (Figure 7B,  $P < 0.0001$ ). Interestingly, this effect was completely prevented when the cells were co-incubated with 20  $\mu\text{M}$  XBD173 and 100  $\mu\text{M}$  aminoglutethimide (Figure 7B). These data suggest that the phagocytosis promoting effect of XBD173 requires pregnenolone synthesis.

### XBD173 reduces the number of LPS-alerted amoeboid microglia in living retinal explants

Finally, we analyzed whether the XBD173-dependent morphological transformation of microglial cells can also be observed in the *ex vivo* retina. Retinas from MacGreen reporter mice were used to enable easy GFP-based analysis of microglial ramification. Retinal explants cultured for 24 h *in vitro* retained their ramified morphology (Figure 8A) and the microglial network was not significantly affected by XBD173 alone (Figure 8B). In contrast, retinal microglia dramatically changed their morphology in the presence of LPS with a large fraction of bloated amoeboid cells (Figure 8C). This LPS-induced morphological transition of microglia was effectively suppressed by XBD173 (Figure 8D). We then performed a quantitative analysis of ramified and amoeboid microglial cells in all retinal explants. As already indicated in Figure 7A-D, the number of amoeboid cells was significantly increased in LPS-treated cultures compared to vehicle-treated explants (Figure 8E,  $P = 0.0012$ ). Interestingly, co-incubation of explants with LPS and XBD173 resulted in a strongly reduced number of alerted amoeboid microglia cells (Figure 8E,  $P < 0.0001$ ). Thus, XBD173 was not only able to influence microglial reactivity *in vitro* but also significantly affected microglia in living mouse retinas.

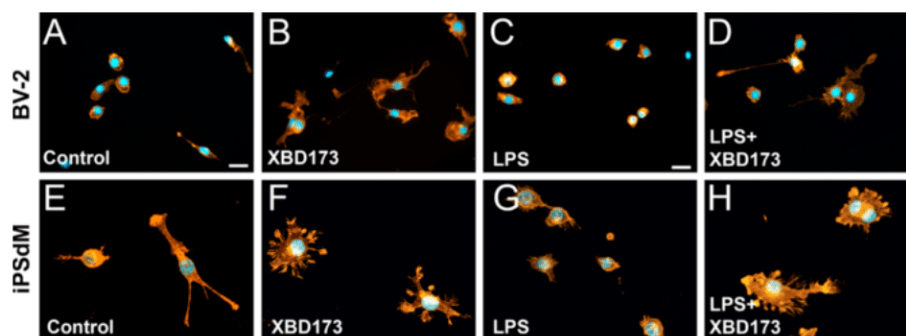
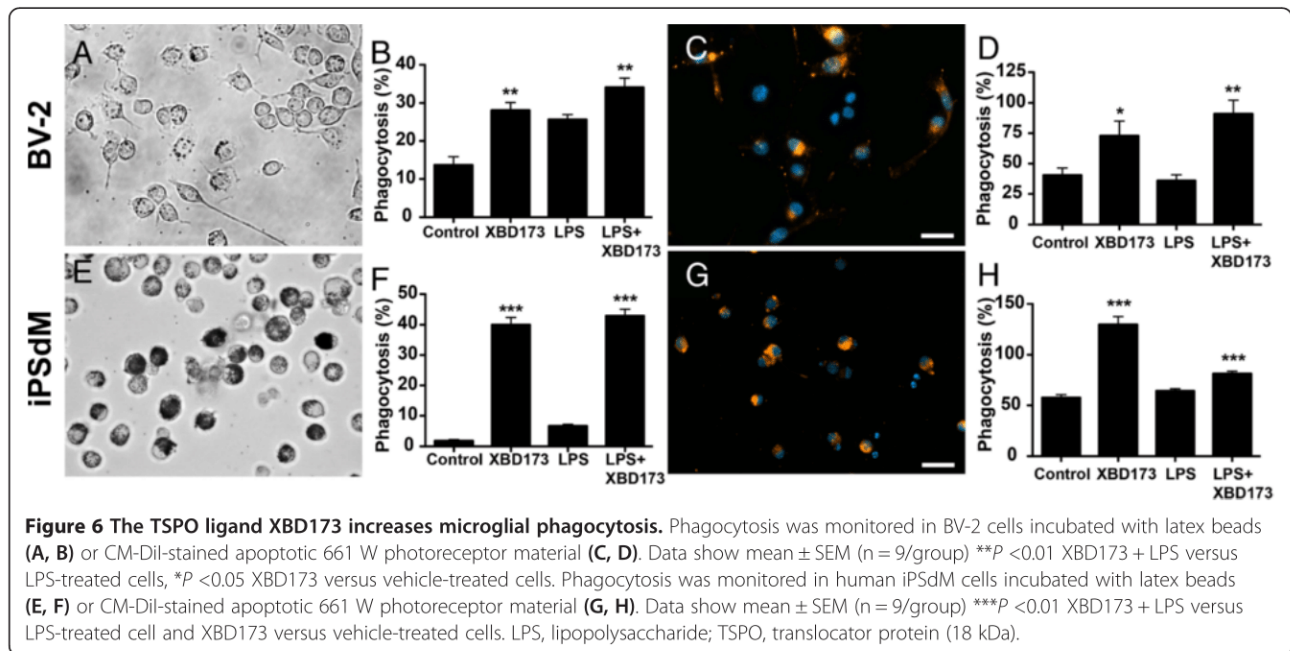


**Figure 5** The TSPO ligand XBD173 promotes microglial filopodia formation. (A-D) Representative images of phalloidin-stained murine BV-2 microglial cells treated with 50  $\mu\text{M}$  XBD173 in the absence or presence of 50 ng/ml LPS. (E-H) Representative images of phalloidin-stained human iPS-derived microglia (iPSdM) treated with 30  $\mu\text{M}$  XBD173 in the absence or presence of 250 ng/ml LPS. LPS, lipopolysaccharide; TSPO, translocator protein (18 kDa).

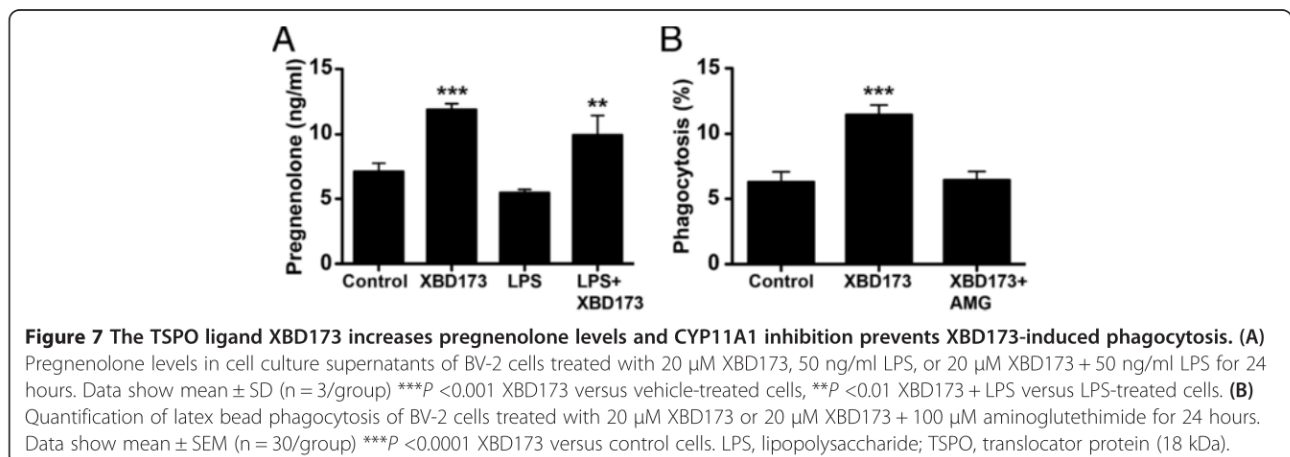


## Discussion

Based on its selective expression in activated glial cells of the brain, TSPO is a marker for brain gliosis and TSPO ligands have been developed for *in vivo* imaging in human and mouse [27,28]. In the present study, we now show that selective up-regulation of TSPO is closely associated with the reactivity of microglia during retinal degeneration. To our knowledge, this is the first report to identify TSPO as a biomarker of activated microglia both in mouse and human retinal tissue. Major questions are why and how TSPO is up-regulated in reactive retinal microglia. Microgliosis in the retina of a mouse model of retinoschisin-deficiency starts at postnatal Day 14, peaks at P21 and then declines to lower levels [29]. The peak of microglial reactivity perfectly overlaps with high induction of TSPO expression levels. In the brain,

TSPO detects activation of both microglia and astrocytes as a result of injury but also during recovery from injury [30,31], indicating that the presence of TSPO on activated glia may be a self-limiting mechanism of activation and proliferation. Our data of up-regulated TSPO expression in LPS-stimulated BV-2 microglia revealed that TLR4 signaling may play a crucial role in TSPO induction. In line with our experiments, up-regulation of TSPO in the recovery phase from neuropathic pain was prevented by pharmacological blockade of TLR4 [13]. We, therefore, hypothesize that retinal damage and the presence of damage-associated molecular patterns may trigger TLR4 signaling on microglia and thereby influence TSPO expression.

Our experiments demonstrate that the selective TSPO ligand XBD173 efficiently reversed the LPS-triggered



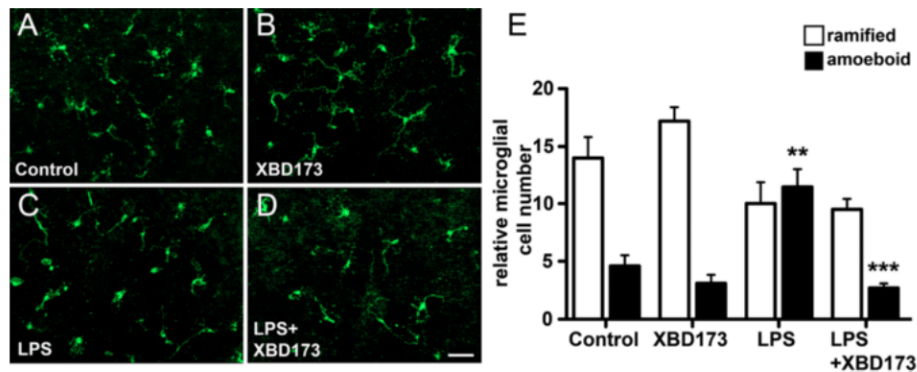


**Figure 8** The TSPO ligand XBD173 reduces the number of alerted amoeboid retinal microglia *ex vivo*. (A-D) Representative GFP images of the retinal microglia network in explanted mouse retinas treated for 24 hours with vehicle (A), 20  $\mu$ M XBD173 (B), 1  $\mu$ g/ml LPS + vehicle (C) and 1  $\mu$ g/ml LPS + 20  $\mu$ M XBD173 (D). (E) Quantification of ramified and amoeboid microglial cells in 10 independent image areas of two individual flat mounts (mean  $\pm$  SEM). \*\* $P$  < 0.01 for amoeboid cells in LPS versus control explants; \*\*\* $P$  < 0.0001, for amoeboid cells in XBD173 + LPS versus LPS-treated explants. GFP, green fluorescent protein; LPS, lipopolysaccharide; TSPO, translocator protein (18 kDa).

production of the pro-inflammatory mediators CCL2, IL6 and iNOS. The TSPO ligand and mitochondrial effector PK11195 effectively inhibited LPS-induced microglial expression of COX-2 and TNF- $\alpha$  via modulation of Ca $^{2+}$ -mediated signaling pathways [32]. The same compound reduced the expression of pro-inflammatory cytokines and neuronal apoptosis in quinolinic-acid-treated rat brain [33]. These findings together with our data on the global influence of XBD173 on gene expression revealed that targeting TSPO has a broad influence on inflammatory signaling in microglia. As we have shown in microglial cell culture, one potential mechanism of the effects of XBD173 could be the synthesis of pregnenolone, as has been previously shown for astrocytes [34]. These findings support the concept that microglia locally synthesize the anti-inflammatory neurosteroid precursor pregnenolone after activation of TSPO by respective ligands.

Our studies revealed that TSPO significantly influenced the f-actin cytoskeleton and fostered the formation of filopodia along with prominent effects on microglial migration and phagocytosis. A high phagocytic activity with a low migratory capacity is a typical hallmark of homeostatic microglia which constantly survey their environment with long protrusions [35]. Over the last years it has also become clear that microglial phagocytosis of apoptotic cells is largely anti-inflammatory [36]. Thus, we hypothesize that induction of TSPO signaling may shift alerted microglia to a more homeostatic and less inflammatory state. In line with this, TSPO ligands have been shown to influence chemotaxis and phagocytosis in peripheral blood cells [37-39]. TSPO overexpression also increased the proliferation and migratory capacity of rat C6 glioma cells whereas treatment with the TSPO ligand PK11195 had a strong anti-proliferative effect and exerted pro-apoptotic activity

on these cells [40]. Treatment of LPS-challenged microglia with XBD173 could effectively reduce the number of amoeboid cells in the explanted mouse retina but did not significantly increase the fraction of ramified cells. This clearly indicates that TSPO signaling may serve to control microglia dynamics during the activation and/or resolution phase of retinal damage. In the native retina, endogenous ligands for TSPO may fulfill this function. Several endogenous molecules that bind TSPO have been identified in steroidogenic tissues, including the protein diazepam binding inhibitor (DBI) [41]. DBI can be cleaved into several active peptide fragments such as octadecaneuropeptide (ODN) and trikontatetraneuropeptide (TTN) which are released from astrocytes [10]. TTN then stimulates neurosynthesis in C6 glioma cells by acting on TSPO [8]. Thus, we hypothesize that either retinal astrocytes or Müller cells may express DBI and secrete active peptides to control microglial activity via targeting of TSPO.

## Conclusions

We have shown that TSPO is highly expressed in reactive retinal microglia and BV-2 cells stimulated with LPS. The selective TSPO ligand XBD173 efficiently dampened pro-inflammatory gene expression in BV-2 microglial cells and reduced their neurotoxic potential on 661 W photoreceptor cells. XBD173 treatment of BV-2 cells and human iPS-derived microglial cells also promoted filopodia formation and phagocytic uptake. In the explanted mouse retina, XBD173 treatment blocked the LPS-dependent accumulation of amoeboid microglial cells. In conclusion, our data implicate that TSPO expression is connected to retinal microglia reactivity and that selective TSPO ligands may be a promising therapeutic approach to dampen microgliosis during retinal degeneration.

#### Abbreviations

CCL2: chemokine (C-C motif) ligand 2; CFSE: carboxyfluorescein diacetate succinimidyl ester; DBI: diazepam binding inhibitor; FACS: Fluorescence Activated Cell Sorting; FCS: fetal calf serum; GFAP: glial fibrillary acid protein; IL: interleukin; iNOS: inducible nitric oxide synthase; iPS: induced pluripotent stem cell; iPScM: induced pluripotent stem cell-derived microglia; LPS: lipopolysaccharide; MAP2: microtubule-associated protein 2; NO: nitric oxide; TSPO: translocator protein (18 kDa).

#### Competing interests

RR has served as a consultant for Novartis developing TSPO ligands as anxiolytics and is a member of Novartis advisory boards. All other authors declare no competing financial interests.

#### Authors' contributions

TL, BW, HN and RR designed the research. MK, CN, AA, KM, FH, RS performed the research. MK, CN, HN and RS analyzed the data. TL and RR wrote the paper. All authors read and approved the final manuscript.

#### Acknowledgements

This work was funded by the Pro Retina Foundation and supported by the Hans- und Marlies Stock-Stiftung. The authors thank Prof. Muayyad Al Ubaidi for providing the 661 W photoreceptor cell line.

#### Author details

<sup>1</sup>Department of Ophthalmology, University of Cologne, D-50931 Cologne, Germany. <sup>2</sup>Department of Psychiatry and Psychotherapy, University of Regensburg, D-93053 Regensburg, Germany. <sup>3</sup>Institute of Reconstructive Neurobiology, University of Bonn, D-53127 Bonn, Germany. <sup>4</sup>Institute of Human Genetics, University of Regensburg, D-93053 Regensburg, Germany.

Received: 10 September 2013 Accepted: 23 December 2013

Published: 8 January 2014

#### References

- Papadopoulos V, Baraldi M, Guilarte TR, Knudsen TB, Lacapere JJ, Lindemann P, Norenberg MD, Nutt D, Weizman A, Zhang MR, Gavish M: **Translocator protein (18 kDa): new nomenclature for the peripheral-type benzodiazepine receptor based on its structure and molecular function.** *Trends Pharmacol Sci* 2006, **27**:402–409.
- McEnery MW, Snowman AM, Trifiletti RR, Snyder SH: **Isolation of the mitochondrial benzodiazepine receptor: association with the voltage-dependent anion channel and the adenine nucleotide carrier.** *Proc Natl Acad Sci U S A* 1992, **89**:3170–3174.
- Papadopoulos V, Liu J, Culty M: **Is there a mitochondrial signaling complex facilitating cholesterol import?** *Mol Cell Endocrinol* 2007, **265–266**:59–64.
- Rupprecht R, Papadopoulos V, Rammes G, Baghai TC, Fan J, Akula N, Groyer G, Adams D, Schumacher M: **Translocator protein (18 kDa) (TSPO) as a therapeutic target for neurological and psychiatric disorders.** *Nat Rev Drug Discov* 2010, **9**:971–988.
- Kuhlmann AC, Guilarte TR: **Cellular and subcellular localization of peripheral benzodiazepine receptors after trimethyltin neurotoxicity.** *J Neurochem* 2000, **74**:1694–1704.
- Maeda J, Higuchi M, Inaji M, Ji B, Haneda E, Okouchi T, Zhang MR, Suzuki K, Suhara T: **Phase-dependent roles of reactive microglia and astrocytes in nervous system injury as delineated by imaging of peripheral benzodiazepine receptor.** *Brain Res* 2007, **1157**:100–111.
- Veiga S, Azcoitia I, Garcia-Segura LM: **Extragonadal synthesis of estradiol is protective against kainic acid excitotoxic damage to the hippocampus.** *Neuroreport* 2005, **16**:1599–1603.
- Papadopoulos V, Berkovich A, Krueger KE, Costa E, Guidotti A: **Diazepam binding inhibitor and its processing products stimulate mitochondrial steroid biosynthesis via an interaction with mitochondrial benzodiazepine receptors.** *Endocrinology* 1991, **129**:1481–1488.
- Girard C, Liu S, Adams D, Lacroix C, Sineus M, Boucher C, Papadopoulos V, Rupprecht R, Schumacher M, Groyer G: **Axonal regeneration and neuroinflammation: roles for the translocator protein 18 kDa.** *J Neuroendocrinol* 2012, **24**:71–81.
- Chen MK, Guilarte TR: **Translocator protein 18 kDa (TSPO): molecular sensor of brain injury and repair.** *Pharmacol Ther* 2008, **118**:1–17.
- Barron AM, Garcia-Segura LM, Caruso D, Jayaraman A, Lee JW, Melcangi RC, Pike CJ: **Ligand for translocator protein reverses pathology in a mouse model of Alzheimer's disease.** *J Neurosci* 2013, **33**:8891–8897.
- Daugherty DJ, Selvaraj V, Chechneva OV, Liu XB, Pleasure DE, Deng W: **A TSPO ligand is protective in a mouse model of multiple sclerosis.** *EMBO Mol Med* 2013, **5**:891–903.
- Wei XH, Wei X, Chen FY, Zang Y, Xin WJ, Pang RP, Chen Y, Wang J, Li YY, Shen KF, Zhou LJ, Liu XG: **The upregulation of translocator protein (18 kDa) promotes recovery from neuropathic pain in rats.** *J Neurosci* 2013, **33**:1540–1551.
- Rupprecht R, Rammes G, Eser D, Baghai TC, Schule C, Nothdurfter C, Troxler T, Gentsch C, Kalkman HO, Chaperon F, Uzunov V, McAllister KH, Bertaina-Anglade V, La Rochelle CD, Tuerck D, Floesser A, Kiese B, Schumacher M, Landgraf R, Holsboer F, Kucher K: **Translocator protein (18 kDa) as target for anxiolytics without benzodiazepine-like side effects.** *Science* 2009, **325**:490–493. Erratum in: *Science* 2009, **325**:1072. Dosage error in article text.
- Nothdurfter C, Rammes G, Baghai TC, Schule C, Schumacher M, Papadopoulos V, Rupprecht R: **Translocator protein (18 kDa) as a target for novel anxiolytics with a favourable side-effect profile.** *J Neuroendocrinol* 2012, **24**:82–92.
- Nothdurfter C, Baghai TC, Schule C, Rupprecht R: **Translocator protein (18 kDa) (TSPO) as a therapeutic target for anxiety and neurologic disorders.** *Eur Arch Psychiatry Clin Neurosci* 2012, **262**(Suppl 2):S107–S112.
- Berger W, Kloeckener-Gruissem B, Neidhardt J: **The molecular basis of human retinal and vitreoretinal diseases.** *Prog Retin Eye Res* 2010, **29**:335–375.
- Langmann T: **Microglia activation in retinal degeneration.** *J Leukoc Biol* 2007, **81**:1345–1351.
- Weber BH, Schrewe H, Molday LL, Gehrig A, White KL, Seeliger MW, Jaissle GB, Friedburg C, Tamm E, Molday RS: **Inactivation of the murine X-linked juvenile retinoschisis gene, Rs1h, suggests a role of retinoschisin in retinal cell layer organization and synaptic structure.** *Proc Natl Acad Sci U S A* 2002, **99**:6222–6227.
- Gehrig A, Langmann T, Horling F, Janssen A, Bonin M, Walter M, Poths S, Weber BH: **Genome-wide expression profiling of the retinoschisin-deficient retina in early postnatal mouse development.** *Invest Ophthalmol Vis Sci* 2007, **48**:891–900.
- Ebert S, Weigelt K, Walczak Y, Drobnik W, Mauerer R, Hume DA, Weber BH, Langmann T: **Docosahexaenoic acid attenuates microglial activation and delays early retinal degeneration.** *J Neurochem* 2009, **110**:1863–1875.
- Sasmono RT, Oceandy D, Pollard JW, Tong W, Pavli P, Wainwright BJ, Ostrowski MC, Himes SR, Hume DA: **A macrophage colony-stimulating factor receptor-green fluorescent protein transgene is expressed throughout the mononuclear phagocyte system of the mouse.** *Blood* 2003, **101**:1155–1163.
- Ebert S, Schoeberl T, Walczak Y, Stoecker K, Stempf T, Moehle C, Weber BH, Langmann T: **Chondroitin sulfate disaccharide stimulates microglia to adopt a novel regulatory phenotype.** *J Leukoc Biol* 2008, **84**:736–740.
- Beutner C, Roy K, Linnartz B, Napoli I, Neumann H: **Generation of microglial cells from mouse embryonic stem cells.** *Nat Protoc* 2010, **5**:1481–1494.
- Roy K, Beutner C, Neumann H: **Perspectives of stem cell-derived microglia for medicine.** In *Embryonic Stem Cells - Recent Advances in Pluripotent Stem Cell-Based Regenerative Medicine*. Edited by Atwood C, Atwood C. Rijeka, Croatia: InTech Europe; 2011:171–188.
- Da Settimo F, Simorini F, Taliani S, La Motta C, Marini AM, Salerno S, Bellandi M, Novellino E, Greco G, Cosimelli B, Da Pozzo E, Costa B, Simola N, Morelli M, Martini C: **Anxiolytic-like effects of N, N-dialkyl-2-phenylindol-3-ylglyoxylamides by modulation of translocator protein promoting neurosteroid biosynthesis.** *J Med Chem* 2008, **51**:5798–5806.
- Chauveau F, Boutin H, Van Camp N, Dollé F, Tavittian B: **Nuclear imaging of neuroinflammation: a comprehensive review of [<sup>11</sup>C]PK11195 challengers.** *Eur J Nucl Med Mol Imaging* 2008, **35**:2304–2319.
- Venneti S, Lopresti BJ, Wiley CA: **Molecular imaging of microglia/macrophages in the brain.** *Glia* 2013, **61**:10–23.
- Karlstetter M, Walczak Y, Weigelt K, Ebert S, Van den Brulle J, Schwer H, Fuchshofer R, Langmann T: **The novel activated microglia/macrophage WAP domain protein, AMWAP, acts as a counter-regulator of proinflammatory response.** *J Immunol* 2010, **185**:3379–3390.
- Chen MK, Baidoo K, Verina T, Guilarte TR: **Peripheral benzodiazepine receptor imaging in CNS demyelination: functional implications of anatomical and cellular localization.** *Brain* 2004, **127**:1379–1392.

31. Chen MK, Guilarte TR: Imaging the peripheral benzodiazepine receptor response in central nervous system demyelination and remyelination. *Toxicol Sci* 2006, **91**:532–539.
32. Choi HB, Khoo C, Ryu JK, van Breemen E, Kim SU, McLarnon JG: Inhibition of lipopolysaccharide-induced cyclooxygenase-2, tumor necrosis factor-alpha and [Ca<sup>2+</sup>]<sub>i</sub> responses in human microglia by the peripheral benzodiazepine receptor ligand PK11195. *J Neurochem* 2002, **83**:546–555.
33. Ryu JK, Choi HB, McLarnon JG: Peripheral benzodiazepine receptor ligand PK11195 reduces microglial activation and neuronal death in quinolinic acid-injected rat striatum. *Neurobiol Dis* 2005, **20**:550–561.
34. Cascio C, Brown RC, Liu Y, Han Z, Hales DB, Papadopoulos V: Pathways of dehydroepiandrosterone formation in rat brain glia. *J Steroid Biochem Mol Biol* 2000, **75**:177–186.
35. Nimmerjahn A, Kirchhoff F, Helmchen F: Resting microglial cells are highly dynamic surveillants of brain parenchyma *in vivo*. *Science* 2005, **308**:1314–1318.
36. Sierra A, Abiega O, Shahraz A, Neumann H: Janus-faced microglia: beneficial and detrimental consequences of microglial phagocytosis. *Front Cell Neurosci* 2013, **7**:6.
37. Ruff MR, Pert CB, Weber RJ, Wahl LM, Wahl SM, Paul SM: Benzodiazepine receptor-mediated chemotaxis of human monocytes. *Science* 1985, **229**:1281–1283.
38. Cosentino M, Marino F, Cattaneo S, Di Grazia L, Francioli C, Fietta AM, Lecchini S, Frigo G: Diazepam-binding inhibitor-derived peptides induce intracellular calcium changes and modulate human neutrophil function. *J Leukoc Biol* 2000, **67**:637–643.
39. Marino F, Cattaneo S, Cosentino M, Rasini E, Di Grazia L, Fietta AM, Lecchini S, Frigo G: Diazepam stimulates migration and phagocytosis of human neutrophils: possible contribution of peripheral-type benzodiazepine receptors and intracellular calcium. *Pharmacology* 2001, **63**:42–49.
40. Rechichi M, Salvetti A, Chelli B, Costa B, Da Pozzo E, Spinetti F, Lena A, Evangelista M, Rainaldi G, Martini C, Gremigni V, Rossi L: TSPO over-expression increases motility, transmigration and proliferation properties of C6 rat glioma cells. *Biochim Biophys Acta* 2008, **1782**:118–125.
41. Guidotti A, Forchetti CM, Corda MG, Konkel D, Bennett CD, Costa E: Isolation, characterization, and purification to homogeneity of an endogenous polypeptide with agonistic action on benzodiazepine receptors. *Proc Natl Acad Sci U S A* 1983, **80**:3531–3535.

doi:10.1186/1742-2094-11-3

**Cite this article as:** Karlstetter *et al.*: Translocator protein (18 kDa) (TSPO) is expressed in reactive retinal microglia and modulates microglial inflammation and phagocytosis. *Journal of Neuroinflammation* 2014 **11**:3.

**Submit your next manuscript to BioMed Central and take full advantage of:**

- Convenient online submission
- Thorough peer review
- No space constraints or color figure charges
- Immediate publication on acceptance
- Inclusion in PubMed, CAS, Scopus and Google Scholar
- Research which is freely available for redistribution

Submit your manuscript at  
www.biomedcentral.com/submit

